

**STRUCTURE-PROPERTY CORRELATIONS OF POLYHEDRAL  
OLIGOMERIC SILSESQUOXANE IN MODEL POLYSTYRENE**

By

Madhu Namani

A DISSERTATION

Submitted to  
Michigan State University  
in partial fulfillment of the requirements  
for the degree of

Chemical Engineering-Doctor of Philosophy

2014

# ABSTRACT

## STRUCTURE - PROPERTY CORRELATIONS OF POLYHEDRAL OLIGOMERIC SILSESQUIOXANE IN MODEL POLYSTYRENE

By

Madhu Namani

In recent years the blending of 0-, 1-, and 2- dimensional inorganic fillers such as POSS, carbon nanotubes, and nano-clay platelets into polymeric matrices enabled exploration of various filler/matrix combinations on mechanical properties. However, a fundamental understanding of the connections amongst the microstructure and macroscopic properties of polymeric based nanocomposites are yet to be fully explored to optimize the truly multifunctional property potential of polymer nanocomposites. Polyhedral oligomeric silsesquioxane (POSS) offers a unique approach to examine the effect of molecularly dispersed nanoscopic fillers on rheological properties of entangled polymer melts. Experiments were performed using a nearly-monodisperse molecular weight polystyrene (PS) blended with varying amounts of two fully condensed POSS molecules surrounded with phenethyl and styrenyl groups. Due to the chemical similarity between these organic moieties surrounding the silicon-oxygen framework ( $\text{SiO}_{1.5}$ ) of POSS and PS, we were able to obtain polymer blends with molecular dispersed nanoscopic fillers needed to study the effect of intermolecular nanoparticle-nanoparticle interactions and the associated intramolecular interactions on the dynamics of the polymer chains. Differential scanning calorimetry (DSC), wide-angle X-ray

diffraction (WAXD) and transmission electron microscopy (TEM) were used to characterize the thermal properties and morphologies of the POSS/PS blends. Oscillatory Shear both small and large amplitude and/or tensile method was used to probe the dynamics of polymer chains as influenced by the addition of different chemical moiety of POSS at the glass transition, rubbery state and the terminal-flow transition regions. Further studies were done with varying molecular weight of PS for understanding of the chain length effects on the phase behavior of the blends, results obtained from the thermal and mechanical characterization methods were compared with morphological observations to better understand the structure-property relationship of polymers containing molecularly dispersed nanoscopic fillers.

# TABLE OF CONTENTS

LIST OF TABLES .....	vi
LIST OF FIGURES.....	vii
CHAPTER 1: REVIEW OF POLYMER NANOCOMPOSITES....	1
1.1 INTRODUCTION.....	1
1.2 SYNTHETIC STRATEGIES TOWARDS HYBRID MATERIALS.....	12
1.2.1 Sol–Gel Process.....	15
1.2.2 Hybrid Materials by the Sol–Gel Process.....	17
1.2.3 Building Block Approach.....	22
1.2.4 Insitu Polymerization Approach.....	26
1.3 TYPES OF HYBRID MATERIALS.....	30
1.4 PROPERTIES AND APPLICATIONS.....	34
1.5 SUMMARY.....	37
RESEARCH OBJECTIVES.....	38
CHAPTER 2: EFFECTS OF CHEMICAL SUBSTITUENTS ON PHASE BEHAVIOR OF POSS - PS BLENDS.....	40
2.1 Introduction.....	40
2.2 Experimental.....	44
2.2.1 Materials.....	44
2.2.2 Sample Preparations.....	47
2.2.2.1 Samples Preparations for Differential Scanning Calorimeter (DSC).....	47
2.2.2.2 Samples Preparations for X-Ray Diffraction.....	47
2.2.2.3 Samples Preparations for Transmission Electron Microscopy (TEM).....	47
2.2.3 Characterization Techniques.....	48
2.2.3.1 Transmission Electron Microscopy (TEM)...	48
2.2.3.2 X-ray Diffraction.....	48
2.2.3.3 Determination of Transition Temperatures of POSS macromers.....	49
2.2.4 Determination of Transition Temperatures of POSS macromers.....	49

2.3 Results and Discussion.....	49
2.3.1 Effects of POSS Corner Groups.....	49
2.3.2 Miscibility in Polystyrene Based on Different POSS.....	52
2.4 Summary.....	64
CHAPTER 3: EFFECTS OF CONCENTRATION ON PHASE BEHAVIOR OF POSS - PS BLENDS.....	67
3.1 Introduction.....	67
3.2 Experimental.....	68
3.2.1 Materials.....	68
3.2.2 Sample Preparation.....	70
3.2.2.1 Melt Rheological Characterization.....	70
3.3 Results and Discussion.....	71
3.3.1 Rheology during the Rubbery State and Flow Transition..	71
3.4 Summary.....	82
CHAPTER 4: EFFECTS OF PS MOLECULAR WEIGHT ON PHASE BEHAVIOR OF POSS - PS BLENDS.....	86
4.1 Introduction.....	86
4.2 Experimental.....	90
4.2.1 Materials.....	90
4.2.2 Sample Preparation.....	90
4.2.2.1 Rheological Characterization.....	90
4.3 Results and Discussion.....	91
4.4 Summary.....	108
CHAPTER 5: FLOW TRANSITIONS OF POSS - PS BLENDS	110
5.1 Introduction.....	110
5.1.1 Large Amplitude Oscillatory Shear (LAOS).....	111
5.2 Experimental.....	115
5.2.1 Thermo-Mechanical Analysis.....	115
5.2.2 Rheological Characterization.....	116
5.3 Results and Discussion.....	117
5.3.1 Glass Transition Region.....	117
5.3.2 Non-linear oscillation measurements.....	122
5.4 Summary.....	128
CHAPTER 6: CONCLUSION.....	130
REFERENCES.....	139

## LIST OF TABLES

<b>Table 2.1:</b> Abbreviations, Chemical Formula and Molecular Weight of POSS Macromers.....	46
<b>Table 2.2:</b> Transition temperatures of POSS macromers (DSC Results) .	52
<b>Table 3.1:</b> The crossover frequency versus POSS weight fraction and the zero-shear viscosity based on an Ellis model fit.....	80

## LIST OF FIGURES

<b>Figure 2.1:</b> POSS Macromers with Different Corner Groups.....	45
<b>Figure 2.2:</b> DSC Curve of Cp <sub>8</sub> POSS Macromer.....	50
<b>Figure 2.3:</b> DSC Curve of Cy <sub>8</sub> POSS Macromer.....	50
<b>Figure 2.4:</b> DSC Curve of Styrenyl <sub>8</sub> POSS Macromer.....	51
<b>Figure 2.5:</b> DSC Curve of Phenthyl <sub>8</sub> POSS Macromer.....	51
<b>Figure 2.6:</b> TEM Image of POSS PS blends at 50 wt% loadings.....	54
<b>Figure 2.7</b> X-Ray plot of Phenethyl POSS (Ph <sub>8</sub> T <sub>8</sub> ) and PS (M <sub>w</sub> = 290K Da) / Phenethyl POSS 20% wt blend.....	57
<b>Figure 2.8</b> X-Ray plot of Styrenyl POSS (St <sub>8</sub> T <sub>8</sub> ) and PS (M <sub>w</sub> = 290K Da) /Styrenyl POSS 20% wt blend.....	58
<b>Figure 2.9:</b> TEM Image of Styrenyl <sub>8</sub> POSS/PS290K Blend (20 wt% POSS).....	61
<b>Figure 2.10:</b> DSC plot of Phenethyl POSS (Ph <sub>8</sub> T <sub>8</sub> ) and PS (M <sub>w</sub> = 290K Da) / Phenethyl POSS 30% wt blend.....	62
<b>Figure 2.11:</b> DSC plot of Styrenyl POSS (St <sub>8</sub> T <sub>8</sub> ) and PS (M <sub>w</sub> = 290K Da) /Styrenyl POSS 30% wt blend.....	63
<b>Figure 3.1</b> Time temperature superposed plots of PS (M <sub>w</sub> = 290K Da) and Phenethyl POSS (Phe <sub>8</sub> T <sub>8</sub> ) blends with varying weight fractions of POSS at 150 <sup>0</sup> C a) Storage Modulus (G') versus Reduced frequency (a <sub>T</sub> ω) b) Reduced viscosity (η <sup>*</sup> /a <sub>T</sub> ) versus Reduced frequency (a <sub>T</sub> ω) c) Shift factors (a <sub>T</sub> ) versus Temperature (Temp).....	73
<b>Figure 3.2</b> Time temperature superposed plots of PS (M <sub>w</sub> = 290K Da) and Styrenyl POSS (St <sub>8</sub> T <sub>8</sub> ) blends with varying weight fractions of POSS at 150 <sup>0</sup> C a) Storage Modulus (G') versus Reduced frequency (a <sub>T</sub> ω) b) Reduced viscosity (η <sup>*</sup> /a <sub>T</sub> ) versus Reduced frequency (a <sub>T</sub> ω) c) Shift factors (a <sub>T</sub> ) versus Temperature (Temp).....	76
<b>Figure 3.3</b> Log-Log plot of Normalized Plateau Modulus (G <sub>N</sub> (φ)/G <sub>N</sub> (1)) versus Volume fraction (φ).....	79
<b>Figure 4.1</b> Time temperature superposed plots of PS (M <sub>w</sub> = 1.6M Da) and Styrenyl POSS (St <sub>8</sub> T <sub>8</sub> ) blends with varying weight fractions of POSS at 150 <sup>0</sup> C a) Storage Modulus	

( $G'$ ) versus Reduced frequency ( $a_T\omega$ ) b) Reduced viscosity ( $\eta^*/a_T$ ) versus Reduced frequency ( $a_T\omega$ ) c) Shift factors ( $a_T$ ) versus Temperature (Temp).....96

**Figure 4.2** Time temperature superposed plots of PS ( $M_w= 650K$  Da) and Styrenyl POSS ( $St_8T_8$ ) blends with varying weight fractions of POSS at  $150^0C$  a) Storage Modulus ( $G'$ ) versus Reduced frequency ( $a_T\omega$ ) b) Reduced viscosity ( $\eta^*/a_T$ ) versus Reduced frequency ( $a_T\omega$ ) c) Shift factors ( $a_T$ ) versus Temperature (Temp).....99

**Figure 4.3** Time temperature superposed plots of PS ( $M_w= 130K$  Da) and Styrenyl POSS ( $St_8T_8$ ) blends with varying weight fractions of POSS at  $150^0C$  a) Storage Modulus ( $G'$ ) versus Reduced frequency ( $a_T\omega$ ) b) Reduced viscosity ( $\eta^*/a_T$ ) versus Reduced frequency ( $a_T\omega$ ) c) Shift factors ( $a_T$ ) versus Temperature (Temp).....102

**Figure 4.4** Time temperature superposed plots of PS ( $M_w= 65K$  Da) and Styrenyl POSS ( $St_8T_8$ ) blends with varying weight fractions of POSS at  $150^0C$  a) Storage Modulus ( $G'$ ) versus Reduced frequency ( $a_T\omega$ ) b) Reduced viscosity ( $\eta^*/a_T$ ) versus Reduced frequency ( $a_T\omega$ ) c) Shift factors ( $a_T$ ) versus Temperature (Temp).....105

**Figure 4.5:** Normalized viscosity ( $\eta^*/a_T$ ) versus volume fraction of Styrenyl POSS..... 108

**Figure 5.1:** Stress, Strain and Strain rate waves during an oscillation measurement. The stress can be decomposed in an elastic and a viscous stress wave. The Lissajous figure results from plotting the stress versus the strain..... 112

**Figure 5.2** Complex Modulus ( $E^*$ ) and  $\tan\delta$  versus Temperature plot for PS ( $M_w= 290K$  Da) and Phenethyl POSS ( $Ph_8T_8$ ) blends with varying weight fractions of POSS..... 118

**Figure 5.3** Complex Modulus ( $E^*$ ) and  $\tan\delta$  versus Temperature plot for PS ( $M_w= 290K$  Da) and Styrenyl POSS ( $St_8T_8$ ) blends with varying weight fractions of POSS.....120

**Figure 5.4:** Strain sweep for the viscoelastic material 290K PS, showing the transition from the linear into the non-linear regime..... 121

**Figure 5.5:** Strain sweep for the viscoelastic material 6%  $Ph_8T_8$  PS 290K blend, showing the transition from the linear into the non-linear regime.....123

**Figure 5.6:** Strain sweep for the viscoelastic material 6%  $St_8T_8$  PS 290K blend, showing the transition from the linear into the non-linear regime.....124



<b>Figure 5.7:</b> Strain sweep for the viscoelastic material 50% Phe <sub>8</sub> T <sub>8</sub> /PS blend, showing the transition from the linear into the non-linear regime.....	125
<b>Figure 5.8:</b> Strain sweep for the viscoelastic material 20% Phe <sub>8</sub> T <sub>8</sub> /PS blend, showing the transition from the linear into the non-linear regime.....	126
<b>Figure 5.9:</b> Strain sweep for the viscoelastic material 20% St <sub>8</sub> T <sub>8</sub> /PS blend, showing the transition from the linear into the non-linear regime.....	127

# **CHAPTER 1**

## **REVIEW OF POLYMER NANOCOMPOSITES**

### **1.1 INTRODUCTION**

Recent technological breakthroughs and the desire for new functions generate an enormous demand for novel materials. Many of the well-established materials, such as metals, ceramics or plastics cannot fulfill all technological desires for the various new applications. Scientists and engineers realized early on that mixtures of materials can show superior properties compared with their pure counterparts. One of the most successful examples is the group of composites which are formed by the incorporation of a basic structural material into a second substance, the matrix. Usually the systems incorporated are in the form of particles, whiskers, fibers, lamellae, or a mesh. Most of the resulting materials show improved mechanical properties and a well-known example is inorganic fiber-reinforced polymers. Nowadays they are regularly used for lightweight materials with advanced mechanical properties, for example in the construction of vehicles of all types or sports equipment. The structural building blocks in these materials which are incorporated into the matrix are predominantly inorganic in nature and show a size range from the lower micrometer to the millimeter range and therefore their heterogeneous composition is quite often visible to the eye. Soon it became evident that decreasing the size of the inorganic units to the same level as the organic building blocks could lead to more homogeneous

materials that allow a further fine tuning of materials' properties on the molecular and nanoscale level, generating novel materials that either show characteristics in between the two original phases or even new properties.

Although we do not know the original birth of hybrid materials exactly it is clear that the mixing of organic and inorganic components was carried out in ancient world. At that time the production of bright and colorful paints was the driving force to consistently try novel mixtures of dyes or inorganic pigments and other inorganic and organic components to form paints that were used thousands of years ago. Therefore, hybrid materials or even nanotechnology is not an invention of the last decade but was developed a long time ago. However, it was only at the end of the 20th and the beginning of the 21st century that it was realized by scientists, in particular because of the availability of novel physico-chemical characterization methods, the field of nanoscience opened many perspectives for approaches to new materials. The combination of different analytical techniques gives rise to novel insights into hybrid materials and makes it clear that bottom up strategies from the molecular level towards materials' design will lead to novel properties in this class of materials.

Apart from the use of inorganic materials as fillers for organic polymers, such as rubber, it was a long time before much scientific activity was devoted to mixtures of inorganic and organic materials. One process changed this situation: the sol-gel process<sup>1-3</sup>. This process, which

will be discussed in more detail later on, was developed in the 1930s using silicon alkoxides as precursors from which silica was produced. In fact this process is similar to an organic polymerization starting from molecular precursors resulting in a bulk material. Contrary to many other procedures used in the production of inorganic materials this is one of the first processes where ambient conditions were applied to produce ceramics. The control over the preparation of multicomponent systems by a mild reaction method also led to industrial interest in that process. In particular the silicon based sol–gel process was one of the major driving forces what has become the broad field of inorganic–organic hybrid materials. The reason for the special role of silicon was its good processability and the stability of the Si—C bond during the formation of a silica network which allowed the production of organic-modified inorganic networks in one step.

Inorganic–organic hybrids can be applied in many branches of materials chemistry because they are simple to process and are amenable to design on the molecular scale. Currently there are four major topics in the synthesis of inorganic–organic materials: (a) their molecular engineering, (b) their nanometer and micrometer-sized organization, (c) the transition from functional to multifunctional hybrids, and (d) their combination with bioactive components. Some similarities to sol–gel chemistry are shown by the stable metal sols and colloids, such as gold colloids, developed hundreds of years ago. In fact sols prepared by the

sol-gel process, i.e. the state of matter before gelation, and the gold colloids have in common that their building blocks are nanosized particles surrounded by a solvent matrix<sup>4</sup>. Such metal colloids have been used for optical applications in nanocomposites for centuries. Glass, for example, was already colored with such colloids centuries ago. In particular many reports of the scientific examination of gold colloids, often prepared by reduction of gold salts, are known from the end of the 18th century. Probably the first nanocomposites were produced in the middle of the 19th century when gold salts were reduced in the presence of gum. Currently many of the colloidal systems already known are being reinvestigated by modern instrumental techniques to get new insights into the origin of the specific chemistry and physics behind these materials.

The term hybrid material is used for many different systems spanning a wide area of different materials, such as crystalline highly ordered coordination polymers, amorphous sol-gel compounds, materials with and without interactions between the inorganic and organic units. Before the discussion of synthesis and properties of such materials we try to delimit this broadly-used term by taking into account various concepts of composition and structure. The most wide-ranging definition is the following: a hybrid material is a material that includes two moieties blended on the molecular scale. The matrix could be either crystalline or amorphous but commonly one of these compounds is inorganic and the other one organic in nature<sup>5</sup>.

A more detailed definition distinguishes between the possible interactions connecting the inorganic and organic species. *Class I* hybrid materials are those that show weak interactions between the two phases, such as van der Waals, hydrogen bonding or weak electrostatic interactions. *Class II* hybrid materials are those that show strong chemical interactions between the components. Because of the gradual change in the strength of chemical interactions it becomes clear that there is a steady transition between weak and strong interactions. For example there are hydrogen bonds that are definitely stronger than for example weak coordinative bonds. In addition to the bonding characteristics structural properties can also be used to distinguish between various hybrid materials. An organic moiety containing a functional group that allows the attachment to an inorganic network, e.g. a trialkoxysilane group, can act as a network modifying compound because in the final structure the inorganic network is only modified by the organic group. Phenyltrialkoxysilanes are an example for such compounds; they modify the silica network in the sol-gel process via the reaction of the trialkoxysilane group without supplying additional functional groups intended to undergo further chemical reactions to the material formed. If a reactive functional group is incorporated the system is called a network functionalizer. The situation is different if two or three of such anchor groups modify an organic segment; this leads to materials in which the inorganic group is afterwards an integral part of the hybrid network<sup>6-8</sup>.

Blends are formed if no strong chemical interactions exist between the inorganic and organic building blocks. One example for such a material is the combination of inorganic clusters or particles with organic polymers lacking a strong (e.g. covalent) interaction between the components. In this case a material is formed that consists for example of an organic polymer with entrapped discrete inorganic moieties in which, depending on the functionalities of the components, for example weak crosslinking occurs by the entrapped inorganic units through physical interactions or the inorganic components are entrapped in a crosslinked polymer matrix. If an inorganic and an organic network interpenetrate each other without strong chemical interactions, so called interpenetrating networks (IPNs) are formed, which is for example the case if a sol–gel material is formed in presence of an organic polymer or vice versa. Both materials described belong to class I hybrids. Class II hybrids are formed when the discrete inorganic building blocks, e.g. clusters, are covalently bonded to the organic polymers or inorganic and organic polymers are covalently connected with each other<sup>9-10</sup>.

After having discussed the above examples one question arises: what is the difference between inorganic–organic hybrid materials and inorganic–organic nanocomposites? In fact there is no clear borderline between these materials. The term nanocomposite is used if one of the structural units, either the organic or the inorganic, is in a defined size range of 1–100 nm. Therefore there is a gradual transition between hybrid

materials and nanocomposites, because large molecular building blocks for hybrid materials, such as large inorganic clusters, can already be of the nanometer length scale. Commonly the term nanocomposites is used if discrete structural units in the respective size regime are used and the term hybrid materials is more often used if the inorganic units are formed in situ by molecular precursors, for example applying sol–gel reactions. Examples of discrete inorganic units for nanocomposites are nanoparticles, nanorods, carbon nanotubes and galleries of clay minerals. Usually a nanocomposite is formed from these building blocks by their incorporation in organic polymers<sup>11</sup>.

The most obvious advantage of inorganic–organic hybrids is that they can favorably combine the often dissimilar properties of organic and inorganic components in one material. Because of the many possible combinations of components this field is very creative, since it provides the opportunity to invent an almost unlimited set of new materials with a large spectrum of known and as yet unknown properties. Another driving force in the area of hybrid materials is the possibility to create multifunctional materials. Probably the most intriguing property of hybrid materials that makes this material class interesting for many applications is their processing. Contrary to pure solid state inorganic materials that often require a high temperature treatment for their processing, hybrid materials show a more polymer-like handling, either because of their large organic content or because of the formation of crosslinked inorganic



networks from small molecular precursors just like in polymerization reactions<sup>12</sup>. Hence, these materials can be shaped in any form in bulk and in films. Although from an economical point of view bulk hybrid materials can currently only compete in very special areas with classical inorganic or organic materials, e.g. in the biomaterials sector, the possibility of their processing as thin films can lead to property improvements of cheaper materials by a simple surface treatment, e.g. scratch resistant coatings. Based on the molecular or nanoscale dimensions of the building blocks, light scattering in homogeneous hybrid material can be avoided and therefore the optical transparency of the resulting hybrid materials and nanocomposites is, dependent on the composition used, relatively high. Furthermore, the materials' building blocks can also deliver an internal structure to the material which can be regularly ordered. While in most cases phase separation is avoided, phase separation of organic and inorganic components is used for the formation of porous materials.

Material properties of hybrid materials are usually changed by modifications of the composition on the molecular scale. If, for example, more hydrophobicity of a material is desired, the amount of hydrophobic molecular components is increased. In sol-gel materials this is usually achieved if alkyl- or aryl-substituted trialkoxysilanes are introduced in the formulation. Hydrophobic and lipophobic materials are composed if partially or fully fluorinated molecules are included. Mechanical

properties, such as toughness or scratch resistance, are tailored if hard inorganic nanoparticles are included into the polymer matrix. Because the compositional variations are carried out on the molecular scale a gradual fine tuning of the material properties is possible. One important subject in materials chemistry is the formation of smart materials, such as materials that react to environmental changes or switchable systems, because they open routes to novel technologies, for example electroactive materials, electrochromic materials, sensors and membranes, biohybrid materials, etc. The desired function can be delivered from the organic or inorganic or from both components. One of the advantages of hybrid materials in this context is that functional organic molecules as well as biomolecules often show better stability and performance if introduced in an inorganic matrix<sup>13-17</sup>.

The transition from the macroscopic world to microscopic, nanoscopic and molecular objects leads, beside the change of physical properties of the material itself, i.e. the so called quantum size effects, to the change of the surface area of the objects. While in macroscopic materials the majority of the atoms are hidden in the bulk of the material it becomes vice versa in very small objects. In small nanoparticles (<10nm) nearly every atom is a surface atom that can interact with the environment. One predominant feature of hybrid materials or nanocomposites is their inner interface, which has a direct impact on the properties of the different building blocks and therefore on the materials'

properties<sup>18</sup>. If the two phases have opposite properties, such as different polarity, the system would thermodynamically phase separate. The same can happen on the molecular or nanometer level, leading to microphase separation. Usually, such a system would thermodynamically equilibrate over time. However in many cases in hybrid materials the system is kinetically stabilized by network forming reactions such as the sol-gel process leading to a spatial fixation of the structure. The materials formed can be macroscopically homogeneous and optically clear, because the phase segregation is of small length scale and therefore limited interaction with visible light occurs. However, the composition on the molecular or nanometer length scale can be heterogeneous. If the phase segregation reaches the several hundred nanometer length scale or the refractive index of the formed domains is very different, materials often turn opaque. Effects like this are avoided if the reaction parameters are controlled in such a way that the speed of network formation is kept faster than the phase separation reactions.

The high surface area of nanobuilding blocks can lead to additional effects; for example if surface atoms strongly interact with molecules of the matrix by chemical bonding, reactions like surface reorganization, electron transfer, etc. can occur which can have a large influence on the physical properties of the nano-building blocks and thus the overall performance of the material formed<sup>19-21</sup>. It is, for example, known that conjugated  $\pi$ -electron systems coordinated to the surface of titania

nanoparticles can lead to charge transfer reactions that influence the color, and therefore the surface electronic properties of the particles. Nanosized objects, such as inorganic nanoparticles, in addition show a very high surface energy. Usually if the surface energy is not reduced by surface active agents (e.g. surfactants), such particles tend to agglomerate in an organic medium. Thus, the physical properties of the nanoparticles (e.g. quantum size effects) diminish, and/or the resulting materials are no longer homogeneous. Both facts have effects on the final material properties. For example the desired optical properties of nanocomposites fade away, or mechanical properties are weakened. However, sometimes a controlled aggregation can also be required, e.g. percolation of conducting particles in a polymer matrix increases the overall conductivity of the material<sup>22</sup>.

Earlier the interaction mechanism between the organic and inorganic species was used to categorize the different types of hybrid materials, furthermore of course the interaction also has an impact on the material properties. Weak chemical interactions between the inorganic and organic entities leave some potential for dynamic phenomena in the final materials, meaning that over longer periods of time changes in the material, such as aggregation, phase separation or leaching of one of the components, can occur. These phenomena can be avoided if strong interactions are employed such as covalent bonds, as in nanoparticle crosslinked polymers. Depending on the desired materials' properties the

interactions can be gradually tuned. Weak interactions are, for example, preferred where a mobility of one component in the other is required for the target properties. This is for example the case for ion conducting polymers, where the inorganic ion (often  $\text{Li}^+$ ) has to migrate through the polymer matrix. In many examples the interactions between the inorganic and organic species are maximized by applying covalent attachment of one to the other species. But there are also cases where small changes in the composition, which on the first sight should not result in large effects, can make considerable differences. It was, for example, shown that interpenetrating networks between polystyrene and sol-gel materials modified with phenyl groups show less microphase segregation than sol-gel materials with pure alkyl groups, which was interpreted to be an effect of  $\pi$ - $\pi$ -interactions between the two materials<sup>23</sup>. In addition the interaction of the two components can have an influence on other properties, such as electronic properties if coordination complexes are formed or electron transfer processes are enabled by the interaction.

## **1.2 SYNTHETIC STRATEGIES TOWARDS HYBRID MATERIALS**

In principle two different approaches can be used for the formation of hybrid materials: Either well-defined preformed building blocks are applied that react with each other to form the final hybrid material in which the precursors still at least partially keep their original integrity or one or both structural units are formed from the precursors that are transformed into a novel (network) structure. Both methodologies have

their advantages and disadvantages and will be described here in more detail.

**Building block approach** As mentioned above building blocks at least partially keep their molecular integrity throughout the material formation, which means that structural units that are present in these sources for materials formation can also be found in the final material. At the same time typical properties of these building blocks usually survive the matrix formation, which is not the case if material precursors are transferred into novel materials. Representative examples of such well-defined building blocks are modified inorganic clusters or nanoparticles with attached reactive organic groups. Cluster compounds often consist of at least one functional group that allows an interaction with an organic matrix, for example by copolymerization. Depending on the number of groups that can interact, these building blocks are able to modify an organic matrix (one functional group) or form partially or fully crosslinked materials (more than one group). For instance, two reactive groups can lead to the formation of chain structures. If the building blocks contain at least three reactive groups they can be used without additional molecules for the formation of a crosslinked material. Beside the molecular building blocks mentioned, nanosized building blocks, such as particles or nanorods could be used to form nanocomposites. The building block approach has one large advantage compared with the *in situ* formation of the inorganic or organic entities: because at least one structural unit (the building block)

is well-defined and usually does not undergo significant structural changes during the matrix formation, better structure–property predictions are possible. Furthermore, the building blocks can be designed in such a way to give the best performance in the materials' formation, for example good solubility of inorganic compounds in organic monomers by surface groups showing a similar polarity as the monomers.

**In situ formation of the components** Contrary to the building block approach the *in situ* formation of the hybrid materials is based on the chemical transformation of the precursors used throughout materials' preparation. Typically this is the case if organic polymers are formed but also if the sol–gel process is applied to produce the inorganic component. In these cases well-defined discrete molecules are transformed to multidimensional structures, which often show totally different properties from the original precursors. Generally simple, commercially available molecules are applied and the internal structure of the final material is determined by the composition of these precursors but also by the reaction conditions. Therefore control over the latter is a crucial step in this process. Changing one parameter can often lead to two very different materials. If, for example, the inorganic species is a silica derivative formed by the sol–gel process, the change from base to acid catalysis makes a large difference because base catalysis leads to a more particle-like microstructure while acid catalysis leads to a polymer-like

microstructure. Hence, the final performance of the derived materials is strongly dependent on their processing and its optimization.

Many of the classical inorganic solid state materials are formed using solid precursors and high temperature processes, which are often not compatible with the presence of organic groups because they are decomposed at elevated temperatures. Hence, these high temperature processes are not suitable for the *in situ* formation of hybrid materials. Reactions that are employed should have more the character of classical covalent bond formation in solutions. One of the most prominent processes which fulfill these demands is the sol–gel process. However, such rather low temperature processes often do not lead to the thermodynamically most stable structure but to kinetic products, which has some implications for the structures obtained. For example low temperature derived inorganic materials are often amorphous or crystallinity is only observed on a very small length scale, i.e. the nanometer range. An example of the latter is the formation of metal nanoparticles in organic or inorganic matrices by reduction of metal salts or organometallic precursors.

### **1.2.1 Sol–Gel Process**

This process is chemically related to an organic polycondensation reaction in which small molecules form polymeric structures by the loss of substituents. Usually the reaction results in a three-dimensional (3-D)



crosslinked network. The fact that small molecules are used as precursors for the formation of the crosslinked materials implies several advantages, for example a high control of the purity and composition of the final materials and the use of a solvent based chemistry which offers many advantages for the processing of the materials formed. The silicon-based sol-gel process is probably the one that has been most investigated; therefore the fundamental reaction principles are discussed using this process as a model system. One important fact also makes the silicon-based sol-gel processes a predominant process in the formation of hybrid materials, which is the simple incorporation of organic groups using organically modified silanes. Si—C bonds have enhanced stability against hydrolysis in the aqueous media usually used, which is not the case for many metal-carbon bonds, so it is possible to easily incorporate a large variety of organic groups in the network formed. Principally  $R_4-nSiX_n$  compounds ( $n = 1-4$ ,  $X = OR'$ , halogen) are used as molecular precursors, in which the Si—X bond is labile towards hydrolysis reactions forming unstable silanols (Si—OH) that condensate leading to Si—O—Si bonds. In the first steps of this reaction oligo- and polymers as well as cyclics are formed subsequently resulting in colloids that define the sol. Solid particles in the sol afterwards undergo crosslinking reactions and form the gel. The reaction could be acid and base catalyzed leading differing architecture based on the pH. More detailed discussions of the sol-gel process can be found in the cited literature<sup>1-3</sup>.

### **1.2.2 Hybrid Materials by the Sol–Gel Process**

Compared with other inorganic network forming reactions, the sol–gel processes show mild reaction conditions and a broad solvent compatibility. These two characteristics offer the possibility to carry out the inorganic network forming process in presence of a preformed organic polymer or to carry out the organic polymerization before, during or after the sol–gel process. The properties of the final hybrid materials are not only determined by the properties of the inorganic and organic component, but also by the phase morphology and the interfacial region between the two components. The often dissimilar reaction mechanisms of the sol–gel process and typical organic polymerizations, such as free radical polymerizations, allow the temporal separation of the two polymerization reactions which offers many advantages in the material formation. One major parameter in the synthesis of these materials is the identification of a solvent in which the organic macromolecules are soluble and which is compatible with either the monomers or preformed inorganic oligomers derived by the sol–gel approach. Many commonly applied organic polymers, such as polystyrene or polymethacrylates, are immiscible with alcohols that are released during the sol–gel process and which are also used as solvents, therefore phase separation is enforced in these cases. This can be avoided if the solvent is switched from the typically used alcohols to, for example, THF in which many organic polymers are soluble and which is compatible with many sol–gel

reactions. Phase separation can also be avoided if the polymers contain functional groups that are more compatible with the reaction conditions of the sol-gel process or even undergo an interaction with the inorganic material formed. In addition, the functional group incorporated changes the properties of the final material, for example fluoro-substituted compounds can create hydrophobic and lipophobic materials, additional reactive functional groups can be introduced to allow further reactions such as amino, epoxy or vinyl groups. Beside molecules with a single trialkoxysilane group also multifunctional organic molecules can be used. by the incorporation of OH-groups that interact with, for example, hydroxyl groups formed during the sol-gel process or by ionic modifications of the organic polymer. Covalent linkages can be formed if functional groups that undergo hydrolysis and condensation reactions are covalently attached to the organic monomers.

If the organic polymerization occurs in the presence of an inorganic material to form the hybrid material one has to distinguish between several possibilities to overcome the incompatibility of the two species. The inorganic material can either have no surface functionalization but the bare material surface; it can be modified with nonreactive organic groups (e.g. alkyl chains); or it can contain reactive surface groups such as polymerizable functionalities. Depending on these prerequisites the material can be pretreated, for example a pure inorganic surface can be treated with surfactants or silane coupling agents to make it compatible

with the organic monomers, or functional monomers can be added that react with the surface of the inorganic material. If the inorganic component has nonreactive organic groups attached to its surface and it can be dissolved in a monomer which is subsequently polymerized, the resulting material after the organic polymerization is a blend. In this case the inorganic component interacts only weakly or not at all with the organic polymer; hence, a Class I material formed. Homogeneous materials are only obtained in this case if agglomeration of the inorganic components in the organic environment is prevented. This can be achieved if the interactions between the inorganic components and the monomers are better or at least the same as between the inorganic components. However, if no strong chemical interactions are formed, the long-term stability of a once homogeneous material is questionable because of diffusion effects in the resulting hybrid material. Examples of such materials are alkyl chain functionalized silica nanoparticles that can be introduced into many hydrophobic polymers, the use of block copolymers containing a poly(vinyl pyridine) segment that can attach to many metal nanoparticles, or the use of hydroxyethyl methacrylates in the polymerization mixture together with metal oxide nanoparticles. In the latter example hydrogen bridges are formed between the polymer matrix and the particle surface. The stronger the respective interaction between the components, the more stable is the final material. The strongest interaction is achieved if class II materials are formed, for example with

covalent interactions. Examples for such strong interactions are the use of surface-attached polymerizable groups that are copolymerized with organic monomers.

If a porous 3-D inorganic network is used as the inorganic component for the formation of the hybrid material a different approach has to be employed depending on the pore size, the surface functionalization of the pores and the stiffness of the inorganic framework. In many cases intercalation of organic components into the cavities is difficult because of diffusion limits. Several porous or layered inorganic materials have already been used to prepare hybrid materials and nanocomposites<sup>24</sup>. Probably the most studied materials, class in this respect is that of two-dimensional (2-D) layered inorganic materials that can intercalate organic molecules and if polymerization between the layers occurs even exfoliate, producing nanocomposites. Contrary to intercalated systems the exfoliated hybrids only contain a small weight percentage of host layers with no structural order. Principally three methods for the formation of polymer–clay nanocomposites can be used:

1. Intercalation of monomers followed by *in situ* polymerization
2. Direct intercalation of polymer chains from solution
3. Polymer melt intercalation

The method applied depends on the inorganic component and on the polymerization technique used and will not be discussed in this introductory chapter.

Contrary to the layered materials, which are able to completely delaminate if the forces produced by the intercalated polymers overcome the attracting energy of the single layers, this is not possible in the case of the stable 3-D framework structures, such as zeolites, molecular sieves and M41S-materials. The composites obtained can be viewed as host-guest hybrid materials. There are two possible routes towards this kind of hybrid material; (a) direct threading of preformed polymer through the host channels (soluble and melting polymers) which is usually limited by the size, conformation, and diffusion behavior of the polymers and, (b) the *in situ* polymerization in the pores and channels of the hosts. The latter is the most widely used method for the synthesis of such systems. Of course, diffusion of the monomers in the pores is a function of the pore size, therefore the pores in zeolites with pore sizes of several hundred picometers are much more difficult to use in such reactions than mesoporous materials with pore diameters of several nanometers. Two methods proved to be very valuable for the filling of the porous structures with monomers: one is the soaking of the materials in liquid monomers and the other one is the filling of the pores in the gas phase. A better uptake of the monomers by the inorganic porous materials is achieved if the pores are pre-functionalized with organic groups increasing the absorption of monomers on the concave surface. In principle this technique is similar to the increase of monomer absorption on the surface of silica nanoparticles by the surface functionalization with silane

coupling agents. Beside of well-defined 3-D porous structures, sol-gel networks are also inherently porous materials. Uniform homogeneous materials can be obtained if the solvent of the sol-gel process is a monomer for a polymerization. This can be polymerized in a second step after the sol-gel process has occurred.

### **1.2.3 Building Block Approach**

In recent years many building blocks have been synthesized and used for the preparation of hybrid materials. Chemists can design these compounds on a molecular scale with highly sophisticated methods and the resulting systems are used for the formation of functional hybrid materials. Many future applications, in particular in nanotechnology, focus on a bottom-up approach in which complex structures are hierarchically formed by these small building blocks. This idea is also one of the driving forces of the building block approach in hybrid materials.

Another point which was also already mentioned is the predictability of the final material properties if well-defined building blocks are used. A typical building block should consist of a well-defined molecular or nanosized structure and of a well-defined size and shape, with a tailored surface structure and composition. In regard of the preparation of functional hybrid materials the building block should also deliver interesting chemical or physical properties, in areas like conductivity, magnetic behavior, thermal properties, switching possibilities, etc. All these characteristics should be kept during the material formation, for

example the embedment into a different phase. Building blocks can be inorganic or organic in nature, but because they are incorporated into another phase they should be somehow compatible with the second phase. Most of the times the compatibility is achieved by surface groups that allow some kind of interaction with a second component.

Prime examples of inorganic building blocks that can keep their molecular integrity are cluster compounds of various compositions. Usually clusters are defined as agglomerates of elements that either exclusively contain pure metals or metals in mixture with other elements. Although the classical chemical understanding of a cluster includes the existence of metal–metal bonds, the term cluster should be used in the context of this book in its meaning of an agglomerate of atoms in a given shape. Regularly pure metal clusters are not stable without surface functionalization with groups that decrease surface energy and thus avoid coalescence to larger particles. Both coalescence and surface reactivity of clusters are closely related to that of nanoparticles of the same composition. Because of this similarity and the fact that the transition from large clusters to small nanoparticles is fluent, we will not clearly distinguish between them. While in commonly applied metal clusters the main role of the coordinating ligands is the stabilization, they also can serve for a better compatibilization or interaction with an organic matrix. Similar mechanisms are valid for binary systems like metal chalcogenide or multicomponent clusters. Hence, the goal in the chemical design of



these systems is the preparation of clusters carrying organic surface functionalizations that tailor the interface to an organic matrix by making the inorganic core compatible and by the addition of functional groups available for certain interactions with the matrix.

Surface-functionalized metal clusters are one prominent model system for well defined inorganic building blocks that can be used in the synthesis of hybrid materials. However, as with many other nanoscaled materials it is not possible to synthesize such pure clusters and to handle them without a specific surface coverage that limits the reactivity of the surface atoms towards agglomeration. From the aspect of the synthesis of hybrid materials this is no problem as long as the surface coverage of the cluster or nanoparticle contains the desired functionalities for an interaction with an organic matrix. Beside pure metal clusters and nanoparticles an interesting class of materials is metal oxides, because they have interesting magnetic and electronic properties often paired with low toxicity. Simple easy-to-synthesize oxidic compounds are silicon-based systems such as silica particles or spherosilicate clusters, therefore these systems are often used as model compounds for the class of metal oxides, although they do not really represent the class of transition metal oxides that are probably more often used in technological relevant areas. Silica particles or spherosilicate clusters both have in common that the surface contains reactive oxygen groups that can be used for further functionalization. Mono-functional polyhedral silsesquioxane (POSS)

derivatives of the type  $R'R_7Si_8O_{12}$  ( $R'$  = functional group,  $R$  = nonfunctional group) are prepared by reacting the incompletely condensed molecule  $R_7Si_7O_9(OH)_3$  with  $R'SiCl_3$ . The eighth corner of the cubic closed structure is inserted by this reaction, and a variety of functional organic groups  $R'$  can be introduced, such as vinyl, allyl, styryl, norbornadienyl, 3-propyl methacrylate, etc. The incompletely condensed compounds  $R_7Si_7O_9(OH)_3$  are obtained when certain bulky groups  $R$  (e.g. cyclopentyl, cyclohexyl, *tert.*-butyl) prevent the formation of the closed structures from  $RSiX_3$  precursors and lead to the precipitation of open-framework POSS. These bulky substituents not only lead to open framework structures but also increase the solubility of the inorganic units in organic solvents. The closed cubic systems still show the high solubility which is necessary if the inorganic building blocks are to be incorporated in an organic environment for the functionalization of organic materials. The simple handling of these systems caused their boom in the preparation of hybrid materials. Other popular silsesquioxanes that have been prepared are the octahydrido- or the octavinyl-substituted molecules, which offer eight reactive sites. The preparation of these systems is still very costly not least because of the low yields of the targeted products. After functionalization usually eight reaction sites are attached to these silica cores. Some typical reactions lead to the attachment of initiating or polymerizable groups at the corners

and therefore the resulting clusters can be used as multifunctional initiators for polymerizations or as crosslinking monomers.

Post synthetic modification means that the cluster or nanoparticle is formed in a first step applying well-established procedures and the functionalization with organic groups is applied in a second step. Reactive surface functionalizations are required that allow a chemical reaction with the surface decorating molecules, for example nucleophilic substitution reactions.

#### **1.2.4 Insitu Polymerization Approach**

In the post-synthesis modification, functionalized building blocks are formed in two steps which are distinctly separate from each other: the inorganic core is formed first, and the functional organic groups are introduced later in a different reaction. An alternative method is the formation of the inorganic building blocks in the presence of functional organic molecules (i.e. the functionalization of the clusters/particles occurs *in situ*). Silsesquioxanes with only one substitution pattern at each silicon atom are typical examples for the *in situ* formation of functionalized building blocks. As mentioned above they are prepared by the hydrolysis and condensation of trialkoxy- or trichlorosilanes, thus they contain inherently one functional group that is also present in the final material. Depending on the reaction procedure either ladderlike polymers or polyhedral silsesquioxanes (POSS) are obtained. The polyhedral compounds  $[\text{RSiO}_{3/2}]_n$  can be considered silicon oxide

clusters capped by the organic groups R. Polyhedral Silsesquioxanes  $[\text{RSiO}_{3/2}]_n$  are obtained by controlled hydrolytic condensation of  $\text{RSiX}_3$  ( $\text{X} = \text{Cl}, \text{OR}'$ ) in an organic solvent. There is a high driving force for the formation of polyhedral rather than polymeric compounds, particularly if the precursor concentration in the employed solvent is low (when the concentration is increased, increasing portions of network polymers may be formed). Which oligomers are produced and at which rate, depends on the reaction conditions, such as solvent, concentration of the monomer, temperature, pH and the nature of the organic group R. Chlorosilanes have a higher reactivity than the corresponding alkoxysilanes. In most cases, intractable mixtures of products are obtained except for those species that precipitate from the solution. The best investigated silsesquioxane cages are the cubic octamers,  $\text{R}_8\text{Si}_8\text{O}_{12}$ . The compound  $[\text{HSiO}_{3/2}]_8$  is, for example, prepared by hydrolysis of  $\text{HSiCl}_3$  in a benzene /  $\text{H}_2\text{SO}_4$  mixture or by using partially hydrated  $\text{FeCl}_3$  as the water source. It is a valuable starting compound for organically substituted derivatives as the Si—H functions of the silsesquioxane can be converted into organofunctional groups either by hydrosilation reactions (in the equation:  $\text{X} = \text{Cl}, \text{OR}', \text{CN}, \text{etc.}$ ). Only a few POSS with functional organic groups are insoluble enough to be obtained directly from the corresponding  $\text{RSiCl}_3$  precursor by precipitation reactions. Examples are  $(\text{CH}_2=\text{CH})_8\text{Si}_8\text{O}_{12}$ ,  $(p\text{-ClCH}_2\text{C}_6\text{H}_4)_8\text{Si}_8\text{O}_{12}$ ,  $(\text{R}_2\text{NCH}_2\text{CH}_2)_8\text{Si}_8\text{O}_{12}$  or  $(\text{ClCH}_2\text{CH}_2)_8\text{Si}_8\text{O}_{12}$ . These compounds can also be transformed to other functional

octa(silsesquioxanes). Examples include epoxidation of vinyl groups or nucleophilic substitution of the chloro group. Nonfunctional organic groups may be converted to functional organic by standard organic reactions. For example, the phenyl groups of the cubic silsesquioxane  $\text{Ph}_8\text{Si}_8\text{O}_{12}$  were first nitrated and then reduced to give  $(\text{H}_2\text{NC}_6\text{H}_4)_8\text{Si}_8\text{O}_{12}$ . The systems prepared in this way can be used as building blocks for materials depending on their functional groups. The polyhedral compounds  $[\text{RSiO}_3/2]_n$  (POSS) or  $[\text{RO—SiO}_3/2]_n$  discussed so far, formed by hydrolysis and condensation of a single precursor, are models for larger silica particles covered by organic groups and prepared from  $\text{RSi}(\text{OR}')_3$  /  $\text{Si}(\text{OR}')_4$  mixtures. The main parameter that controls the mutual arrangement of the  $[\text{SiO}_4]$  and  $[\text{RSiO}_3/2]$  building blocks is the pH. It was shown that upon sol–gel processing of  $\text{RSi}(\text{OR}')_3$  /  $\text{Si}(\text{OR}')_4$  mixtures (with nonbasic groups R) under basic conditions  $\text{Si}(\text{OR}')_4$  reacts first and forms a gel network of agglomerated spherical nanoparticles. The  $\text{RSi}(\text{OR}')_3$  precursor reacts in a later stage and condenses to the surface of the pre-formed silica nanoparticulate network. This kinetically controlled arrangement of the two building blocks from  $\text{RSi}(\text{OR}')_3$  /  $\text{Si}(\text{OR}')_4$  mixtures is another method to obtain surface-modified spherical Stöber particles.

Interactions between metals or metal oxides cores to molecules that act as surface functionalizations are similar on a molecular scale and therefore do not usually change with the size of the core. Thus, the

chemistry developed for isolated and structurally characterized metal and metal oxide clusters can also be applied for the functionalization of larger nanoparticles. This interface analogy offers the chance to study the chemistry on the molecular scale, which can be analyzed by conventional spectroscopic techniques much more easily, and transfer the obtained conclusions to the larger scale. There are many examples which show these similarities. Generally, as already mentioned above, the organic groups present in the reaction mixture and attached to the surface after the particle formation were mainly used to limit the growth of the derived particles by blocking reactive surface sites and guarantee a stable suspension in a specific solvent. Only recently have these groups been used to introduce a different surface characteristic to the surface of these building blocks or to add chemical functionalities to the surface of the particles and on their preparation route. The head groups of these capping agents can also be other functional molecules or polymers to graft them on the surface of the inorganic nanobuilding blocks.

Beside the surface-functionalized inorganic building blocks described, of course organic building blocks can also be used for the formation of hybrid materials. Typical examples are oligo- and polymers as well as biological active molecules like enzymes. In principal, similar methods have to be applied as in the case of inorganic systems to increase the compatibility and the bonding between the two organic phases.

### 1.3 TYPES OF HYBRID MATERIALS:

**Small molecules** The modification of inorganic networks with small organic molecules can be defined as the origin of hybrid materials. This is particularly true for sol–gel derived silicon-based materials. The mild conditions of the sol–gel process permit the introduction into the inorganic network of any organic molecule that consists of groups which do not interfere with these conditions, e.g. an aqueous and an acid or alkaline environment; it can then either be physically trapped in the cavities or covalently connected to the inorganic backbone. The latter is achieved by the modification of the organic molecules with hydrolysable alkoxysilane or chlorosilane groups. Phase separation is usually avoided by matching the polarity of the often hydrophobic molecules to that of the hydrophilic environment. If such a match can be obtained nearly every organic molecule can be applied to create hybrid materials. In recent years functional hybrids have been the particular focus of interest. Organic dyes, nonlinear optical groups, or switchable groups are only a small selection of molecules which have already been used to prepare hybrid materials and nanocomposites.

**Macromolecules** Oligo- and polymers as well as other organic macromolecules often show different solubilities in specific solvents compared with their monomers; most often the solubility of the polymers is much lower than that of the monomers. However, many formation mechanisms for hybrid materials and nanocomposites are based on solvent

chemistry, for example the sol–gel process or the wet chemistry formation of nanoparticles.<sup>25-26</sup> Therefore, if homogeneous materials are targeted, an appropriate solvent for both the inorganic and the organic macromolecules is of great benefit. For example many macromolecules are soluble in THF which is also a reasonable good reaction environment for the sol–gel process. Additional compatibilization is obtained if the polymers contain groups that can interact with the inorganic components. Similar mechanisms of interactions can be employed as already mentioned above, i.e. groups that interact via the formation of covalent bonds or others that compatibilize between the organic and inorganic components. A particularly interesting group of macromolecules are block copolymers, consisting of a hydrophilic and a hydrophobic segment. They can be tailored in such a way that they can react with two phases that reveal totally different chemical characters and therefore, they are known as good compatibilizers between two components. These surfactants were for example often used for the modification of nanoparticles, where one segment interacts with the surface of the particle, and the other segment sticks away from this surface. In technology such systems are often used to overcome interfaces, for example when inorganic fillers are used for the modification of organic polymers. Novel controlled polymerization methods of late have allowed the preparation of block copolymers with a plethora of functional groups and therefore novel applications will soon be available.



**Particles and particle-like structures** Organic colloids formed from physically or chemically crosslinked polymers can also be used as building blocks for inorganic–organic hybrid materials and nanocomposites. The good control over their properties, such as their size, the broad size range in which they can be produced, from several nanometers to micrometers, accompanied by their narrow size distribution makes them ideal building blocks for many applications. Similarly to dendrimers, special interest in these systems is achieved after their surface modification, because of their self-assembling or simply by their heterophase dispersion. As already mentioned above these latex colloids are formed in aqueous dispersions which, in addition to being environmentally more acceptable or even a mandatory choice for any future development of large output applications, can provide the thermodynamic drive for self-assembling of amphiphilics, adsorption onto colloidal particles or partitioning of the hybrid's precursors between dispersed nanosized reaction loci, as in emulsion or mini-emulsion free-radical polymerizations. For the use as precursors in inorganic–organic hybrid materials styrene or acrylate homo- and copolymer core latex particles are usually modified with a reactive comonomer, such as trimethoxysilylpropyl methacrylate, to achieve efficient interfacial coupling with silica environment during the sol–gel process.<sup>32-34</sup> Organic colloidal building blocks were in particular used for the preparation of 3-D colloidal crystals that were subsequently applied as templates in whose

voids inorganic precursors were infiltrated and reacted to inorganic materials followed by removal of the colloids. Furthermore, discrete core-shell particles can also be produced consisting of an organic core and an inorganic shell. After removal of the organic core, for example by calcination, hollow inorganic spheres are obtained. Another type of organic macromolecular building block is the hyperbranched molecules, so-called dendrimers. Dendrimers are highly branched regular 3-D monodisperse macromolecules with a tree-like structure. These macromolecules offer a wide range of unusual physical and chemical properties mainly because they have a well-defined number of peripheral functional groups that are introduced during their synthesis as well as internal cavities (guest–host systems). In particular the deliberate control of their size and functionality makes these compounds also interesting candidates as nanoscopic building blocks for hybrid materials. Spherically shaped dendrimers are, for example, ideal templates for porous structures with porosities that are determined by the radius of the dendrimeric building block. Generally approaches for surface functionalizations of these molecules are the modification with charged end-groups or the use of reactive organic groups. The end groups of dendrimers can also be used for an interaction with metal clusters or particles and thus nanocomposites are formed often by simply mixing the two components. Multifunctionalized inorganic molecules can also act as the core of dendrimers. POSS and spherosilicate cages were, for example, used as the

core units from which dendrons were either grown divergently or to which they were appended convergently. Applying both silsesquioxanes and end-group functionalized dendrimers, both as multifunctional molecules crosslinked hybrid materials were obtained where welldefined inorganic molecules acted as crosslinking components.<sup>27-31</sup>

Beside their role as crosslinking building blocks dendrimers can form hybrid materials by themselves. For example in their outer or inner shell precursors for nanoparticle synthesis can be attached to functional groups introduced during the synthesis and afterwards nanoparticles are grown within the branches of the dendrimers.

#### **1.4 PROPERTIES AND APPLICATIONS**

There is almost no limit to the combinations of inorganic and organic components in the formation of hybrid materials. Therefore materials with novel composition– property relationships can be generated that have not yet been possible. Because of the plethora of possible combinations this introductory chapter can only present some selected examples. Many of the properties and applications are dependent on the properties of the precursors and the reader is therefore referred to the following chapters. Based on the increased importance of optical data transmission and storage, optical properties of materials play a major role in many high-tech applications. The materials used can reveal passive optical properties, which do not change by environmental excitation, or active optical properties such as photochromic (change of color during

light exposure) or electrochromic (change of color if electrical current is applied) materials. Both properties can be incorporated by building blocks with the specific properties, in many cases organic compounds, which are incorporated in a matrix. Hybrid materials based on silicates prepared by the sol-gel process and such building blocks reveal many advantages compared with other types of materials because silica is transparent and if the building blocks are small enough, does not scatter light, and on the other hand organic materials are often more stable in an inorganic matrix. One of the most prominent passive features of hybrid materials already used in industry are decorative coatings obtained by the embedment of organic dyes in hybrid coatings. Another advantage of hybrid materials is the increased mechanical strength based on the inorganic structures. Scratch-resistant coatings for plastic glasses are based on this principle. One of the major advantages of hybrid materials is that it is possible to include more than one function into a material by simply incorporating a second component with another property into the material formulation. In the case of scratch resistant coatings, for example, additional hydrophobic or antifogging properties can be introduced. However, in many cases the precursors for hybrid materials and nanocomposites are quite expensive and therefore the preparation of bulk materials is economically not feasible. One of the advantages of hybrid materials, namely, their quite simple processing into coatings and thin films, can be one solution to this disadvantage. Applying such coatings to cheaper supports can be

advantageous. Silica is preferred as the inorganic component in such applications because of its low optical loss. Other inorganic components, for example zirconia, can incorporate high refractive index properties, or titania in its rutile phase can be applied for UV absorbers. Functional organic molecules can add third order nonlinear optical (NLO) properties and conjugated polymers, conductive polymers can add interesting electrical properties. Nanocomposite based devices for electronic and optoelectronic applications include light-emitting diodes, photodiodes, solar cells, gas sensors and field effect transistors.<sup>35</sup> While most of these devices can also be produced as fully organic polymer-based systems, the composites with inorganic moieties have important advantages such as the improvement of long term stability, the improvement of electronic properties by doping with functionalized particles and the tailoring of the band gap by changing the size of the particles. The enhancement of mechanical and thermal properties of polymers by the inclusion of inorganic moieties, especially in the form of nanocomposites, offers the possibility for these materials to substitute classical compounds based on metals or on traditional composites in the transportation industry or as fire retardant materials for construction industry. Medical materials are also one typical application area of hybrid materials, as their mechanical properties can be tailored in combination with their biocompatibility, for example nanocomposites for dental filling materials. A high content of inorganic particles in these materials provides the necessary toughness

and low shrinkage, while the organic components provide the curing properties combined with the paste-like behavior. Additional organic groups can improve the adhesion properties between the nanocomposites and the dentine. Composite electrolyte materials for applications such as solid-state lithium batteries or super capacitors are produced using organic–inorganic polymeric systems formed by the mixture of organic polymers and inorganic moieties prepared by sol–gel techniques. In these systems at least one of the network-forming species should contain components that allow an interaction with the conducting ions. This is often realized using organic polymers which allow an interaction with the ions, for example via coordinative or by electrostatic interactions. One typical example is proton conducting membranes which are important for the production of fuel cells. The application of hybrid composites is interesting for these systems because this membrane is stable at high temperatures compared with pure organic systems. These are only some applications for hybrid materials and there is a plethora of systems under development for future applications in various fields.

## **1.5 SUMMARY**

Hybrid materials represent one of the most fascinating developments in materials chemistry in recent years. The tremendous possibilities of combination of different properties in one material initiated an explosion of ideas about potential materials and applications. However, the basic science is sometimes still not understood, therefore

investigations in this field in particular to understand the structure–property relationships are crucial. This introduction has shown the importance of the interface between the inorganic and organic materials which has to be tailored to overcome serious problems in the preparation of hybrid materials. Different building blocks and approaches can be used for their preparation and these have to be adapted to bridge the differences of inorganic and organic materials. Beside the preparation of hybrid materials, their nano- and microstructure formation, processing and analysis is important.

## **RESEARCH OBJECTIVES**

Why are these POSS/polymer studies significant? Polymers have properties which make them very useful industrially and commercially. Most polymers in common use such as polyethylene and polypropylene are organic in nature and have limited thermal stability. My goal was to study and therefore be in a position to guide in the development of even more useful materials (i.e. plastics) which have properties intermediate between these traditional organic systems and inorganic ceramics - hybrid materials, in other words. POSS macromers, having the general formula  $(\text{RSiO}_{1.5})_n$ , can be incorporated into the traditional linear, thermoplastic systems either as pendants or as part of the polymer backbone to impart thermal stability, resistance to oxidation, flame and heat resistance, while avoiding the formation of intractable, crosslinked networks. While a number of these systems have been synthesized, it was important to

achieve an understanding of the structure-properties relationships in these organic-inorganic hybrid polymers, in particular, the origin of the reinforcing and enhancing effects of the POSS structure and the nature of the POSS-polymer interactions.

Even though POSS can be attached onto the backbone of the polymers, in this study we use only fully condensed POSS systems where by altering the organic functional groups appended to Si-O core where different extent of compatibility can be controlled. The focus of this study is to investigate the influence of the various organic groups on the interactions between POSS and polymer which would govern the properties of the POSS-polymer blends.

- 1) *Dispersibility of POSS Moieties. Miscibility effects on Polymer Microstructure.*
- 2) *Understanding the morphology/rheology properties of various POSS-polymer blends.*
- 3) *Nanoparticulate loading effects in polymer blends with respect their Viscoelastic properties*
- 4) *Polymer Chain length effects on the linear rheological properties of the nanoparticle/polymer blends.*
- 5) *Effect of large deformations on the dynamics of the polymer chain segments and their segmental motions.*



## **CHAPTER 2**

### **EFFECTS OF CHEMICAL SUBSTITUENTS ON PHASE BEHAVIOR OF POSS – PS BLENDS**

#### **2.1 INTRODUCTION**

Literatures regarding the synthesis, structure and properties have their origins in the late 1940's. The first oligomeric organo silsequioxanes were first synthesized by Scott in 1946<sup>41</sup> and this work in later years was done by Brown<sup>42</sup>. The research on POSS based systems has been stagnant until the early 90's when researchers like Feher<sup>43-44</sup> and Lichtenhan<sup>45</sup> focused on exploiting the advantages of this unique silica cage like frameworks containing various functionalities. A variety of POSS nanostructured chemicals have been prepared which can either be chemically inert or containing reactive chemical functionalities which can be used to grafting, polymerization, surface bonding or other transformations<sup>46-47</sup>.

The synthesis of POSS and its derivatives can be formed through various reactions which can be categorized into two main types. The first being the formation of new Si-O-Si bonds which eventually leads to the cage framework of POSS containing different organic functionalities, the second being the variation of the group on the Si through different techniques. There are two excellent reviews by Voronkov<sup>12</sup> and Feher<sup>13</sup>

which extensively talk about the various reactions available in literature for the synthesis of POSS macromers and its derivatives.

POSS macromers can be incorporated into polymeric systems through two techniques. First through producing hybrid polymers containing POSS, where POSS macromers which contain functional organic reactive sites are polymerized or copolymerized with other organic species to produce a variety of organic-inorganic hybrid homopolymers or copolymers. The second being POSS/polymer nanoscopic blends where POSS macromers are used as nano-reinforcing agents, are blended with polymers to produce inorganic/organic nano-reinforced materials.

POSS macromers can be polymerized using standard polymerization protocols like radical polymerizations, condensation polymerizations, ring opening polymerizations etc., to provide polymers with a variety of architectures. Depending on the type of functionality contained on the POSS macromers and on the desired polymer architecture, POSS macromers can be introduced into macromolecular systems as either a main chain, side chain, or as chain terminus groups<sup>39</sup>.

Several POSS homopolymers and copolymers have been synthesized and characterized, for example: POSS-Styryl based homopolymers and copolymers<sup>48-49</sup>, methacrylates-POSS polymers<sup>50</sup>, norboryl- POSS copolymers<sup>51</sup>, POSS-siloxane copolymers<sup>52</sup>, POSS-epoxy polymers<sup>53-54</sup>, POSS-polyurethane copolymers<sup>55-56</sup>. The property studies of these POSS

containing polymers showed that because the massive inorganic groups (i.e. POSS cages) are attached to polymer chains, the POSS-polymer chains act like nanoscale reinforcing fibers or like a hard block phase separated from a soft block, producing enhanced heat resistance and mechanical properties.

Currently there are relatively few literatures concerning the investigation of POSS/polymer nano-materials, where POSS macromers are incorporated into polymer by blending. Though comparatively a lot of POSS copolymer work has been published which talk about the POSS incorporation benefits but most of them have no systematic chemistry involved. Lichtenhan<sup>46</sup> was the first to work on POSS/polymers blends in the early and mid 90's where most of the work was done on PMMA and POSS blends and talks mostly with reference to thin films rather than the bulk property influence.

Later Fu, Yang, Somani, etc<sup>58</sup>. studied the aggregation behavior of isotactic polypropylene containing nanostructured POSS at quiescent and shear states. The results showed that the addition of POSS significantly increased the crystallization rate during shear. The authors postulate that POSS molecules behave as weak cross linkers in polymer melts and increase the relaxation time of iPP chains after shear. Therefore, the overall orientation of the polymer chains is improved and a faster crystallization rate is obtained with the addition of POSS. Most of the

literature published and the current progress in POSS/polymer systems are covered in a recent review articles by Pittman<sup>59</sup> and Shawn Phillips<sup>60</sup>.

Molecular dynamic simulations on POSS filled polymers have been done by Starr et al<sup>61</sup> and Glotzer et al<sup>62</sup> which talk about the influence on the polymer chains near the surface of the nanoscopic filler and hence the influence on the glass transition temperature and the agglomeration behavior of POSS respectively. Most recently a McKinley's group from MIT has published their work which talks about the influence of POSS on PMMA both when tethered and untethered onto PMMA chains<sup>63</sup>. The authors talk about that POSS acting as plasticizers at very low concentrations (<5wt %) and at higher concentrations POSS agglomerates in the matrix.

The detailed synthesis of the POSS used in this work is presented in a polymer preprint paper by Blanski et al<sup>64</sup>. The MALDI of the POSS used in this study were done by Bowers et al<sup>65</sup>. The combining of POSS macromers with polymer by blending is a new approach to achieve nanomaterials, there are still a lot of unknown domains that need to be investigated for this technique. The key issue in this field is to develop new design principles that allow to control POSS macromers at nanometer level and to achieve effective POSS-polymer interface. The recent development of POSS macromers affords an opportunity for the preparation of new polymers (thermoset, thermoplastics, and elastomers) and new polymeric blends. As part of our ongoing effort to understand,

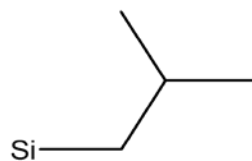
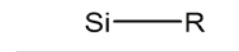
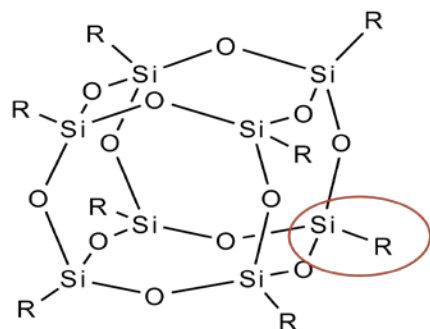
and develop these materials an investigation into the morphology and thermal properties of these POSS macromers was initiated. This study is essential to optimizing the processing of the POSS/Polymer blends, and for understanding the structure-property relationships of the blends, since any given property of a multi-component system is some (more or less complex) function of the properties of the constituents and of the interactions between them.

In the following chapter, the morphology and thermal properties of the POSS macromers were examined, using X-ray diffraction, Transmission Electron Microscopy (TEM) and Differential Scanning Calorimetry (DSC), with special emphasis given to the effects of the organic corner groups on the POSS cages. We expect that the chemistry of the corner groups affect the degree of miscibility inside the POSS Polymer blends.

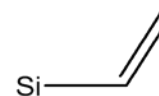
## **2.2 EXPERIMENTAL**

### **2.2.1 Materials:**

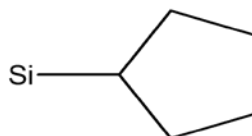
POSS Macromers used in this study are all  $T_8$  cages bearing different corner groups. These POSS macromers were obtained from Hybrid Plastics Corporation. Their chemical formulae, structures, abbreviations and molecular weight (M.W.) are shown in Table 2.2 and Figure 2.2. Monodispersed PS was obtained from Pressure Chemicals. PS2M:  $M_w=2316000$ , (polydispersity less than 1.6) and PS 290K: polystyrene with  $M_w=290K$  Daltons (polydispersity less than 1.1).



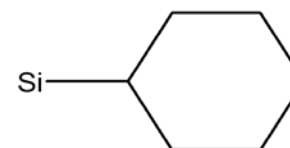
Isobutyl POSS



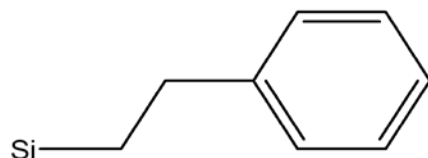
Vinyl POSS



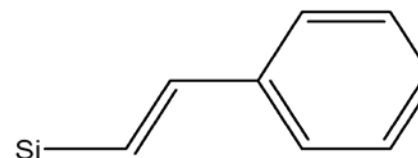
Cyclopentyl POSS



Cyclohexyl POSS



Phenethyl POSS



Styrenyl POSS

**Figure 2.1: POSS Macromers with Different Corner Groups**

<b>Full Chemical Name</b>	<b>Abbreviations for POSS</b>	<b>Chemical Formula</b>	<b>Molecular Weight</b>
Octa-Cyclopentyl-POSS	(Cp) <sub>8</sub> POSS	C <sub>40</sub> H <sub>72</sub> Si <sub>8</sub> O <sub>12</sub>	969.7
Octa-Cyclohexyl-POSS	(Cy) <sub>8</sub> POSS	C <sub>48</sub> H <sub>88</sub> Si <sub>8</sub> O <sub>12</sub>	1081.9
Octa-Styrenyl-POSS	(St) <sub>8</sub> POSS	C <sub>64</sub> H <sub>56</sub> Si <sub>8</sub> O <sub>12</sub>	1241.8
Octa-Phenethyl-POSS	(Phe) <sub>8</sub> POSS	C <sub>64</sub> H <sub>72</sub> Si <sub>8</sub> O <sub>12</sub>	1257.9
Octa-Isobutyl-POSS	(iBu) <sub>8</sub> POSS	C <sub>32</sub> H <sub>72</sub> Si <sub>8</sub> O <sub>12</sub>	873.6
Octa-Vinyl-POSS	(Vi) <sub>8</sub> POSS	C <sub>16</sub> H <sub>24</sub> Si <sub>8</sub> O <sub>12</sub>	633

**Table 2.1: Abbreviations, Chemical Formula and Molecular Weight of POSS Macromers**

### **2.2.2 Sample Preparations:**

#### **2.2.2.1 Samples Preparations for Differential Scanning Calorimeter (DSC)**

POSS powders were used directly for DSC tests. Preparation of POSS/PS blends were performed by dissolving PS and POSS macromers in chloroform and stirring the solution for 12 hours using a magnetic stirrer and crashing the sample out by using a bad solvent methanol. The precipitated sample on crashing out of the solvent is filtered and then dried under vacuum for more than 12 hours at 60°C.

#### **2.2.2.2 Samples Preparations for X-Ray Diffraction:**

POSS macromers were used as they were, POSS/PS blends were prepared by dissolving both POSS and PS in chloroform and stirred for 12 hours with a magnetic stirrer. The mixture was poured on a glass surface and covered with a slight gap to allow slow evaporation of solvent to form a thin polymer film. The as-cast film was dried in a vacuum oven for 24 hours at 60°C.

#### **2.2.2.3 Samples Preparations for Transmission Electron Microscopy (TEM):**

TEM images were obtained using a JEOL 100CX TEM using an acceleration voltage of 120 KV. PS and POSS were dissolved in THF at a concentration of 5 mg per ml of THF and stirred for more than 3 hours. The solution was then dropped onto a glass slide and let to dry in air. The film was removed from the glass slide by slowly immersing the slide into



a vessel of water at an angle of 45° to the surface. TEM grids were dropped onto the film and the test assembly was lifted out of the water using a section of paper. The samples were dried on filter paper and subsequently carbon coated to increase their beam stability.

### **2.2.3 Characterization Techniques:**

#### **2.2.3.1 Transmission Electron Microscopy (TEM)**

TEM was utilized to characterize the morphologies of the POSS/PS blends.

#### **2.2.3.2 X-ray Diffraction:**

X-ray diffraction was employed to identify the morphological changes of POSS macromers after they were blended with PS. X-ray diffraction measurements were performed using a Scintag 2000 XRD with Cu-K $\alpha$  target ( $\lambda=1.5406\text{\AA}$ ) radiation generated at 45 kV and 200 mA. The diffraction angle was ranged from 5° to 30°, with step size and scan rate of 0.05° and 2° per minute, respectively.

The X-ray diffraction pattern obtained from a diffractometer records the X-ray intensity as a function of diffraction angle. The inter-atomic spacing is determined by Bragg's law:

$$d = n \lambda / (2\sin\theta)$$

Where d is the inter-atomic spacing;  $\lambda$  is the wavelength of the x-ray ( $\lambda=1.5406\text{\AA}$  for Cu target);  $\theta$  is the diffraction angle.

### **2.2.3.3 Determination of Transition Temperatures of POSS macromers:**

Transition temperatures were determined using a Mettler-Toledo 821e/400 Differential Scanning Calorimeter (DSC) under a flow of nitrogen and with a heating rate of 10°C per minute. The transition temperature is taken as the inflection point of the transition region.

## **2.3 RESULTS AND DISCUSSION**

### **2.3.1 Effects of POSS Corner Groups:**

Differential Scanning Calorimetry (DSC) was used to test the transition temperatures of POSS macromers with different corner groups. The DSC results are showed in Figures 2.2 to 2.5, and the transition temperature data are listed in Table 2.2. Some of these transitions shown in the DSC figures are the fusions of POSS crystalline structures, and some of them are the destruction of POSS weak associations. The heats of these fusions or disassociations of POSS macromers are very weak (between 2~40J/g).

We can see that the Cp<sub>8</sub>POSS (Figures 2.2), Styrenyl<sub>8</sub>POSS (Figure 2.4), have two transition peaks: 12.5°C (disassociation) and 29.9°C (disassociation) for Cp<sub>8</sub>POSS; 189.1°C (disassociation) and 274.3°C (melting) for St<sub>8</sub>POSS; and 49.6°C (disassociation) and 272.1°C (melting) for Isobu<sub>8</sub>POSS. The disassociation temperature of the Cy<sub>8</sub>POSS is around 23.7°C. Ph<sub>8</sub>POSS, have a melting temperature at 76.5°C.

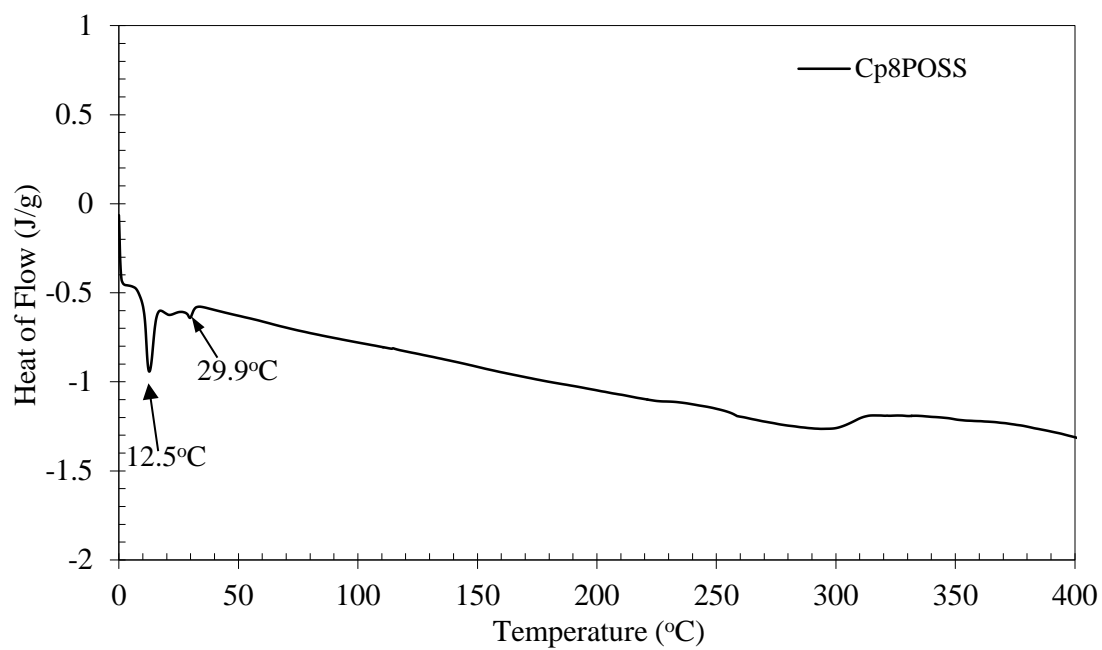


**Figure 2.2: DSC Curve of Cp<sub>8</sub>POSS Macromer**

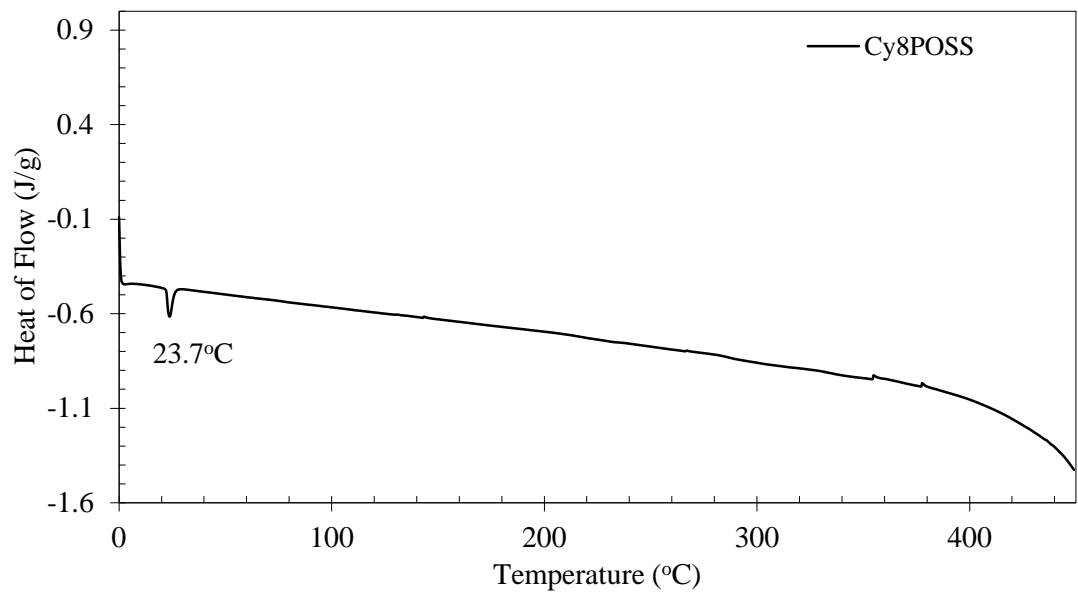


**Figure 2.3: DSC Curve of Cy<sub>8</sub>POSS Macromer**

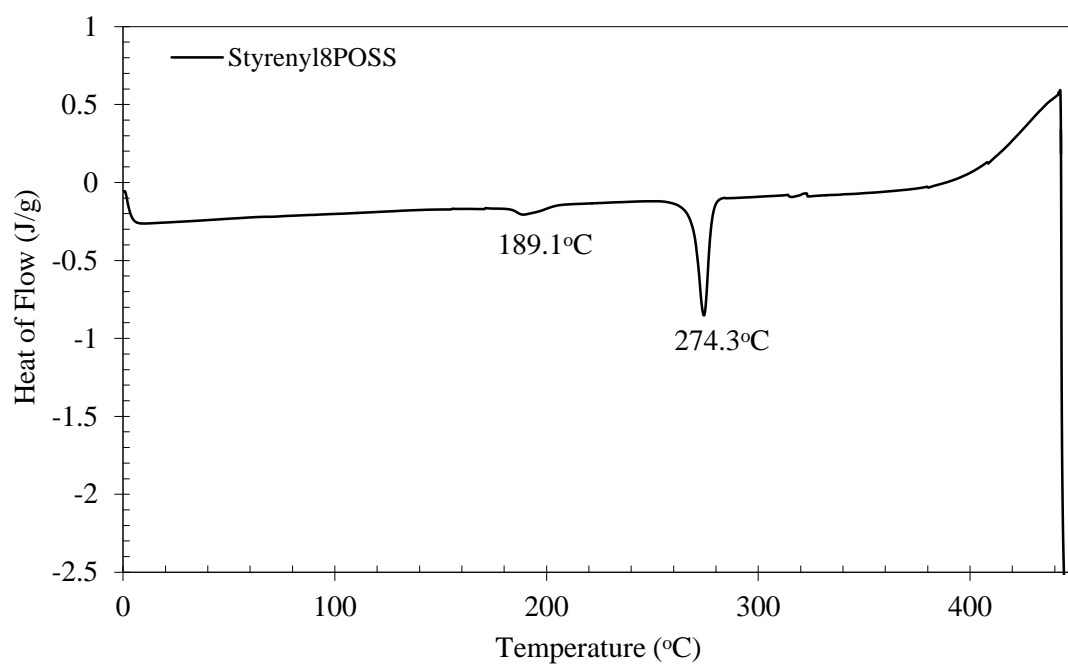


**Figure 2.4: DSC Curve of Styrenyl<sub>8</sub>POSS Macromer**

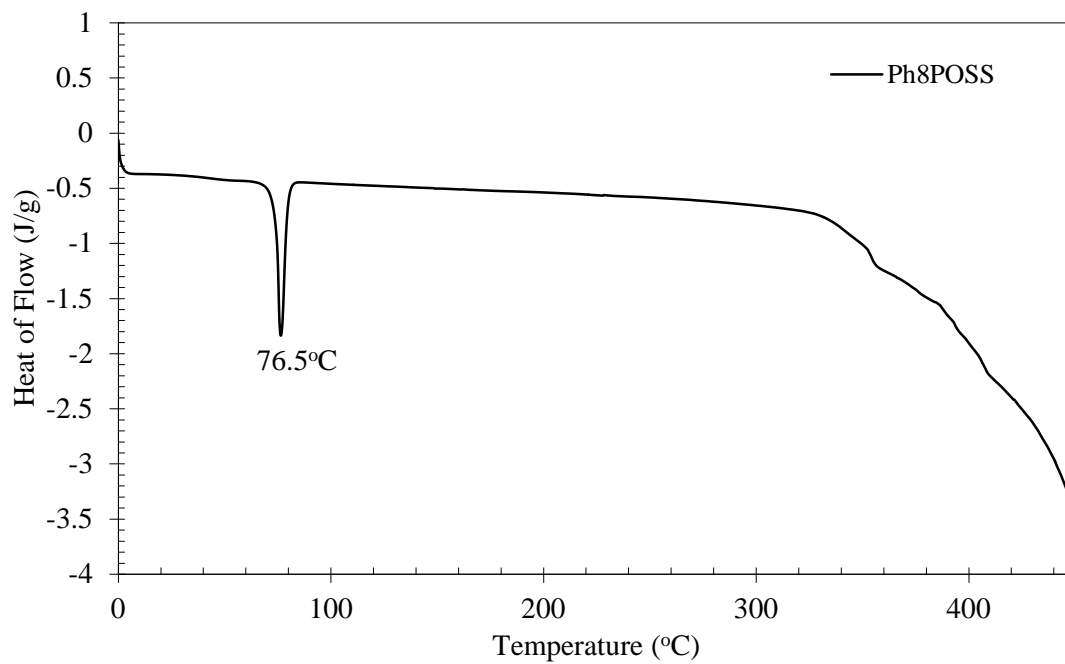


**Figure 2.5: DSC Curve of Phe<sub>8</sub>POSS Macromer**

POSS Macromers	Transition Temperature (°C)		Heat of Dissociation (J/g)	
	1	2	1	2
Cp <sub>8</sub> POSS	12.5	29.9	4.4	6.2
Cy <sub>8</sub> POSS	23.7	~	2.5	~
Styrenyl <sub>8</sub> POSS	189.1	274.3	4.5	29.6
Ph <sub>8</sub> POSS	76.5	~	37.8	~

**Table 2.2: Transition temperatures of POSS macromers (DSC Results)**

The melting transition of St<sub>8</sub>POSS is observed in the DSC experiments having higher heat of fusion, relatively Cp<sub>8</sub>POSS, Cy<sub>8</sub>POSS and Ph<sub>8</sub>T<sub>8</sub>macromers are observed to have very low heat of fusion in their DSC curves, and we assume that it is because of the weak interactions between the POSS macromers. The small disassociation peaks found in Cp<sub>8</sub>POSS, Cy<sub>8</sub>POSS and Styrenyl<sub>8</sub>POSS macromers are also indicative of destruction of weak aggregations in these POSS macromers.

### **2.3.2 Miscibility in Polystyrene Based on Different POSS:**

The morphology of the PS/POSS blends was observed by using a Transmission Electron Microscope. These experiments were done to study the effects of different chemical moieties of POSS used under similar POSS loadings on the morphological structures of the PS/POSS blends. From previous studies done in our group by haipeng different phase characteristics have been observed in these blends. A higher molecular

weight PS was used, 1.6M Da to facilitate better mechanical properties to the film especially since very dilute solutions were employed to cast the sample films.

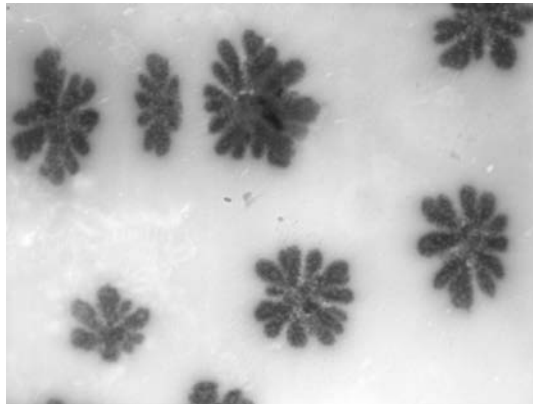
Figure 2.6 depict the TEM photographs of PS2M (Molecular weight 2M Daltons) blended with Cp<sub>8</sub>POSS, St<sub>8</sub>POSS, Phe<sub>8</sub>POSS, Cy<sub>8</sub>POSS. A high POSS loading (50wt %) is used in this study to facilitate better contrast between the dispersed and the continuous phases; if at all phase separation is observed.

As shown in Figure 2.6, the Cp<sub>8</sub>POSS/PS2M blend has two phases with PS as the continuous phase and snowflake like Cp<sub>8</sub>POSS macromers as the disperse phase. The dimensions of the Cp<sub>8</sub>POSS aggregates are in order of a micron. The substitution of all the cyclopentyl groups in the Cp<sub>8</sub>POSS macromer with styrenyl groups (Styrenyl<sub>8</sub>POSS) renders a two phase system in the Styrenyl<sub>8</sub>POSS/PS2M blend: PS rich phase (white round particles) becomes the disperse phase, and the continuous phase is the POSS rich Phase, is a mixture of Styrenyl<sub>8</sub>POSS and PS. The replacement of all the cyclopentyl groups in Cp<sub>8</sub>POSS macromer with phenethyl groups dramatically improves the compatibility between Ph<sub>8</sub>POSS and PS. The Ph<sub>8</sub>POSS macromer is homogeneously dispersed in the PS matrix. There is no phase separation in the Ph<sub>8</sub>POSS/PS2M blend. A phase separation is also observed in Cy<sub>8</sub>POSS/PS2M, with POSS being the disperse phase, PS as the continuous phase.

# POSS-Molecular Silica Blends

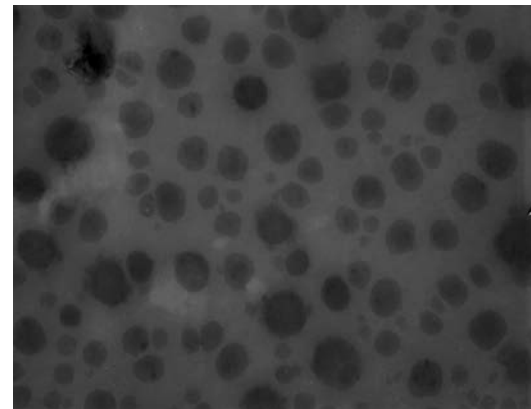
Blended into 1.6M Da MW Polystyrene

R = cyclopentyl



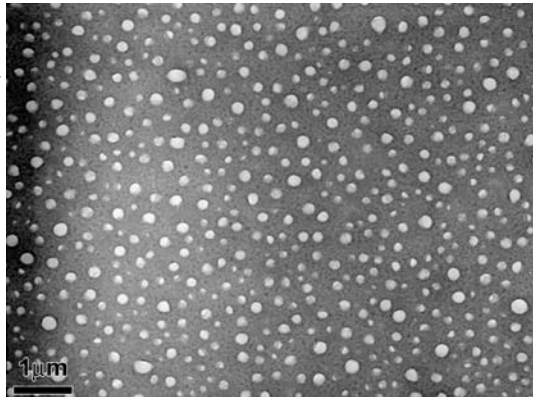
domain formation

R = Cyclohexyl



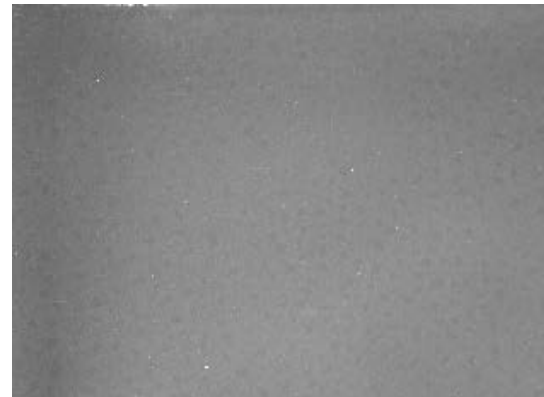
partial compatibility

R = styrenyl



phase inversion

R = penethyl



transparent

Figure 2.6: TEM Image of POSS PS blends at 50 wt% loadings

From the morphology studies it clearly suggests that the organic pendent group on the POSS macromers play a crucial role in determining the dispersibility of the nanoparticulates, self similar systems similar to the polymer matrix tend to show better dispersibility than other systems.

For better understanding of the blend characteristics we have considered the two cases of Ph<sub>8</sub>T<sub>8</sub>POSS/PS and the St<sub>8</sub>T<sub>8</sub>POSS/PS blends due to the similarity of the organic pendent group with the polymer matrix and also based on the TEM images showed the better miscibility among the blend systems. Even though in the case of St<sub>8</sub>T<sub>8</sub>POSS/PS2M blends phase separation takes place into a two phase system where both POSS and PS seem to exist in both the continuous and the dispersed phases lack of well defined crystallite domains like in the case of Cp<sub>8</sub>T<sub>8</sub> and Cy<sub>8</sub>T<sub>8</sub> suggests that something different was driving the phase behavior of these blends.

TEM images showing phase separation in the case of St<sub>8</sub>T<sub>8</sub>POSS/PS1.6M blends suggests either the high molecular weight of PS used and higher loadings of POSS used might have shifted the Phase diagram to show a two phase system or the higher molecular weight might have hindered the crystallization process of the POSS macromers. To further elucidate on this issue lower molecular weight polystyrene system has been used with lower POSS loadings since concentration is a driving force for phase behavior, to study the miscibility of St<sub>8</sub>T<sub>8</sub> POSS in PS. To further examine the microstructures of POSS macromers, TEM, DSC and



X-Ray diffraction analysis was performed. The study below is mainly focused on the impacts of styrenyl and phenethyl on the morphology of the POSS/PS blend systems.

The effects of the PS on the crystalline structures of POSS were studied by comparing the X-ray diffraction patterns of the POSS macromers in the POSS/PS blends with those of the neat POSS macromers. The X-ray diffraction pattern obtained from a diffractometer records the X-ray intensity as a function of the diffraction angle  $2\theta$ , and it gives the information about the orderly packing of the molecules in crystals. Figure 2.7 shows the X-ray diffraction curves of  $\text{Ph}_8\text{T}_8\text{POSS}$  macromers with and without PS; Figure 2.8 shows the X-ray diffraction curves of  $\text{St}_8\text{T}_8\text{POSS}$  macromers with and without PS. Table 2.5 has their corresponding diffraction data (peak positions, inter-atomic spacing, and the  $2\theta$  width of the diffraction peaks). Only some weak and broad peaks are found in  $\text{Ph}_8\text{POSS}$  macromer, and Styrenyl $_8\text{POSS}$  macromer has only one weak peak in its diffraction pattern.

From Figures 2.8 and 2.9, it could be seen that the crystalline POSS peak in the case of PS blends containing 20 wt% of POSS disappear for  $\text{Phe}_8\text{T}_8$  and  $\text{St}_8\text{T}_8$  respectively compared to the pure POSS macromers results, suggesting the absence of crystallite domains and indicating good compatibility between the POSS macromers and PS. The disappearance of the crystalline POSS peak suggests that the POSS macromers are completely dispersed in the PS matrix.

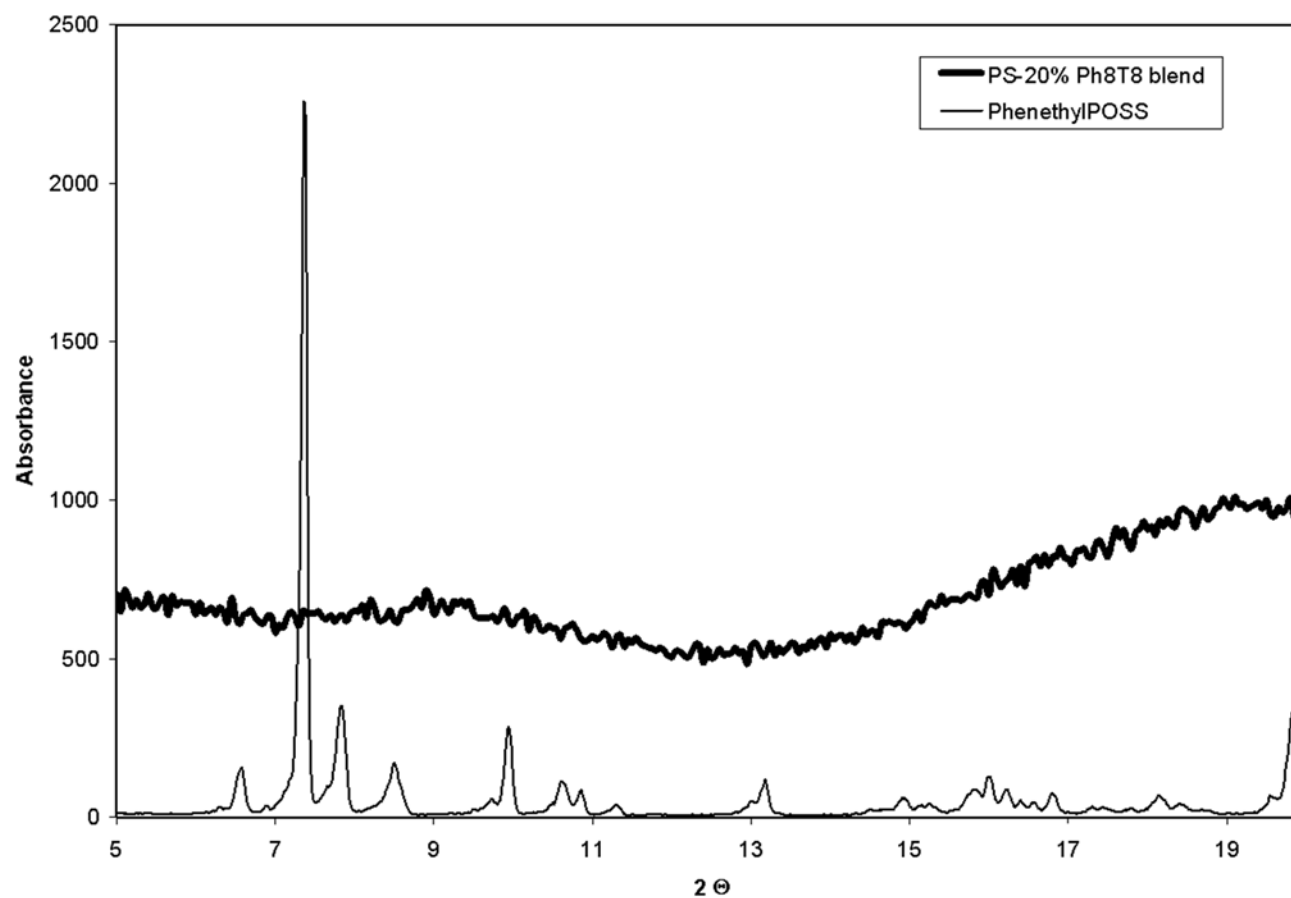


**Figure 2.7: X-Ray plot of Phenethyl POSS (Ph<sub>8</sub>T<sub>8</sub>) and PS (M<sub>w</sub>= 290K Da) / Phenethyl POSS 20%wt blend**

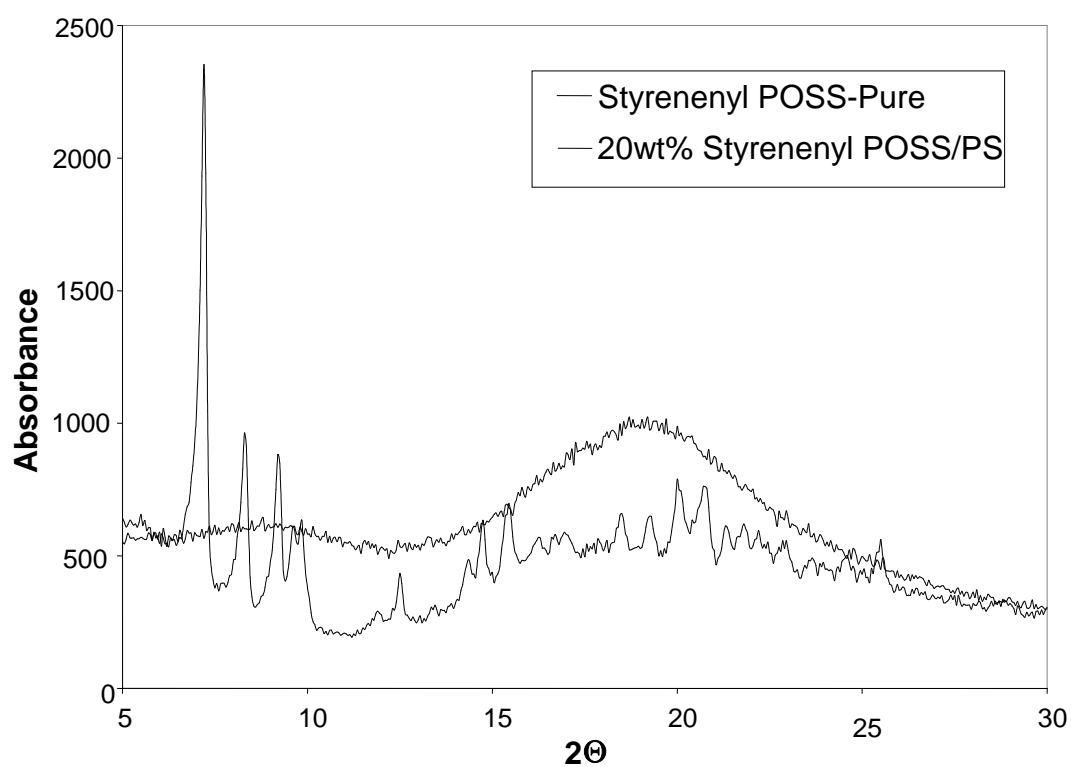


**Figure 2.8 X-Ray plot of Styrenyl POSS ( $\text{St}_8\text{T}_8$ ) and PS ( $M_w = 290\text{K Da}$ ) /Styrenyl POSS 20%wt blend**

The X Ray diffraction of the polymer blend systems suggest miscibility contrary what we have observed in the TEM images showing phase separation in the case of St<sub>8</sub>POSS/PS blends, this suggests the high molecular weight of PS used and higher loadings of POSS used might have shifted the Phase diagram to show a two phase system and also the polymer chains might have hindered the crystallization process of the POSS macromers, to further verify the above observations DSC experiments have been performed along with TEM to get further insight on the phase characteristics of these blends. Figure 2.10 shows the TEM images of St<sub>8</sub>POSS macromers with 290K PS, Figure 2.10 suggests the existence of two phase system behavior with both the polymer rich phase and the POSS rich phase. The results reflect the degree of compatibility between the POSS macromers and PS.

Figures 2.10 and 2.11 depicted DSC curves of Ph<sub>8</sub>T<sub>8</sub> POSS, its blend with PS, St<sub>8</sub>T<sub>8</sub> POSS and its blend with PS, respectively. As observed from these DSC curves, the value of heat of fusion for Ph<sub>8</sub>T<sub>8</sub> and St<sub>8</sub>T<sub>8</sub> POSS is nearly identical (~ 37.7 kJ/mole). In addition, for the case of 30wt% POSS/PS blends, we did not observe any crystalline melting peaks associated with the pure POSS macromers, which suggests that POSS-PS blends form a single phase mixture.

The melting transition temperature from the DSC measurement can be used to estimate the strength of associations within the POSS crystallites. As determined from the DSC, the onset of melting transition

peak for St<sub>8</sub>T<sub>8</sub> is around 274°C and Ph<sub>8</sub>T<sub>8</sub> was at 77°C. The higher transition temperature indicates a stronger POSS-POSS association in St<sub>8</sub>T<sub>8</sub> as compared to Ph<sub>8</sub>T<sub>8</sub>.

DSC results were also used to examine the effect of POSS addition on the T<sub>g</sub> of blends. For the case of PS blended with Ph<sub>8</sub>T<sub>8</sub> POSS, the value of T<sub>g</sub> decreases on the addition of POSS macromers from 106.07C for the pure PS to around 91.88C with POSS, in the case of Styrenyl POSS blend the T<sub>g</sub> decreases to 103.66. We believe the suppression of T<sub>g</sub> in the case of Ph<sub>8</sub>T<sub>8</sub> blends was caused by the well-dispersed POSS clusters in PS and the excellent mutual solubility between Ph<sub>8</sub>T<sub>8</sub> and PS thereby causing a swelling in the polymer network, similar to that of solvent plasticization effect, which was further evaluated by rheological measurements in the next chapter.

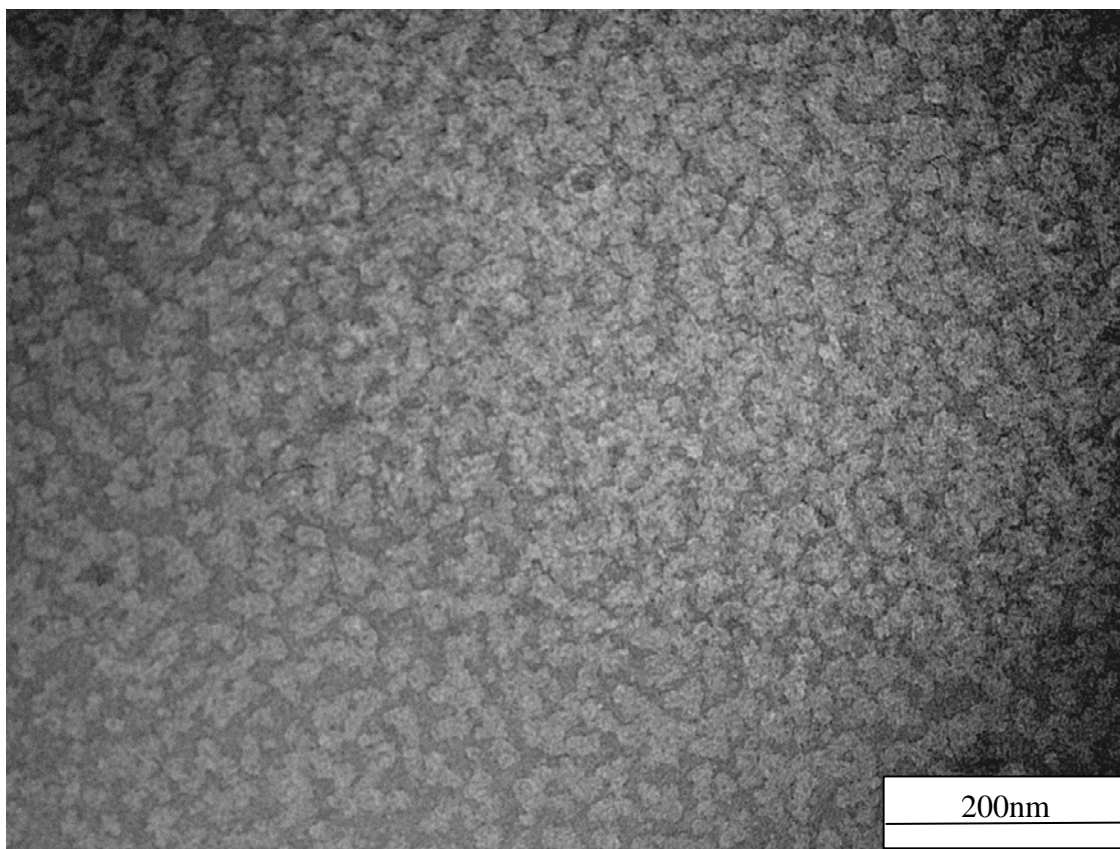


**Figure 2.9: TEM Image of Styrenyl<sub>8</sub>POSS/PS290K Blend (20 wt% POSS)**

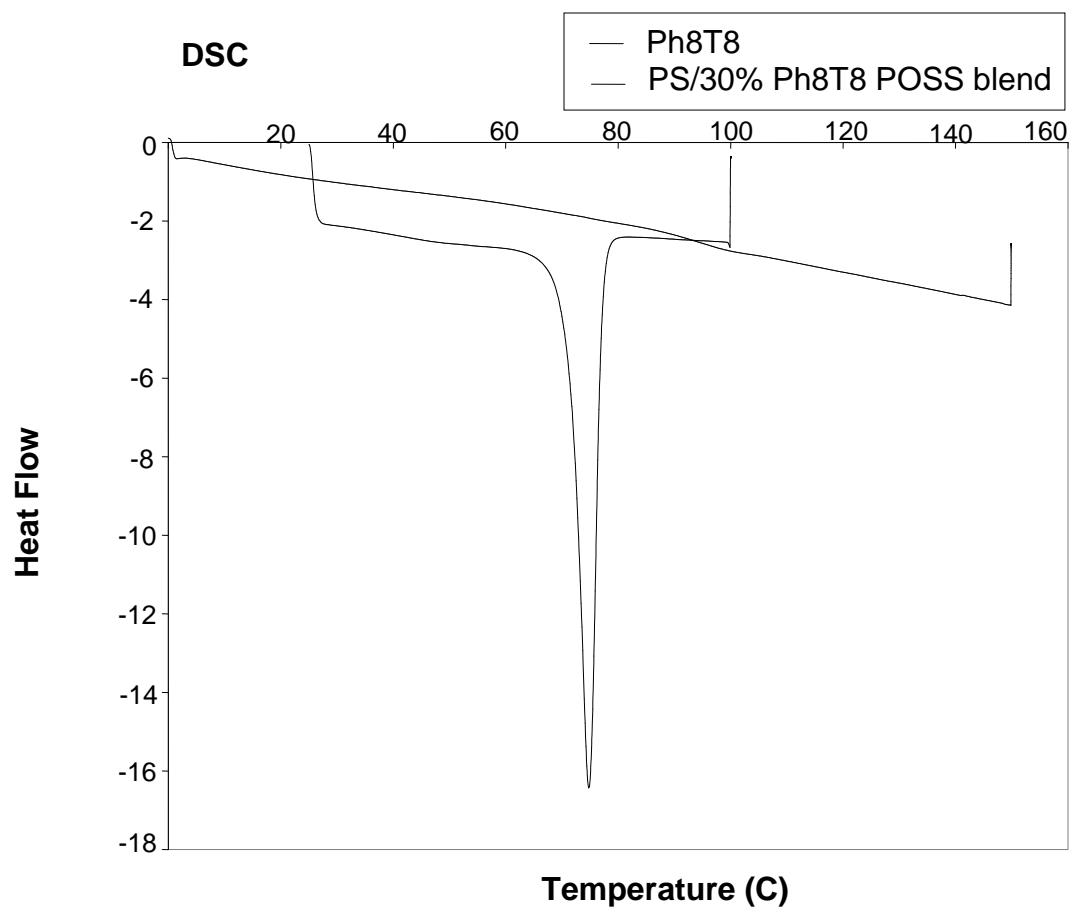


**Figure 2.10: DSC plot of Phenethyl POSS (Ph<sub>8</sub>T<sub>8</sub>) and PS (M<sub>w</sub>= 290K Da) / Phenethyl POSS 30%wt blend**

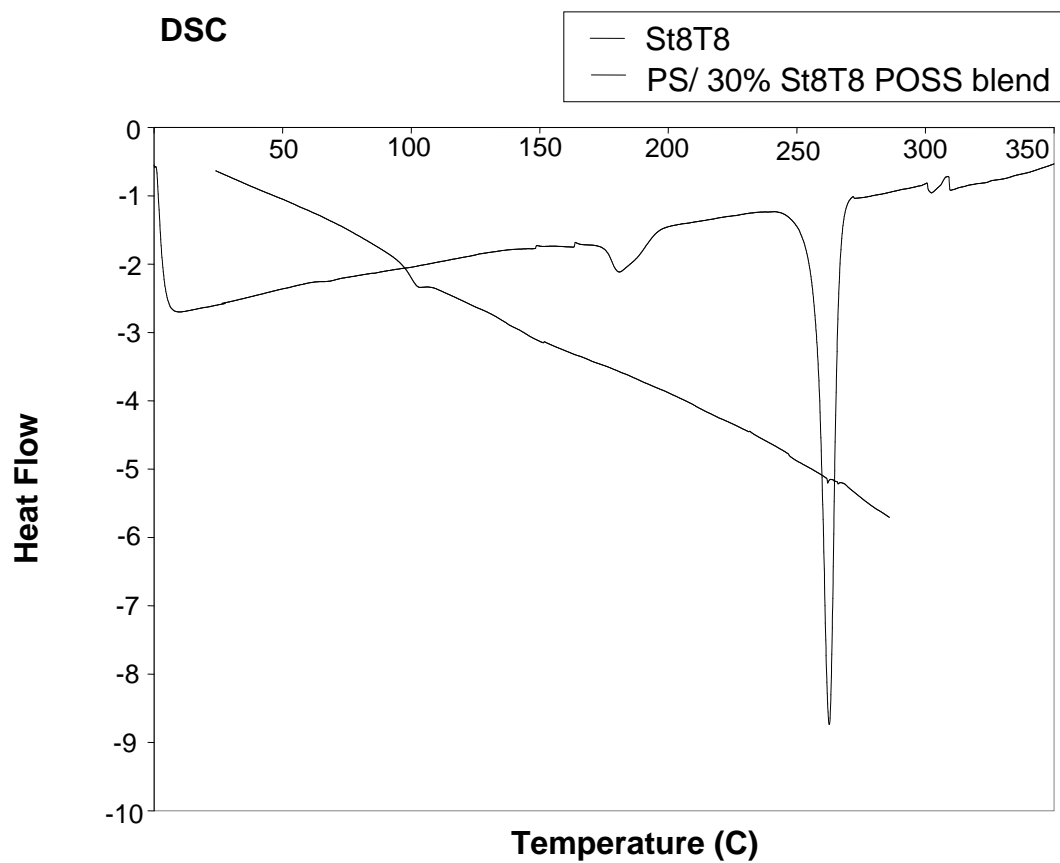


**Figure 2.11: DSC plot of Styrenyl POSS (St<sub>8</sub>T<sub>8</sub>) and PS (M<sub>w</sub>= 290K Da) /Styrenyl POSS 30%wt blend**



As for St<sub>8</sub>T<sub>8</sub>/PS blends, although POSS may be well dispersed, but there was a lack of interaction between POSS and PS due to the two phase system obtained from the TEM Images. The reason for us to believe it being dispersed is from the lack of any melting peaks as seen from the DSC thermogram. The lack of thermal transitions indicates the domains present if present are too small for the DSC to differentiate through a change in heat flow signal. The presence of two phases as indicated by TEM images may have occurred because of a shift in the phase diagram due to the solvent evaporation technique employed in preparing the samples. The evaporating solvent may have driven the POSS blend to form a two phase system. To further investigate various blends with different POSS loadings have been used and their corresponding rheological characterization done to evaluate the phase characteristics in the next chapter.

## **2.4 SUMMARY**

The chemistry of POSS macromers plays an important role in determining the morphologies of the POSS/PS blends. Depending on the attached chemical groups on the POSS macromer, the morphologies of POSS/PS blends ranged from a complete phase separation between POSS and PS to a homogeneous dispersion of POSS in the PS matrix in a nanoscopic scale. Among the five POSS macromers used, Ph<sub>8</sub>POSS is the most compatible one with PS and can be homogeneously dispersed in PS

matrix. All other POSS/PS blends display a certain amount of phase separation to a various degrees.

The morphology of a blend depends on the compatibility between the two components, the type of molecular interaction and the resultant interface of the components and the processing history. For POSS/Polymer blends, the following factors influence the compatibility between the two components, and hence the morphologies of the blends. The chemistry of POSS, the chemical structures of the corner groups on the POSS cage greatly influence the compatibility between POSS and polymers. The above studies showed that the compatibilities between POSS and PS varied with different POSS chemical structures. Notably, among the five POSS macromers studied, the  $\text{Ph}_8\text{POSS}$  macromer is the most compatible one with PS and, hence, it is the one which can be homogenously dispersed in the PS matrix. The degree of the crystallinity of POSS macromers also affects the morphologies of the POSS/PS blends. The potential for achieving miscible blends in which one or both components are crystalline is low because of the heat of fusion which would have to be overcome to achieve the necessary thermodynamic criteria for mixing. High crystallinity POSS does not favor the formation of homogeneous dispersion of the POSS. POSS macromers with a strong tendency to crystallize are inclined to aggregate and phase separate from the polymer host.

The chemistry of the corner groups on the POSS cage affects the morphological structures of the POSS macromers. The higher the symmetry and regularity of the POSS macromers, and the smaller the size of the corner groups, the more ordered the POSS macromers.

# **CHAPTER 3**

## **EFFECTS OF CONCENTRATION ON PHASE BEHAVIOR OF POSS – PS BLENDS**

### **3.1 INTRODUCTION**

The effect of concentration on the viscometric properties of the nanocomposite blends has been investigated. Rheological measurements well above  $T_g$  have been used to determine the time-temperature superposition behavior of these thermorheologically simple materials. The size of POSS macromers on similar length scales when compared to the entanglement spacing of the polymer chains makes it interesting to study the role these nano-structured constituents would play in controlling the polymer chain dynamics. However as we have seen Chapter 2 various organic groups on the POSS macromers led to the complex morphologies of various POSS/PS blends, some miscible some showing two phase behavior with both phases containing both the components and some showing complete segregation as filler systems. The rheological response of the filler systems has been widely studied and the effect a filler has on the viscoelastic properties widely understood, the part which is still sketchy is the understanding of the presence of miscible or partly miscible nanoparticulates in the polymer matrix, and the part to be yet answered is do these changes in microstructure cause profound changes to the relaxation of the polymer backbones. To address the above issue we took

two POSS macromers having the organic pendant group as the same or nearly similar as the monomer unit as the polymer. Rheological characterization was done for understanding the chain dynamics due to the presence of POSS or due to the domains formed due to the presence of POSS.

## **3.2 EXPERIMENTAL DETAILS**

### **3.2.1 Materials**

Nearly monodisperse molecular weight distribution of polystyrene with  $M_w = 290K$  Daltons (polydispersity less than 1.1) were purchased from Pressure Chemicals. Two fully condensed POSS, Styrenyl<sub>8</sub>-POSS (St<sub>8</sub>T<sub>8</sub>, **1**) and Phenethyl<sub>8</sub>-POSS (Ph<sub>8</sub>T<sub>8</sub>, **2**) and were used in this study.

### **Synthesis of POSS macromers used in the study<sup>64</sup>**

Degassed toluene (Fisher) was purified by elution through an alumina column. Grubbs Catalyst  $Cl_2Ru(=CHPh)(PCy_3)_2$  (Strem) was used as received. Styrene (Aldrich) was purified by distillation under diminished pressure onto ~10 ppm of catechol. Hydrogen (Scott Specialty Gases) and 10% Palladium on Carbon (Aldrich) were used as received. NMR Spectra were taken on a Bruker Avance 300 spectrometer

**Synthesis of Styrenyl<sub>8</sub>T<sub>8</sub> (1):** A 500 mL round bottom flask was charged with 15 grams (26.7 mmol, 189.5 mmol vinyl) of Vinyl<sub>8</sub>T<sub>8</sub>, 35mL (305 mmol) of Styrene, 50 mL of toluene and a stir bar under nitrogen. 200 mg (0.24 mmol) of the  $Cl_2Ru(=CHPh)(PCy_3)_2$  (dissolved in 10 mL of toluene) was added to the reaction via syringe. A slight vacuum was applied to the

flask to assist in the volatilization of ethylene that was generated in the process and the mixture was allowed to stir overnight. The volatiles were removed under vacuum and redissolved in toluene. To this mixture was added 30 grams of montmorillonite clay and the mixture stirred for 45 minutes. The reaction was filtered through Celite and the colorless filtrate is evaporated to give a colorless solid. This solid is heated under vacuum at 150 °C for two hours and then 100 °C overnight to remove any stilbene formed. 27 grams of **1** is obtained as a free flowing solid (92% yield).

**Synthesis of Phenethyl<sub>8</sub>T<sub>8</sub> (2):** A 300 mL Parr reactor was charged with 20 grams of Styrenyl<sub>8</sub>T<sub>8</sub>, 50 mg of 10% palladium on carbon, and 30 mL of toluene. The reactor was pressurized to 500 psi of hydrogen and allowed to stir overnight at 50 °C. The reaction was cooled to ambient temperature and the solution filtered through Celite. The volatiles were removed and the remaining liquid was heated to 150 °C under vacuum for two hours. 19.5 grams of a colorless solid was obtained (97% yield.) <sup>1</sup>H NMR (300.1 MHz, CDCl<sub>3</sub>) δ 7.381 (m, 5H, C<sub>6</sub>H<sub>5</sub>), δ 2.904 (m, 2H, CH<sub>2</sub>Ph), δ 1.152 (m, 2H, Si-CH<sub>2</sub>). <sup>13</sup>C NMR (75.5 MHz, CDCl<sub>3</sub>) δ 143.97, 128.32, 127.84, 125.74, 28.93, 13.73. <sup>29</sup>Si NMR (59.6 MHz, CDCl<sub>3</sub>) δ -67.2.

### **3.2.2 Sample Preparation**

#### **3.2.2.1 Melt Rheological Characterization**

Preparations of POSS/PS blends were performed by dissolving PS and POSS macromers in chloroform and stirring the solution for 12 hours using a magnetic stirrer and crashing the sample out by using a bad solvent methanol. The precipitated sample on crashing out of the solvent is filtered and then dried under vacuum for more than 12 hours at 60°C.

Rheological measurements were carried out using a Rheometric Scientific ARES rheometer equipped with a force convection oven in the parallel plate geometry. Parallel plate geometry with diameter of 8 mm and gap of 0.5 mm was used for all measurements obtained in this study. Rheological behavior of all samples was investigated using a series of isothermal, small-strain oscillatory shear with oscillatory frequency ranging from 100 to 0.1 radian/second and oscillatory shear strain amplitude of 5%. To examine the validity of the time-temperature superposition principle and the effect of POSS addition on the values of time-temperature shift factor, sample was tested at temperatures ranging from  $T_g+10^{\circ}\text{C}$  to  $T_g+100^{\circ}\text{C}$  with  $10^{\circ}\text{C}$  intervals. Values of storage modulus,  $G'(\omega)$ , loss modulus,  $G''(\omega)$ , and damping factor,  $\tan\delta(\omega) = G''(\omega)/G'(\omega)$ , were determined using software provided by Rheometric Scientific. Samples tested under the same experimental conditions were repeated two to three times to confirm their reproducibility. Master curves for  $G'$ ,  $G''$  and  $\tan\delta$  were also obtained

with software package provided by Rheometric Scientific and a reference temperature of  $T_{ref}=150^{\circ}\text{C}$  for pure polymers and blends was used.

### 3.3 RESULTS AND DISCUSSION

#### 3.3.1 Rheology during the Rubbery State and Flow Transition

The effect of POSS loading and distribution of POSS macromers in PS is understood through the thermal and morphological studies. Rheology experiments were performed to address the effect of POSS macromers on the chain dynamics of PS. Since rheological measurements and their correlation to polymer chain dynamics using narrow molecular weight PS properties were well documented, our measurements of POSS/PS blends will provide insight into how the POSS macromers affect the polymer chain dynamics.

The melt rheological experiments were carried out using small-strain amplitude oscillatory shear so to minimize deformation on sample morphology. The dynamic properties of the POSS/PS blends were investigated as a function of frequency at different temperatures. Changes in  $G_C(\omega)$ ,  $\omega_C$ ,  $G_N^0$  and  $\lim_{\omega \rightarrow 0} \eta^*(\omega)$  were compared for all studied systems. In addition, the validity of time-temperature superposition was also verified for all the samples used in this study.

#### **Ph<sub>8</sub>T<sub>8</sub> POSS / PS blends:**

Figure 3.1(a) is the time-temperature master curves shifted to  $150^{\circ}\text{C}$  for the PS (Molecular weight 290K Daltons) blended with varying amounts of Ph<sub>8</sub>T<sub>8</sub> POSS. The corresponding plot of reduced complex



viscosity versus reduced frequency is shown in Figure 3.1(b). The temperature shift factor versus temperature is plotted in Figure 3.1(c). From the various reduced storage modulus curves shown in Figure 3.1(a), we observed that these curves shift downwards and towards the right with increasing amount of Ph<sub>8</sub>T<sub>8</sub> POSS blended. In addition, the values of the plateau modulus,  $G_N^0$ , and the cross-over frequency,  $\omega_C$ , as shown in Table 3.1, decrease with increasing amount of Ph<sub>8</sub>T<sub>8</sub> POSS added. These observations correspond to PS chains becoming less entangled when blended with Ph<sub>8</sub>T<sub>8</sub> POSS, which suggests that the Ph<sub>8</sub>T<sub>8</sub> POSS molecules are completely dissolved into PS and form a homogeneous solution. The concept of Ph<sub>8</sub>T<sub>8</sub> POSS as a good solvent for polystyrene is verified by plotting the normalized plateau modulus,  $G_N^0(c) / G_N^0(1)$ , versus the concentration of solution as depicted in Figure 3.3. For a good solvent, we expect a power law dependence whose concentration dependant exponent is approximately 2.3 irrespective of the type of solvent in which the polymer chains are present<sup>66</sup>. As shown in Figure 3.3, the concentration dependant exponent is slightly less than 2.3, thus confirming that the observed viscosity reduction in Ph<sub>8</sub>T<sub>8</sub> POSS/PS blends is due to the solvent effect.

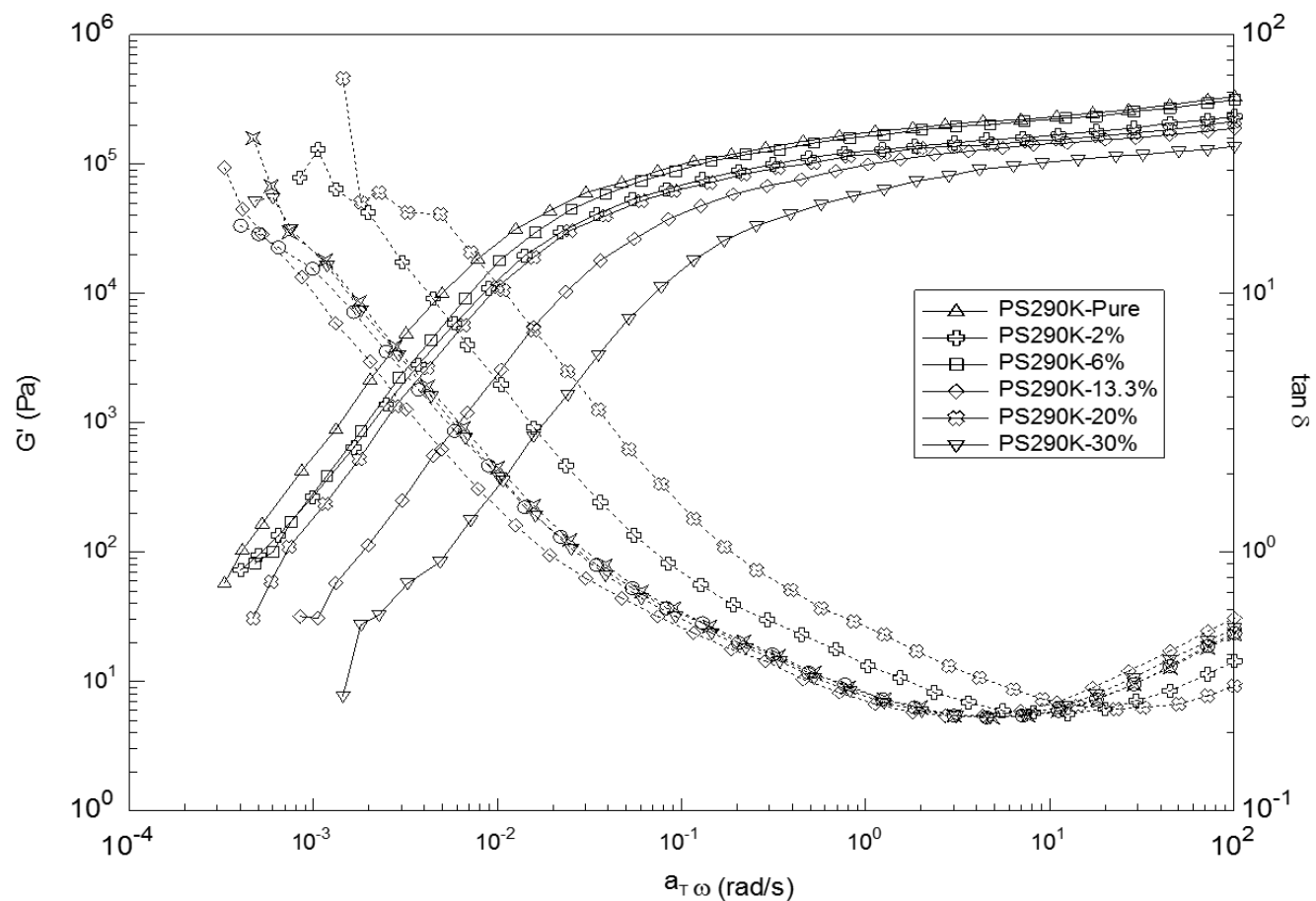


Figure 3.1(a)

**Figure 3.1** Time temperature superposed plots of PS ( $M_w = 290\text{K Da}$ ) and Phenethyl POSS ( $\text{Ph}_8\text{T}_8$ ) blends with varying weight fractions of POSS at  $150^\circ\text{C}$  a) Storage Modulus ( $G'$ ) versus Reduced frequency ( $a_T\omega$ ) b) Reduced viscosity ( $\eta^*/a_T$ ) versus Reduced frequency ( $a_T\omega$ ) c) Shift factors ( $a_T$ ) versus Temperature (Temp)

Figure 3.1 (cont'd)

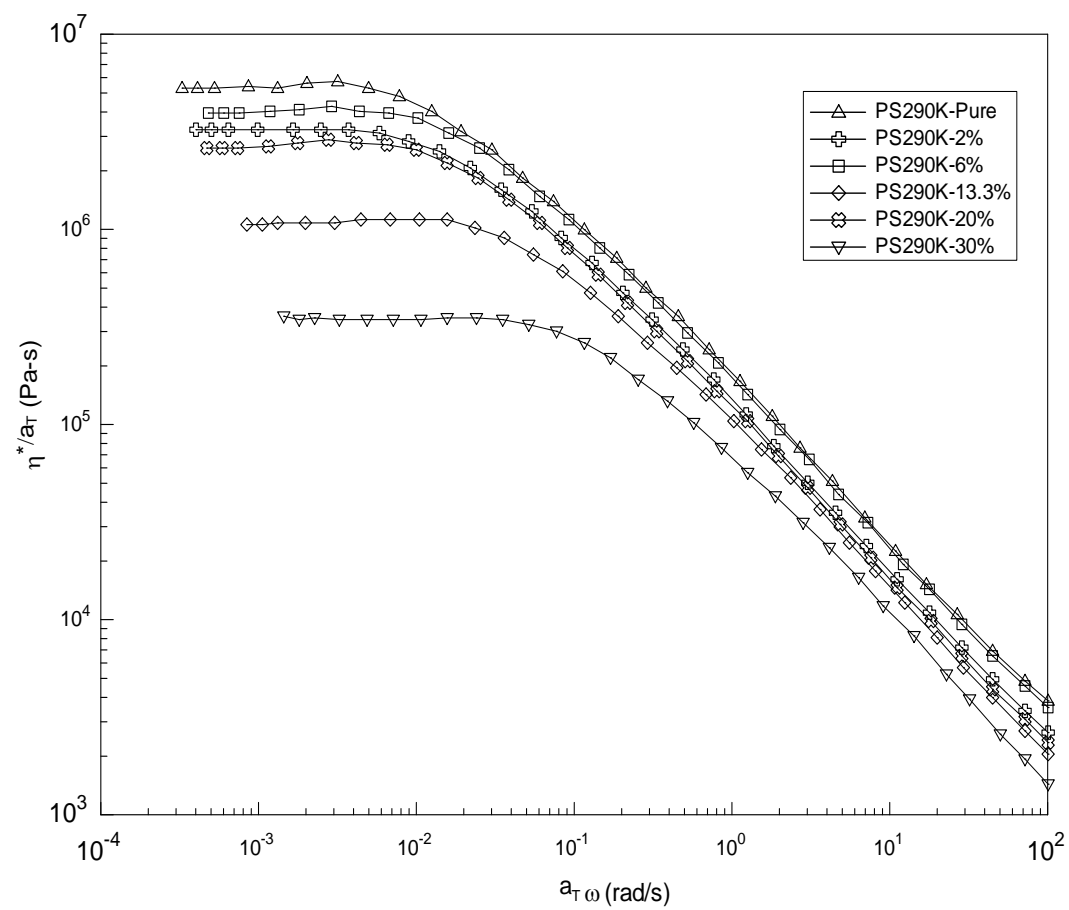


Figure 3.1(b)

Figure 3.1 (cont'd)

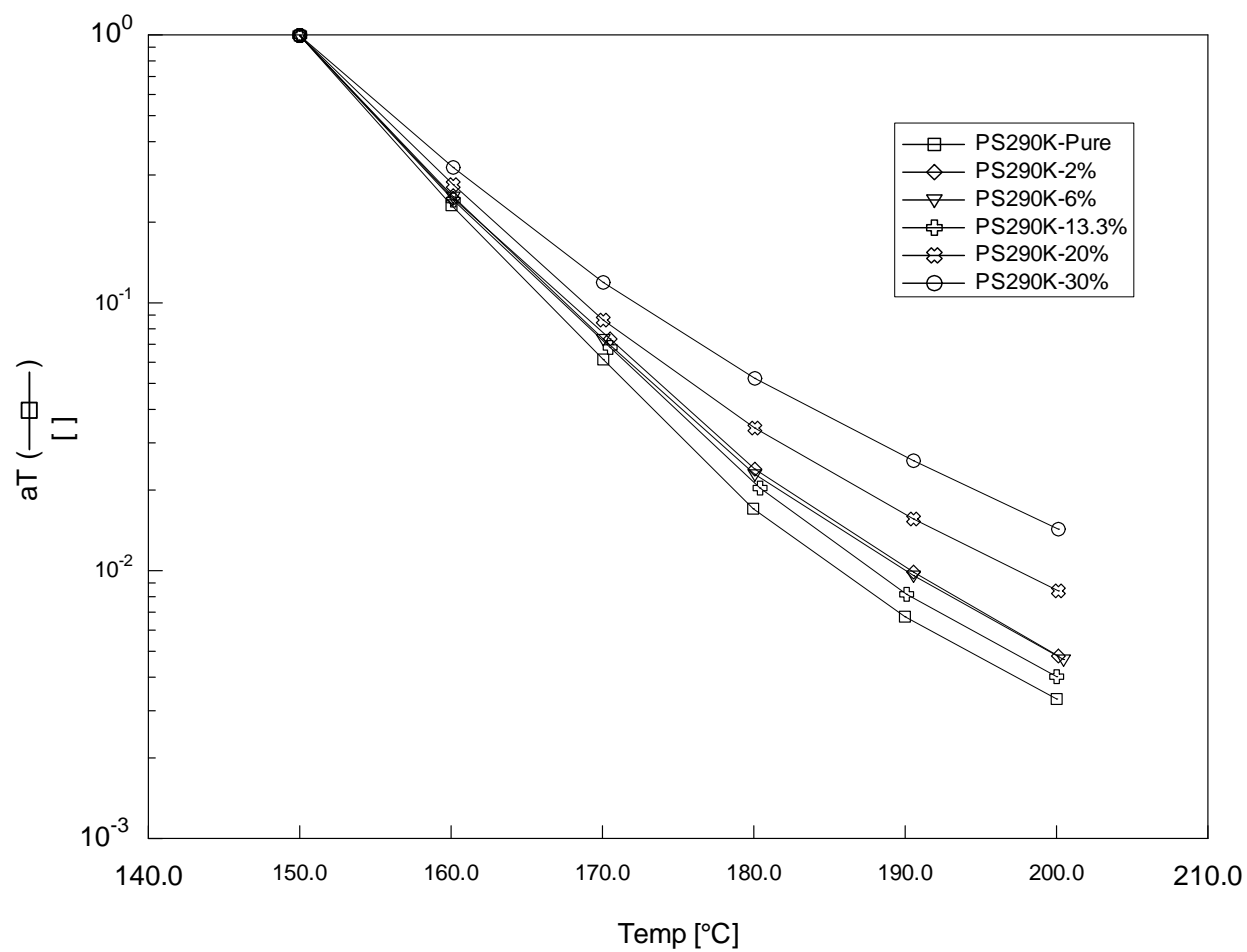


Figure 3.1(c)

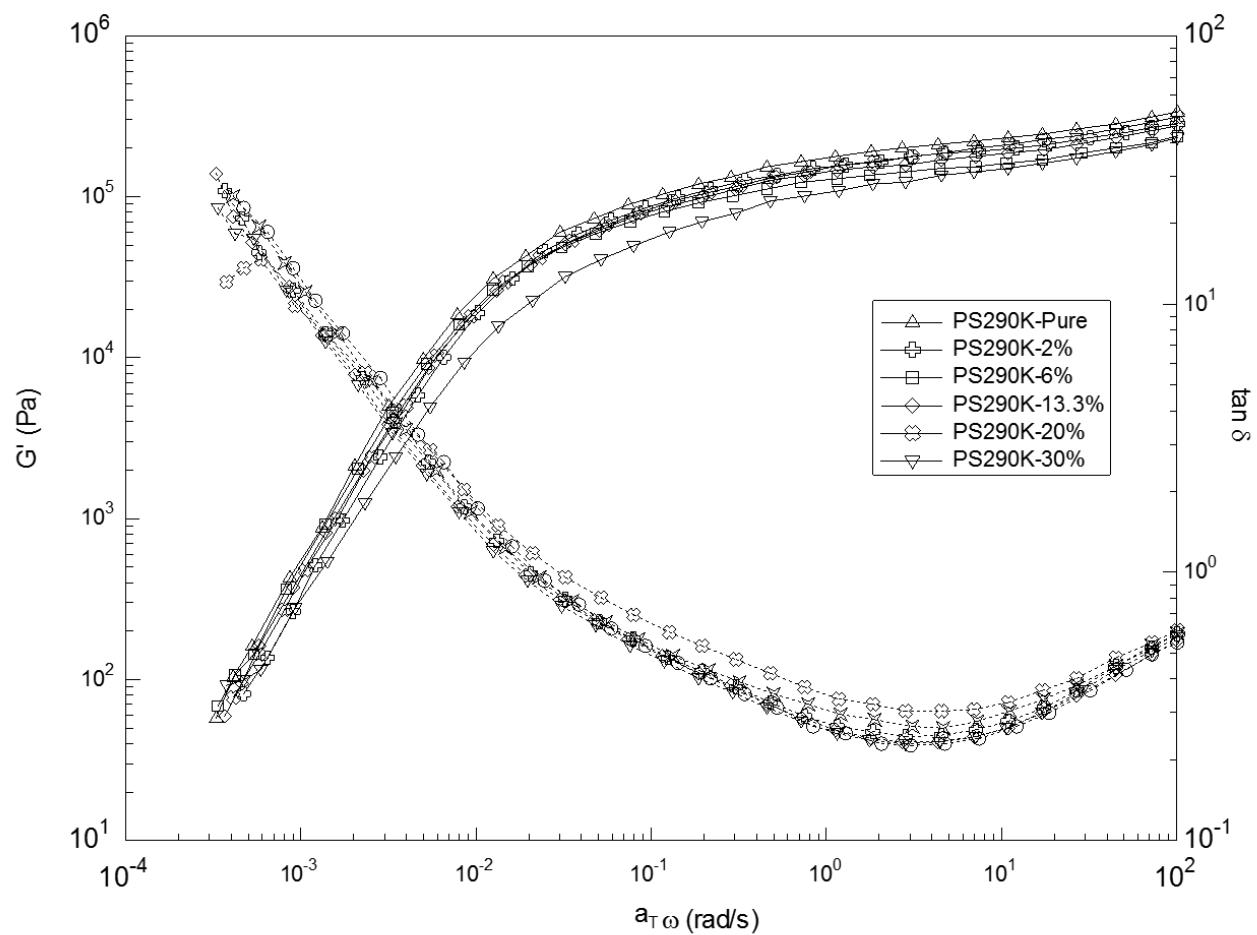


Figure 3.2(a)

**Figure 3.2** Time temperature superposed plots of PS ( $M_w = 290$  K Da) and Styrenyl POSS (St<sub>8</sub>T<sub>8</sub>) blends with varying weight fractions of POSS at 150°C a) Storage Modulus ( $G'$ ) versus Reduced frequency ( $a_T \omega$ ) b) Reduced viscosity ( $\eta^* / a_T$ ) versus Reduced frequency ( $a_T \omega$ ) c) Shift factors ( $a_T$ ) versus Temperature (Temp)

Figure 3.2 (cont'd)

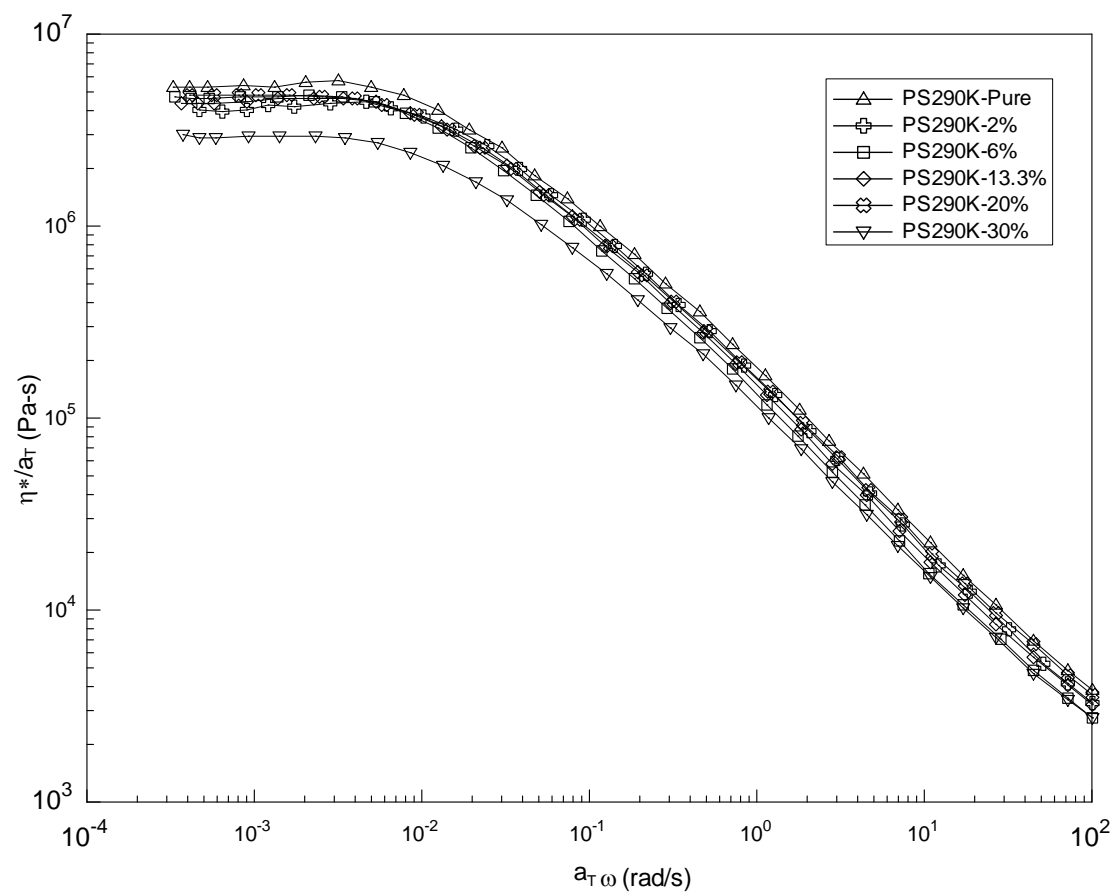


Figure 3.2(b)

Figure 3.2 (cont'd)

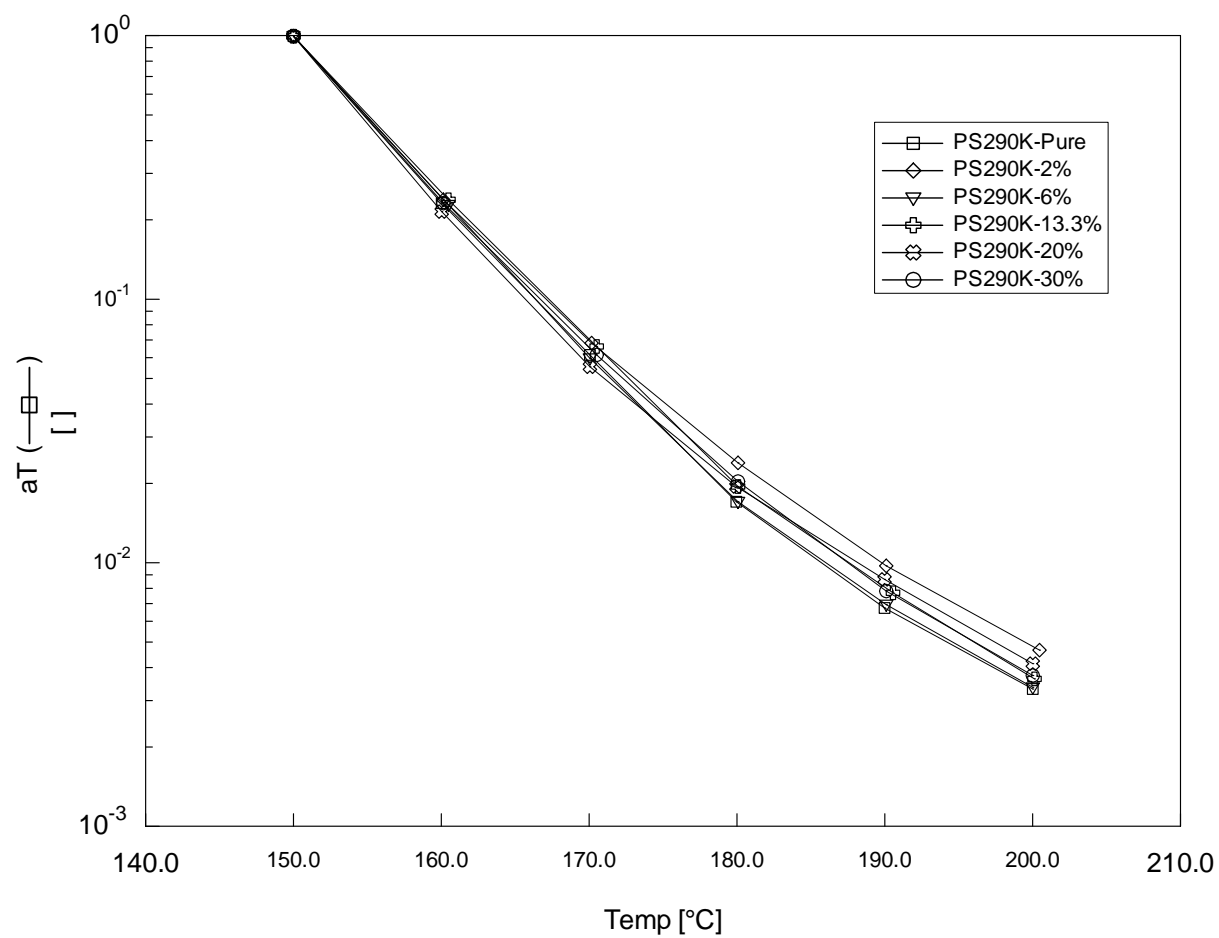
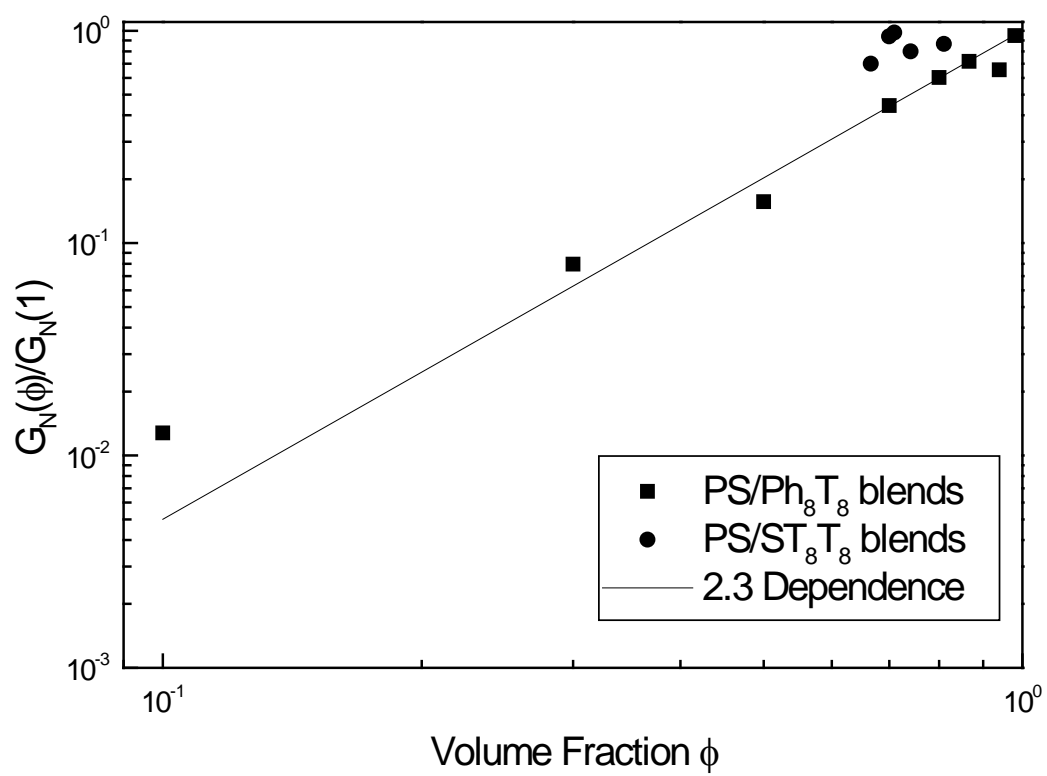


Figure 3.2(c)



**Figure 3.3** Log-Log plot of Normalized Plateau Modulus ( $G_N(\phi)/G_N(1)$ ) versus Volume fraction ( $\phi$ )



	$\Phi$	$T_g$	$\omega_c$	$G_c(\omega)$	$\lim_{\omega \rightarrow 0} \eta^*(\omega)$	$G_N^0$
		$^{\circ}\text{C}$	rad/s	Pa	Pa-s	Pa
<b>PS 290K Pure</b>		106.07	0.0182	4.182E+04	6.02E+06	2.352E+05
<b>Ph8T8/PS</b>						
	<b>2%</b>	102.23	0.02609	4.68E+04	4.51E+06	2.231E+05
	<b>6%</b>	100.75	0.02947	3.432E+04	2.98E+06	1.543E+05
	<b>13.3%</b>	101.44	0.02757	3.506E+04	3.58E+06	1.686E+05
	<b>20%</b>	98.57	0.07089	3.27E+04	1.19E+06	1.416E+05
	<b>30%</b>	91.88	0.1827	2.71E+04	3.77E+05	1.045E+05
	<b>50%</b>	N/A	N/A	N/A	N/A	3.680E+04
	<b>70%</b>	N/A	N/A	N/A	N/A	1.870E+04
	<b>90%</b>	N/A	N/A	N/A	N/A	3.005E+03
<b>St8T8/PS</b>	<b>2%</b>	105.39	0.02271	4.27E+04	4.27E+06	1.667E+05
	<b>6%</b>	104.67	0.01703	3.325E+04	3.325E+06	1.644E+05
	<b>13.3%</b>	104.91	0.02003	3.724E+04	3.724E+06	1.904E+05
	<b>20%</b>	105.75	0.02037	3.979E+04	3.979E+06	1.742E+05
	<b>30%</b>	103.66	0.02854	2.912E+04	2.912E+06	1.566E+05

**Table 3.1** The crossover frequency versus POSS weight fraction and the zero-shear viscosity based on an Ellis model fit

$\Phi = \text{POSS}$  weight fraction is  $\approx$  volume fraction since densities of both POSS and PS are approximately 1.

$G_N^0$  is the plateau modulus and is determined as the value of  $G'$  at minimum  $\tan\delta$  position.

$T_g$  is determined as the midpoint of onset and end set of transition from the DSC curve.

$\omega_c$  is the crossover frequency and  $G_c(\omega)$  is the modulus at the crossover frequency

$\lim_{\omega \rightarrow 0} \eta^*(\omega)$  is the zero shear viscosity from the master curve at 150°C based on Ellis model.

N/A Not Available

**St<sub>8</sub>T<sub>8</sub> POSS / PS blends:**

St<sub>8</sub>T<sub>8</sub> POSS is used to study the effect of POSS-POSS interactions on the polymer chain dynamics, since it is known that the POSS-POSS interaction in the case of St<sub>8</sub>T<sub>8</sub> is greater compared to Ph<sub>8</sub>T<sub>8</sub> POSS from the DSC studies. Figure 3.2(a) is the time-temperature master curves shifted to 150°C for the PS (Molecular weight 290K Daltons) blended with different amount of St<sub>8</sub>T<sub>8</sub> POSS. The crossover frequency versus POSS weight fraction and the zero-shear viscosity based on an Ellis model fit were tabulated and shown in Table 3.1. The reduced-complex viscosity versus frequency curves for various St<sub>8</sub>T<sub>8</sub> POSS fractions are shown in Figure 3.2(b). Data were shown for the 2%, 6%, 13.3%, 20%, and 30% St<sub>8</sub>T<sub>8</sub> POSS blends with 290K PS on the same plot.

In Figure 3.2(a) the storage modulus curve and the cross over frequency,  $\omega_c$ , from Table 1 shifts downwards with the addition of St<sub>8</sub>T<sub>8</sub> POSS. Although there are some similarities to the effect observed in the case of Ph<sub>8</sub>T<sub>8</sub>/PS blends, however, no systemic change on  $\omega_c$  and  $G_N^0$  were observed. This is in agreement with the DSC results, where no significant  $T_g$  depression is observed. We believe this observation can be explain based on the effect of miscibility of St<sub>8</sub>T<sub>8</sub> POSS in PS as influenced by a stronger POSS-POSS interaction and the thermorheological behavior of well-dispersed, albeit inert, nano-particulate filled polymer. As discussed previously, the POSS-POSS association is stronger for St<sub>8</sub>T<sub>8</sub> POSS as

compared to  $\text{Ph}_8\text{T}_8$  POSS. Consequently, the stronger POSS-POSS interaction affect the miscibility curve of  $\text{St}_8\text{T}_8$  in PS in such a manner that concentration fluctuations might occur thus leading to a two phase behavior, one POSS-rich and the other polymer-rich, as shown in the TEM images in Chapter 2. Furthermore, the two-phase morphology remains even with increases in the total POSS concentration. The formation of white drop-like domains can be seen as the dispersed PS domains with lower POSS concentration, where the difference in free energies in both the phases leads to the formation of drops in the homogeneous blend where spinodal decomposition occurs. We believe the droplet domain which is rich in PS can reinforce the polymer matrix thus the value of plateau modulus,  $G_N^0$ , and  $\omega_c$  are not strongly affected by the addition of  $\text{St}_8\text{T}_8$  POSS. Although the value of  $G_N^0$  and  $\omega_c$  are not strongly affected by the addition of  $\text{St}_8\text{T}_8$  POSS, however we observed a systemic decrease in the value of zero-shear viscosity,  $\lim_{\omega \rightarrow 0} \eta^*(\omega)$ , and the cross-over modulus,  $G_c(\omega)$ , as amounts of  $\text{St}_8\text{T}_8$  POSS increase. This is consistent with some other investigations of nano-particle filled polymers<sup>67</sup>, where the presence of nanoparticles decreases the viscosity of the polymer blend.

### 3.4 SUMMARY

Rheological experiments were performed to investigate the influence of POSS addition on the melt dynamics of the polymer chains.

We are particularly interested in the influence of well-dispersed, nano-particulate additions on the zero-shear viscosity,  $\lim_{\omega \rightarrow 0} \eta^*(\omega)$ , plateau modulus,  $G_N^0$  and the cross-over frequency,  $\omega_c$  of polymer melts.

In the Ph<sub>8</sub>T<sub>8</sub> POSS/PS blends, because of the low POSS-POSS interaction, any POSS interactions are screen-out by the presence of PS. Ph<sub>8</sub>T<sub>8</sub> POSS/PS blend forms a homogeneous solution. The rheological responses of these blends are the same as if as a good solvent was added to PS. We observed a systemic decrease in the zero-shear viscosity, plateau modulus, cross-over frequency as the concentration of Ph<sub>8</sub>T<sub>8</sub> POSS increases, as shown in Table 1.

For St<sub>8</sub>T<sub>8</sub> POSS/PS blends, due to a stronger POSS-POSS association, the blend forms a two-phase morphology. Regardless to the concentration of St<sub>8</sub>T<sub>8</sub> POSS in PS, the POSS-rich form a continuous phase and PS-rich domain as the discontinuous phase. As we increase the concentration of St<sub>8</sub>T<sub>8</sub> POSS, only the fraction of PS-rich discontinue phase is increased. Since St<sub>8</sub>T<sub>8</sub> POSS is molecularly dispersed in PS, the zero shear viscosity of the blends decreases with the addition of St<sub>8</sub>T<sub>8</sub> POSS which is similar to that observed in the case of Ph<sub>8</sub>T<sub>8</sub>/PS blends (shown in Table 1). However due to persistence of the two-phase morphology, no systematic changes in  $\omega_c$  and  $G_N^0$  was observed with increasing concentration of POSS since phase behavior controls the rheological behavior of these blends.

The effect of concentration on the viscometric properties of the nanocomposite blends has been investigated. Rheological measurements well above  $T_g$  have been used to determine the time-temperature superposition behavior of these thermorheologically simple materials. The size of POSS macromers on similar length scales when compared to the entanglement spacing of the polymer chains makes it interesting to study the role these nano-structured constituents would play in controlling the polymer chain dynamics. However due to the complex morphologies of various POSS/PS blends, similar rheological behavior may be obtained due to two different mechanisms. DSC, X-ray, TEM were used to understand the morphology of the blends. Rheological characterization was done for understanding the chain dynamics due to the presence of POSS or due to the domains formed due to the presence of POSS.

The shape of the POSS macromers plays an important role in governing the microstructure in the blend. The changes in microstructure cause profound changes to the relaxation of the polymer backbones. Our findings clearly suggest that POSS nanoparticles which are compatible with the polymer chains could be used to lower the free energy of the polymer mixture and also reduce the viscosity of a polymer mixture as a plasticizer. Though miscibility and aggregation kinetics could be controlled in these types of nanocomposites since the chemistry of POSS particles can be modified depending on the system to be used, it should be noted that restrictions on the organic pendant group on the silicone cage

plays an important role in governing the dynamics of systems involving POSS. Interestingly in the case of Octa styrenyl POSS PS Blends, at small volume fractions, free (untethered) POSS nano-dispersed in the melt appears to act as a plasticizer, reducing the magnitude of selected material properties such as plateau modulus or zero-shear rate viscosity at a given temperature, while simultaneously causing a decrease in free volume (estimated from WLF coefficient analysis). As the volume of dispersed POSS increases, steric effects of the filler dominate and the rheological properties of the melt (modulus, relaxation time, viscosity) are all enhanced.

# **CHAPTER 4**

## **EFFECTS OF PS MOLECULAR WEIGHT ON PHASE BEHAVIOR OF POSS – PS BLENDS**

### **4.1 INTRODUCTION**

Molecular weight is the main structural parameter of polymer flow behavior at temperatures above the glass transition temperature (for an amorphous material) or the melting point (for a semi-crystalline polymer). Melt viscosity is a constant at low shear rates or frequencies. The viscosity in this region is known as the zero shear, or Newtonian, viscosity  $\eta_0$ . For low molecular weight polymers in which chain entanglement is not a factor, the zero shear viscosity is proportional to the polymers molecular weight. However, above a critical molecular weight, chains begin to entangle and the zero shear viscosity depends much stronger on molecular weight, proportional now to about the 3.4 power of the molecular weight. Rheological measurements are therefore ideal for studying the effects of molecular weight differences in resins as small differences in molecular weight are manifested in large changes in viscosity. Whether a blend is compatible or not, also depends on temperature; in this case the blend is considered partially miscible. If blends are incompatible, mechanical energy is needed to disperse the minor phase (mixing) and coalescence occurs if the blend morphology is not stabilized. Interfacial forces such as the interfacial tension become

important and can change the rheological signature of the blend significantly. Moreover the elastic properties of non-compatible blends depend on energy storage mechanisms at the interphase. The relaxation of the dispersed phase itself is often much longer than the relaxation of the polymer chains of the individual components. As a result of this fact, the morphology can be modified to change the final product specific properties.

The reptation model describes the motion of a polymer along its contour as it passes the physical constraints imposed by the surrounding polymers and predicts the molecular weight dependence of the macroscopic diffusion coefficient. Polymer diffusion studies first focused on simple linear chains in matrices of equally simple polymers while subsequent studies explored more complex architectures including branched molecules, star molecules, and loops. Here we investigate the diffusion of linear polymers in the presence of nanoparticles. Nanoparticles with desirable properties are now widely available, and there has been an explosion of activities focused on combining nanoparticles with polymers to create polymer nanocomposites with unique and valuable properties. Nanoparticles also provide access to a new range of size differences between particles and polymers, wherein the radius of gyration ( $R_g$ ) of the polymer is considerably larger than the nanoparticle. For example, POSS have diameters of 1.2 nm and a polystyrene (PS) of 290 000 g/mol molecular weight has  $2R_g = 30$  nm.



The addition of nanoparticles to polymers provides a new challenge to building a fundamental understanding of polymer dynamics in complex environments. In the example of POSS and PS, one might predict that the addition of the nanoparticles to a polymer would act as a diluent and thereby smoothly increase both the free volume of the system and the diffusion coefficient as the POSS concentration increases as observed in the previous chapter in the case of Phenethyl POSS PS blends. Also in the same study the Styrenyl POSS PS blends reports that the additional POSS produces a minimum in zero shear viscosity with increasing nanoparticle concentration. Thus, the addition of nanoparticles to polymers has unforeseen consequences on polymer diffusion, which in turn has direct impact on practical problems, such as the stability of nanoparticle dispersions. Since the 1980s, elastic recoil detection (ERD) has been used to study polymer diffusion and thereby played a key role in testing leading polymer diffusion theories including reptation, constraint release, and mutual diffusion. ERD is an ion beam technique that directly provides a concentration profile of diffusing species, typically a deuterated polymer, as a function of depth into a matrix. But a more practical route is the study of the polymer dynamics using rheology, the limitation being its use in low nanoparticle concentrations to avoid solid like behavior. Using rheology, we follow the crossover frequency along with the plateau modulus and the zero shear viscosity in polystyrene (PS) nanocomposites to understand the influence of POSS on polymer dynamics. This new

understanding will enable better manipulation of polymer nanocomposite properties and melt processing, and could impact our understanding of macromolecular movement in hybrid materials.

Based on our results in the previous chapter which indicate the ability for POSS to very locally interact with the matrix molecules altering their mobility, and thereby able to either stiffen or plasticize the material. Apart from understanding the concentration dependence on the phase behavior the polymer molecular weight plays a crucial role in the phase characteristics of the hybrid materials. Not only the phase characteristics the corresponding dynamics involving the polymer chains blended with the POSS spheres effects the dynamics of the blended system. In a confined system like an entangled polymer melt blended with POSS, the motion of either the POSS macromer or the polymer chain or both should in some way be affected. Though this problem is studied previously, several hypothesizes have arised and several model theories like the reptation theory along with constraint release mechanisms have been used to explain what exact mechanisms control the dynamics of the polymer chains due to the presence of huge (on a molecular length scale) cage like particles. There are however, many questions left due to the absence of a systematic study. Will the higher molecular weight polymer chains take a longer time to relax due to the interference by POSS macromers? Or the dynamics of POSS macromers within the entangled polymer chain play a role in governing the rheological characteristics of

these blends. We intend to address this problem through the study of POSS-PS blends by varying the molecular weight of the linear nearly monodisperse PS ranging from around 30KDa to around 1.6MDa.

## **4.2 EXPERIMENTAL**

### **4.2.1 Materials**

Nearly monodisperse molecular weight distribution of polystyrene with  $M_w$  = 1.6M, 650K, 290K, 130K and 65K Daltons (polydispersity less than 1.1) were purchased from Scientific Polymers. Two fully condensed POSS, Styrenyl<sub>8</sub>-POSS (St<sub>8</sub>T<sub>8</sub>, **1**) and Phenethyl<sub>8</sub>-POSS (Ph<sub>8</sub>T<sub>8</sub>, **2**) and were used in this study.

### **4.2.2 Sample Preparation**

**4.2.2.1 Rheological Characterization:** Preparations of POSS/PS blends were performed by dissolving PS and POSS macromers in chloroform and stirring the solution for 12 hours using a magnetic stirrer and crashing the sample out by using a bad solvent methanol. The precipitated sample on crashing out of the solvent is filtered and then dried under vacuum for more than 12 hours at 60°C.

Rheological measurements were carried out using a Rheometric Scientific ARES rheometer equipped with a force convection oven in the parallel plate geometry. Parallel plate geometry with diameter of 8 mm and gap of 0.5 mm was used for all measurements obtained in this study. Rheological behavior of all samples was investigated using a series of isothermal, small-strain oscillatory shear with oscillatory frequency

ranging from 100 to 0.1 radian/second and oscillatory shear strain amplitude of 5%. To examine the validity of the time-temperature superposition principle and the effect of POSS addition on the values of time-temperature shift factor, sample was tested at temperatures ranging from  $T_g+10^{\circ}\text{C}$  to  $T_g+100^{\circ}\text{C}$  with  $10^{\circ}\text{C}$  intervals. Values of storage modulus,  $G'(\omega)$ , loss modulus,  $G''(\omega)$ , and damping factor,  $\tan\delta(\omega) = G''(\omega)/G'(\omega)$ , were determined using software provided by Rheometric Scientific. Samples tested under the same experimental conditions were repeated two to three times to confirm their reproducibility. Master curves for  $G'$ ,  $G''$  and  $\tan\delta$  were also obtained with software package provided by Rheometric Scientific and a reference temperature of  $T_{ref}=150^{\circ}\text{C}$  for pure polymers and blends was used. These data was also used to see the differences in the polymer relaxation times, which is the inverse of the frequency corresponding to the intersection of the storage modulus and the loss modulus. Furthermore, the plateau storage modulus at high frequencies was observed for all of the nanocomposites, demonstrating the effect of POSS on the entanglement molecular weight ( $M_e$ ) of the PS.

### **4.3 RESULTS & DISCUSSION**

The effect of POSS loading and distribution of POSS macromers in varying molecular weights of PS is understood through the rheological studies. Rheology experiments were performed to address the effect of POSS macromers on the chain dynamics of PS. Since rheological

measurements and their correlation to polymer chain dynamics using narrow molecular weight PS properties were well documented, our measurements of POSS/PS blends will provide insight into how the POSS macromers affect the polymer chain dynamics.

The melt rheological experiments were carried out using small-strain amplitude oscillatory shear so to minimize deformation on sample morphology. The dynamic properties of the POSS/PS blends were investigated as a function of frequency at different temperatures. Changes in  $G_C(\omega)$ ,  $\omega_C$ ,  $G_N^0$  and  $\lim_{\omega \rightarrow 0} \eta^*(\omega)$  were compared for all studied systems. In addition, the validity of time-temperature superposition was also verified for all the samples used in this study.

Figure 4.1(a) is the time-temperature master curves shifted to 150°C for the PS (Molecular weight 1.6M Daltons) blended with varying amounts of St<sub>8</sub>T<sub>8</sub> POSS. The corresponding plot of reduced complex viscosity versus reduced frequency is shown in Figure 4.1(b). The temperature shift factor versus temperature is plotted in Figure 4.1(c). From the various reduced storage modulus curves shown in Figure 4.1(a), we observed that these curves shift downwards and towards the right with increasing amount of St<sub>8</sub>T<sub>8</sub> POSS blended. In addition, the values of the plateau modulus,  $G_N^0$ , and the cross-over frequency,  $\omega_C$ , as shown in Figure 4.1, decrease with increasing amount of St<sub>8</sub>T<sub>8</sub> POSS added expect for very high loading of 30wt%. These observations correspond to PS chains becoming less entangled when blended with St<sub>8</sub>T<sub>8</sub> POSS. There are two

ways of looking at the individual polymer blends from a volumetric point of view to look at effect on free volume of the blends and secondly the viscometric effect arising from the phase behavior in these blends. For the really high molecular weight 1.6M PS POSS blend system, observed is a difference in the shifting parameter with increasing POSS loadings based on the shift factor curve 4.1(c), the higher the concentration the lower the shift factor, which is indicative of increased free volume, at the same time based on the zero shear viscosity there seems to a drop in zero shear viscosities at low volume loadings indicative of the free volume changes but with weight loadings the zero shear viscosity tends to go up along with an increase in the plateau modulus indicative of filler like behavior, which suggests a two phase behavior.

By decreasing the molecular weight to around 650K as observed in Fig 4.2, there is an increased effect on the shift factor plot Fig 4.2 (c), which suggests the free volume effect dominating the volumetric effects hence a reduction in the zero shear viscosity at higher weight loadings. Similar behavior has been observed in the previous chapter with blend systems with 290K PS.

Figures 4.1 to 4.4 (a) is the time-temperature master curves shifted to 150°C for the PS, Molecular weight 1.6M, 650K, 130K and 65K Daltons respectively blended with different amount of St<sub>8</sub>T<sub>8</sub> POSS. The crossover frequency versus POSS weight fraction has not changed but the the zero-shear viscosity has had a minimum before filler type phase

separation behavior dominates the viscoelastic response of these blends. The reduced-complex viscosity versus frequency curves for various St<sub>8</sub>T<sub>8</sub> POSS fractions are shown in Figure 4.1 to Figures 4.4(b). Data were shown for the 2%, 6%, 20%, and 30% St<sub>8</sub>T<sub>8</sub> POSS blends with varying molecular weight of PS on the same plot.

Although there are some similarities to the effect observed in the case of Ph<sub>8</sub>T<sub>8</sub>/PS blends, however, no systemic change on  $\omega_c$  and  $G_N^0$  were observed. We believe this observation can be explain based on the effect of miscibility of St<sub>8</sub>T<sub>8</sub> POSS in PS as influenced by a stronger POSS-POSS interaction and the thermo rheological behavior of well-dispersed, albeit inert, nano-particulate filled polymer. As discussed previously, the POSS-POSS association is stronger for St<sub>8</sub>T<sub>8</sub> POSS as compared to Ph<sub>8</sub>T<sub>8</sub> POSS. Consequently, the stronger POSS-POSS interaction affect the miscibility curve of St<sub>8</sub>T<sub>8</sub> in PS in such a manner that concentration fluctuations might occur thus leading to a two phase behavior, one POSS-rich and the other polymer-rich, as shown in the TEM images in Chapter 2. Furthermore, the two-phase morphology remains but shifts horizontally with varying polymer molecular weight as observed in Fig 4.5.

Based on the Figure we report a minimum in the zero shear viscosity as the nanoparticle concentration increases in polymer composites with spherical nanoparticles. POSS particles give rise to polymer nanocomposites with much larger specific interfacial areas, such that even a modest perturbation in the vicinity of the nanoparticles can

have significant ramifications on the observed polymer properties. The minimum in the zero shear viscosity diffusion is inconsistent with a simple reptation model; for example, the significant changes in  $D$  are not coupled with changes in  $M_e$ . A possible physical interpretation of the anisotropic diffusion could involve a disruption of polymer reptation near nanoparticles. Reptation describes the motion of a polymer chain along a confining tube that is defined by constraints or entanglements within a high molecular weight polymer melt. With sufficient thermal energy and time the entanglements that define the confining tube relax because these entangled polymers have diffused out of their own tubes. Perhaps, in the vicinity of nanoparticles, the confining tube for polymer reptation is perturbed such that diffusion becomes locally anisotropic.. We have several studies underway that are designed to determine the range of materials showing a minimum in the diffusion coefficient with nanoparticle concentration and to ascertain the underlying polymer physics.



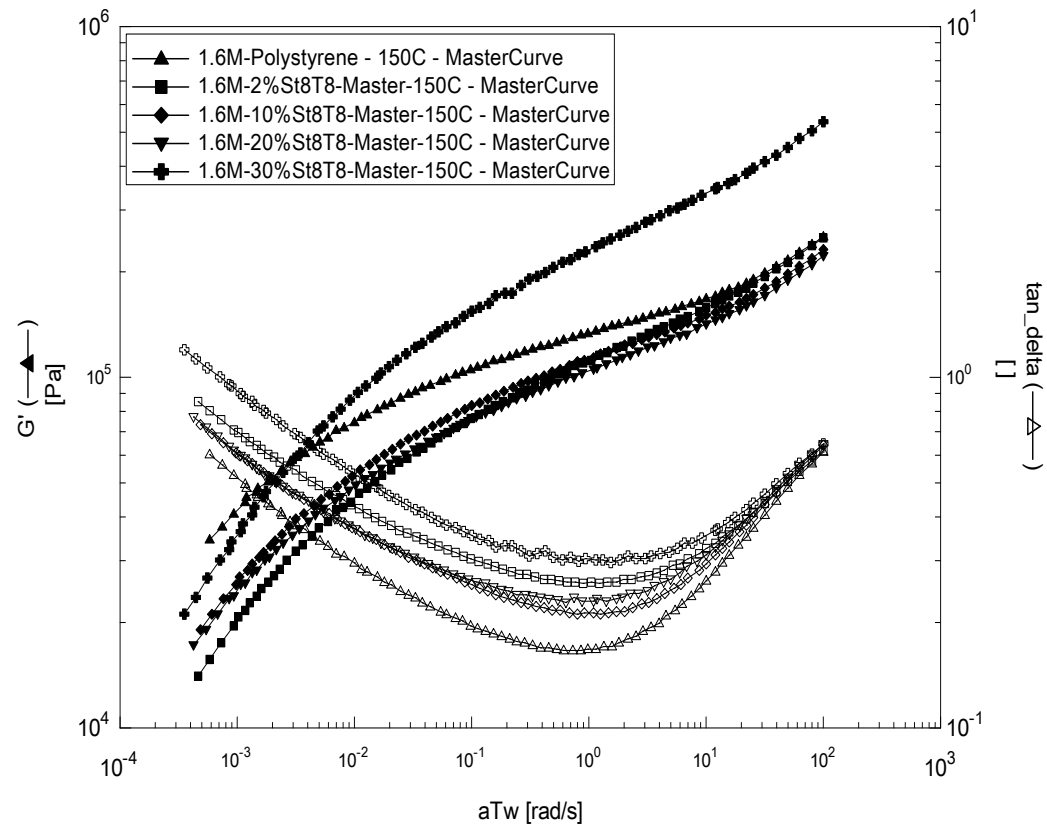


**Fig 4.1 (a)**

**Figure 4.1** Time temperature superposed plots of PS ( $M_w = 1.6$  M Da) and Styrenyl POSS (St<sub>8</sub>T<sub>8</sub>) blends with varying weight fractions of POSS at 150°C a) Storage Modulus ( $G'$ ) versus Reduced frequency ( $a_T \omega$ ) b) Reduced viscosity ( $\eta^* / a_T$ ) versus Reduced frequency ( $a_T \omega$ ) c) Shift factors ( $a_T$ ) versus Temperature (Temp)

**Figure 4.1** (cont'd)

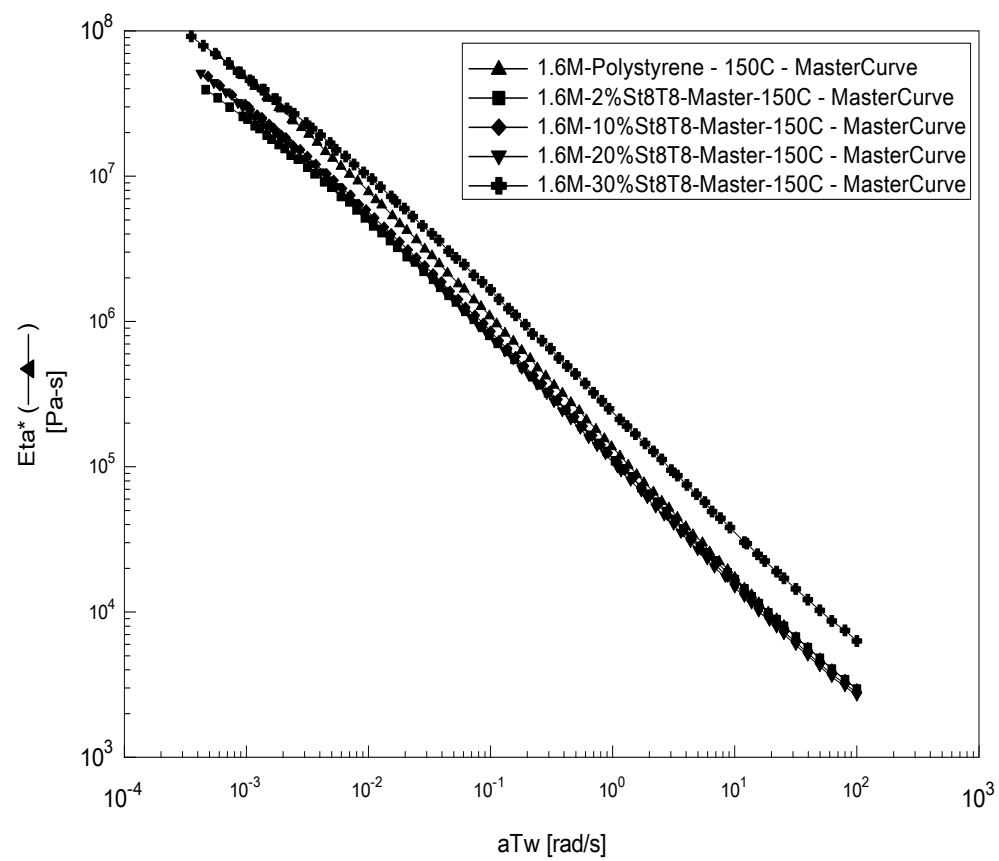


**Figure 4.1 (b)**

**Figure 4.1 (cont'd)**

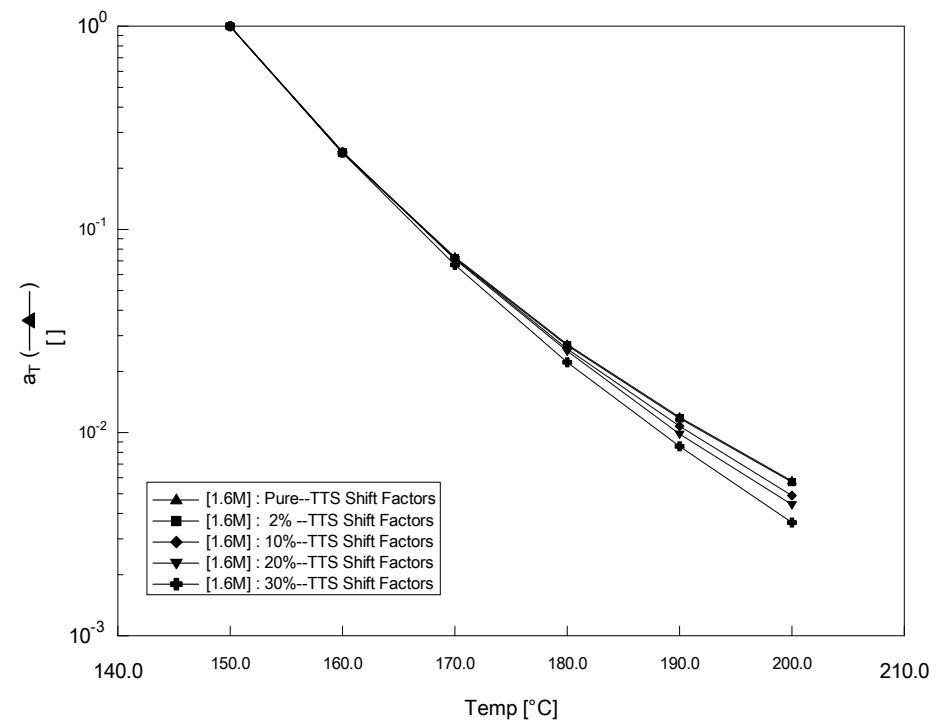


**Figure 4.1 (c)**

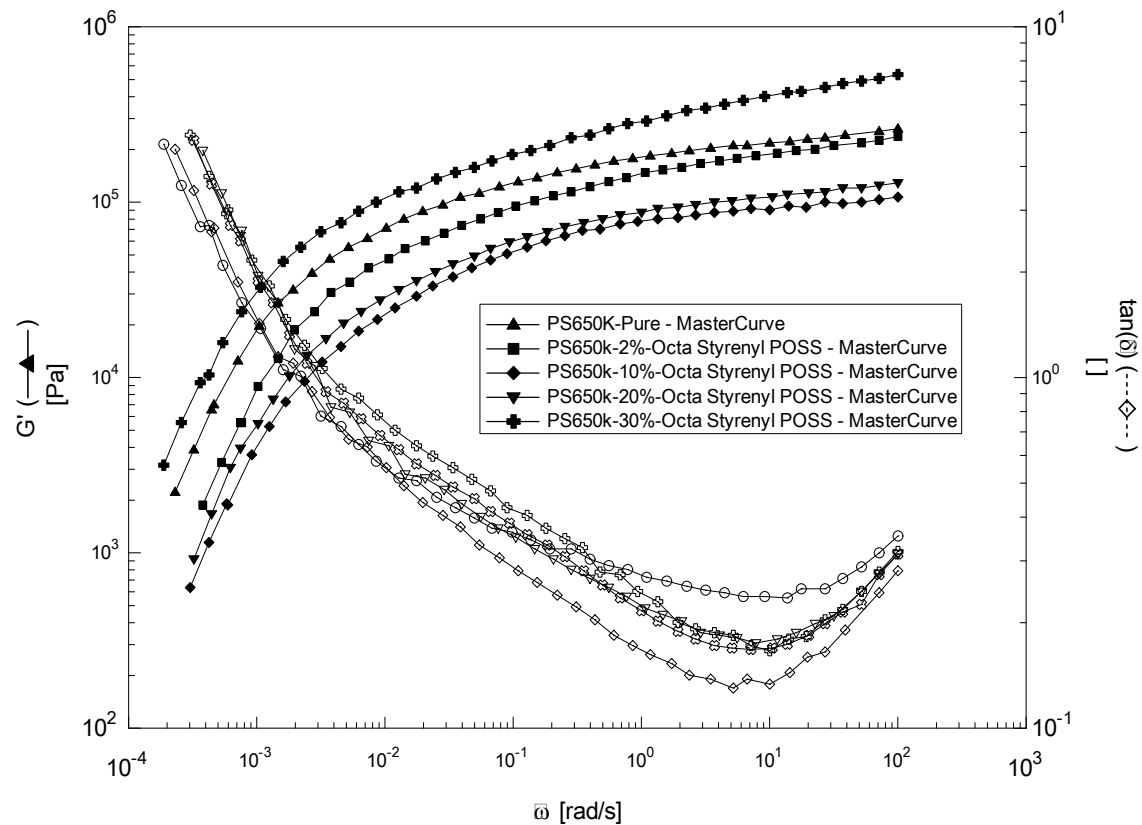


**Figure 4.2 (a)**

**Figure 4.2** Time temperature superposed plots of PS ( $M_w = 650\text{K Da}$ ) and Styrenyl POSS ( $\text{St}_8\text{T}_8$ ) blends with varying weight fractions of POSS at  $150^\circ\text{C}$  a) Storage Modulus ( $G'$ ) versus Reduced frequency ( $a_T\omega$ ) b) Reduced viscosity ( $\eta^*/a_T$ ) versus Reduced frequency ( $a_T\omega$ ) c) Shift factors ( $a_T$ ) versus Temperature (Temp)

**Figure 4.2 (cont'd)**

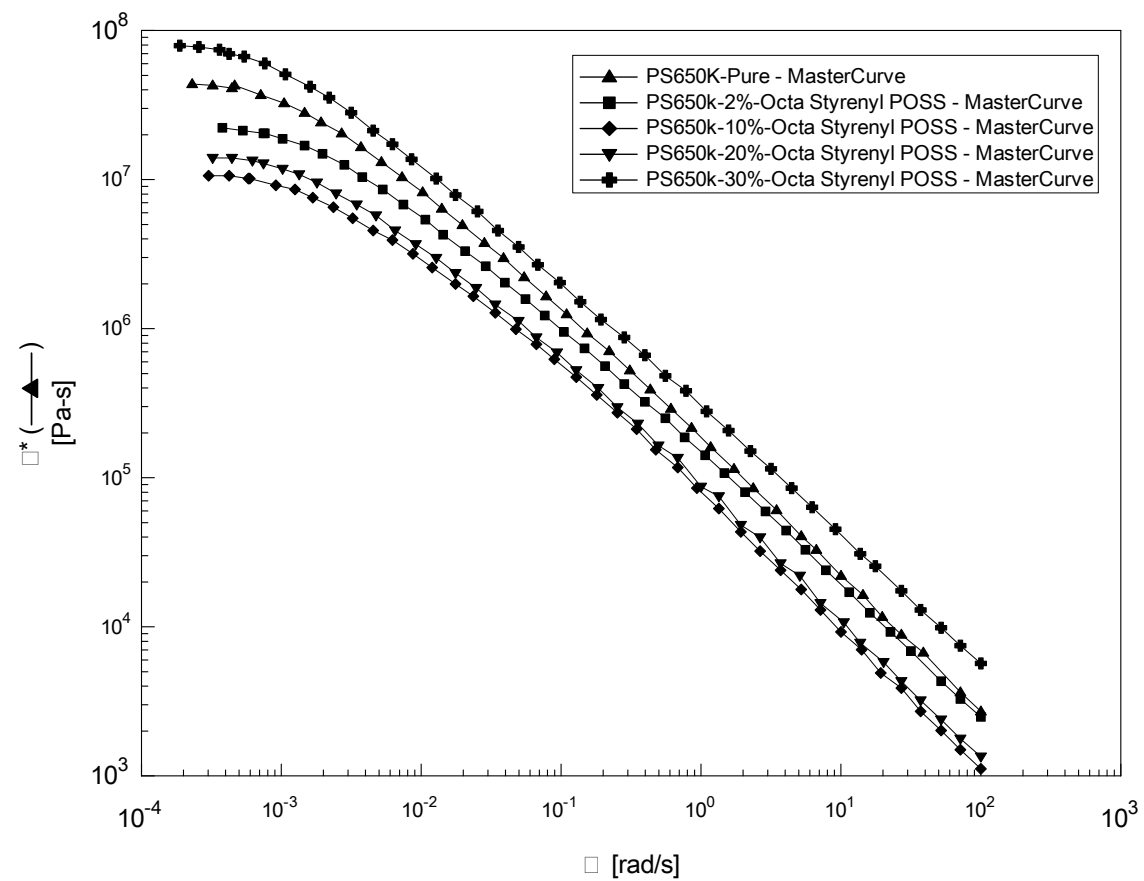


**Figure 4.2 (b)**

**Figure 4.2 (cont'd)**

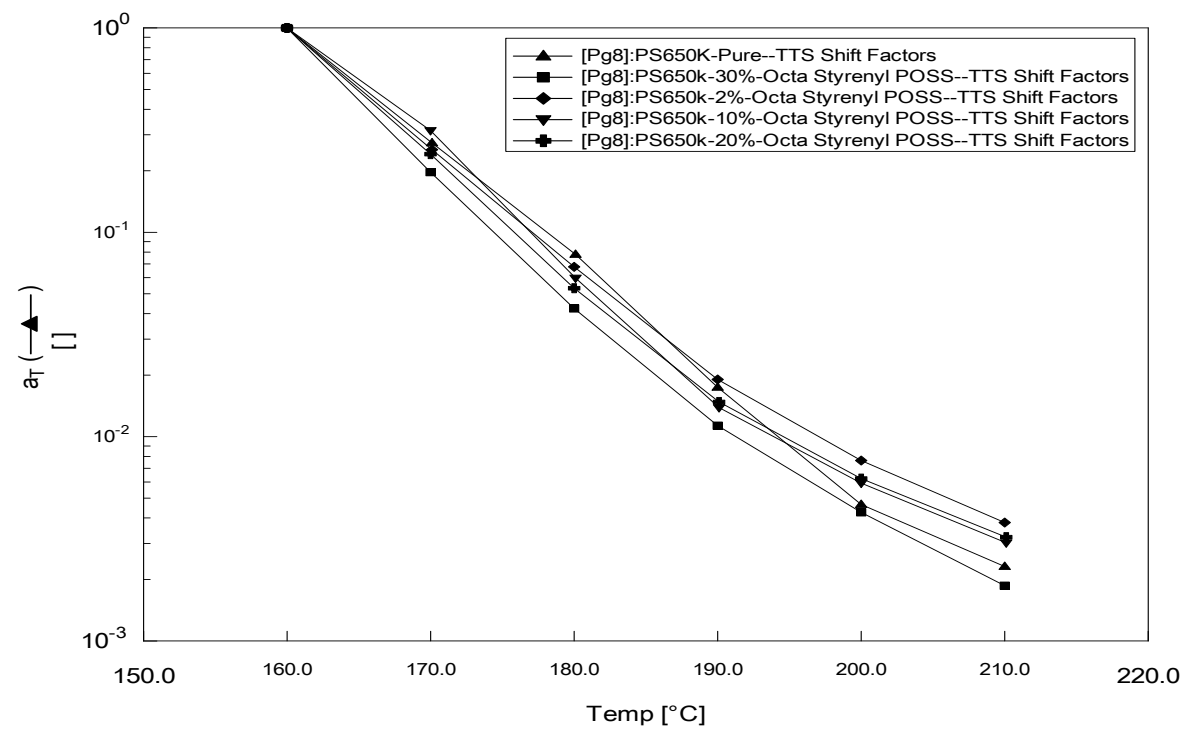


**Figure 4.2 (c)**

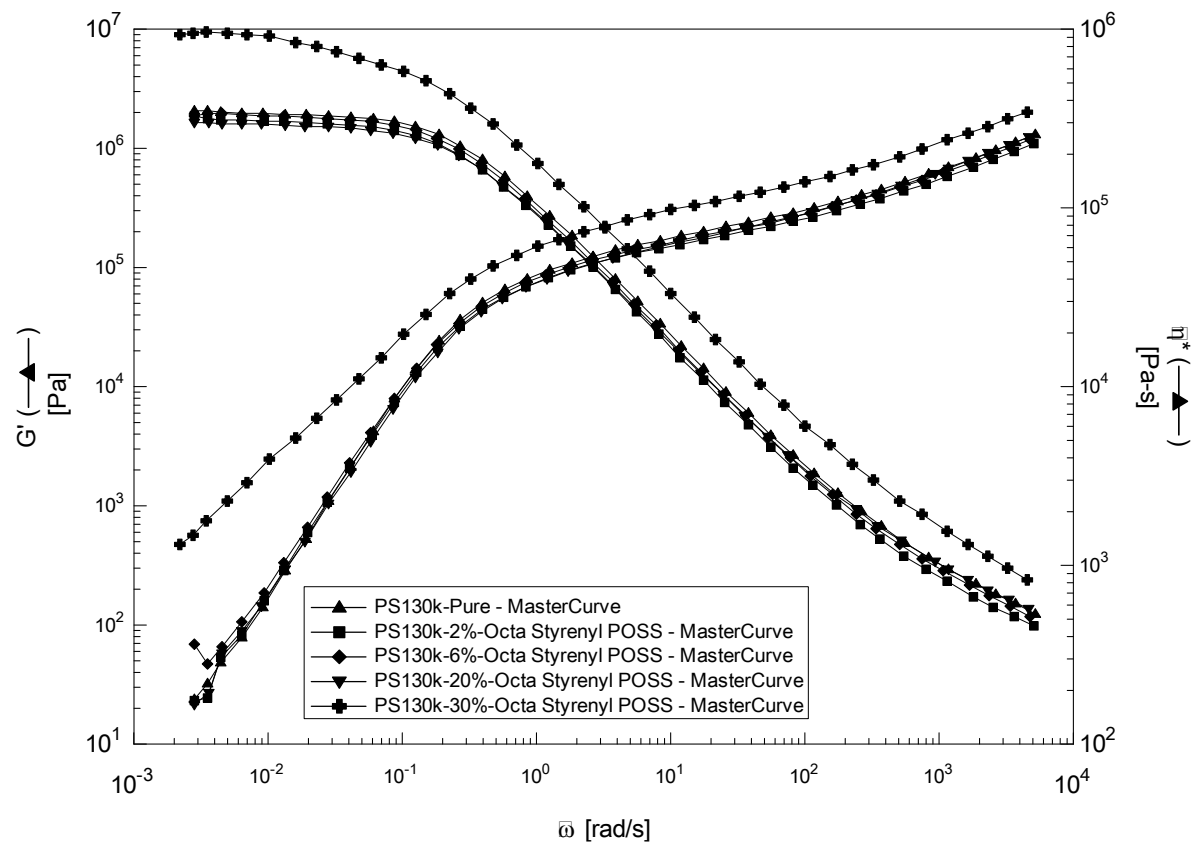


**Figure 4.3(a)**

**Figure 4.3** Time temperature superposed plots of PS ( $M_w = 130K$  Da) and Styrenyl POSS ( $St_8T_8$ ) blends with varying weight fractions of POSS at  $150^\circ C$  a) Storage Modulus ( $G'$ ) versus Reduced frequency ( $a_T\omega$ ) b) Reduced viscosity ( $\eta^* / a_T$ ) versus Reduced frequency ( $a_T\omega$ ) c) Shift factors ( $a_T$ ) versus Temperature (Temp)

**Figure 4.3 (cont'd)**

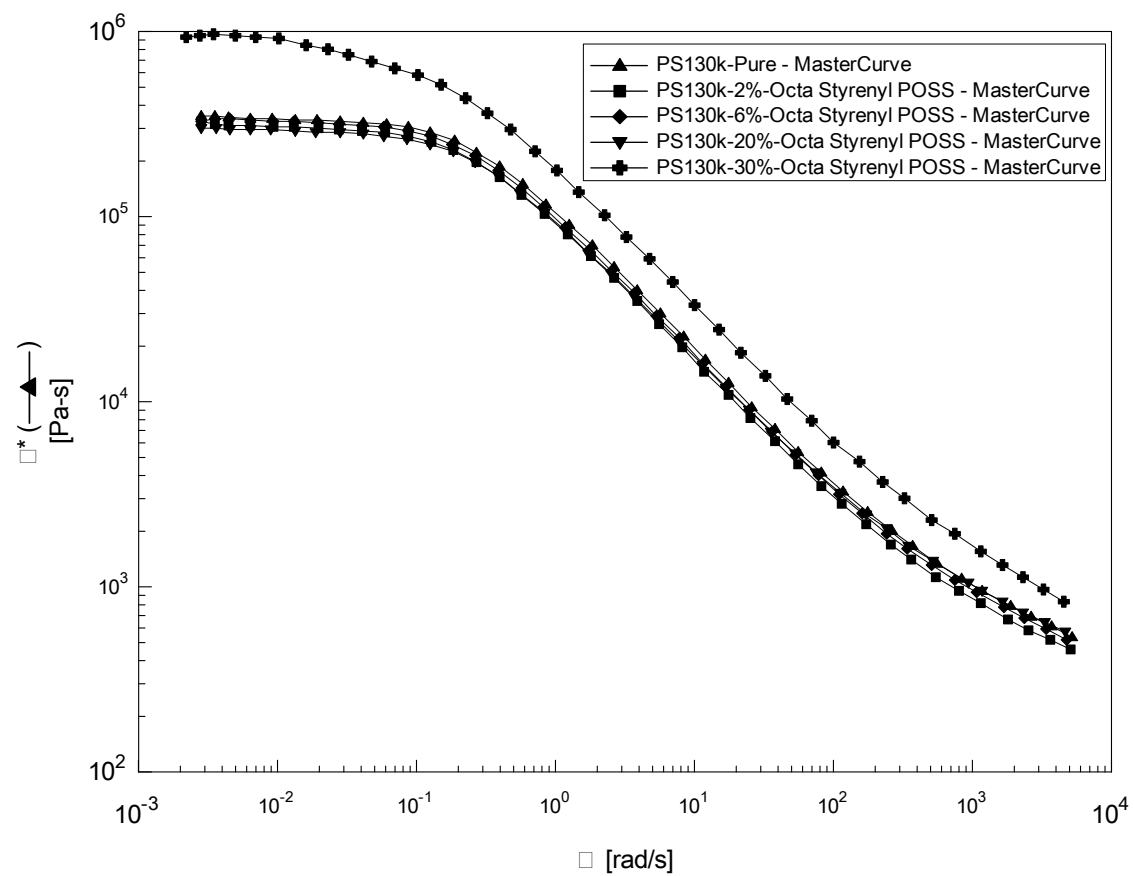


**Figure 4.3 (b)**



**Figure 4.3 (cont'd)**

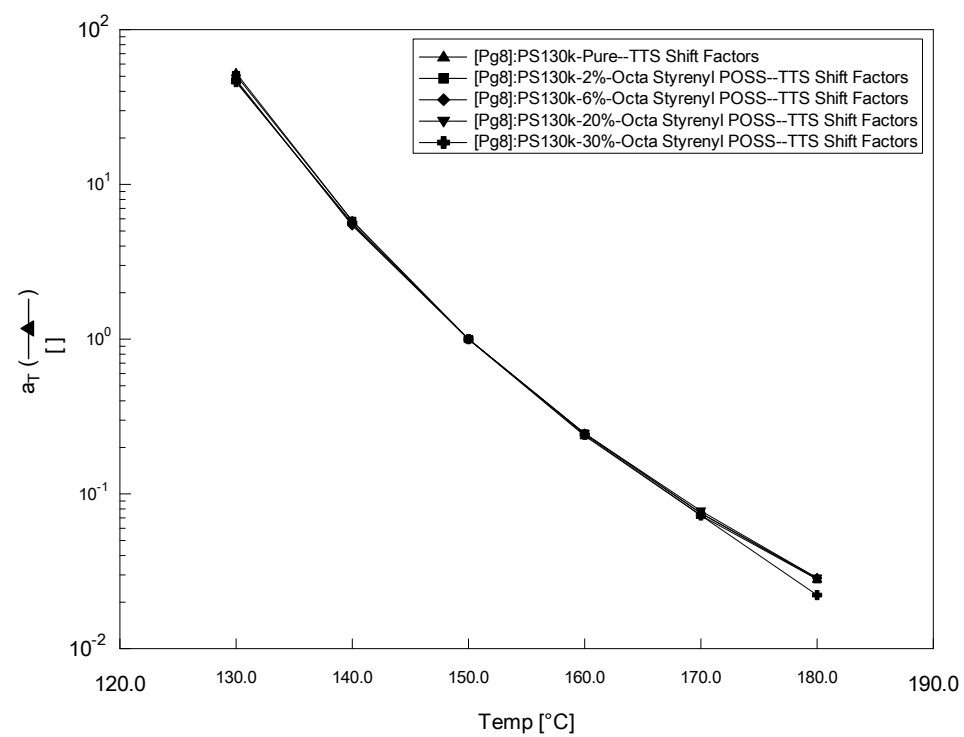


**Figure 4.3 (c)**

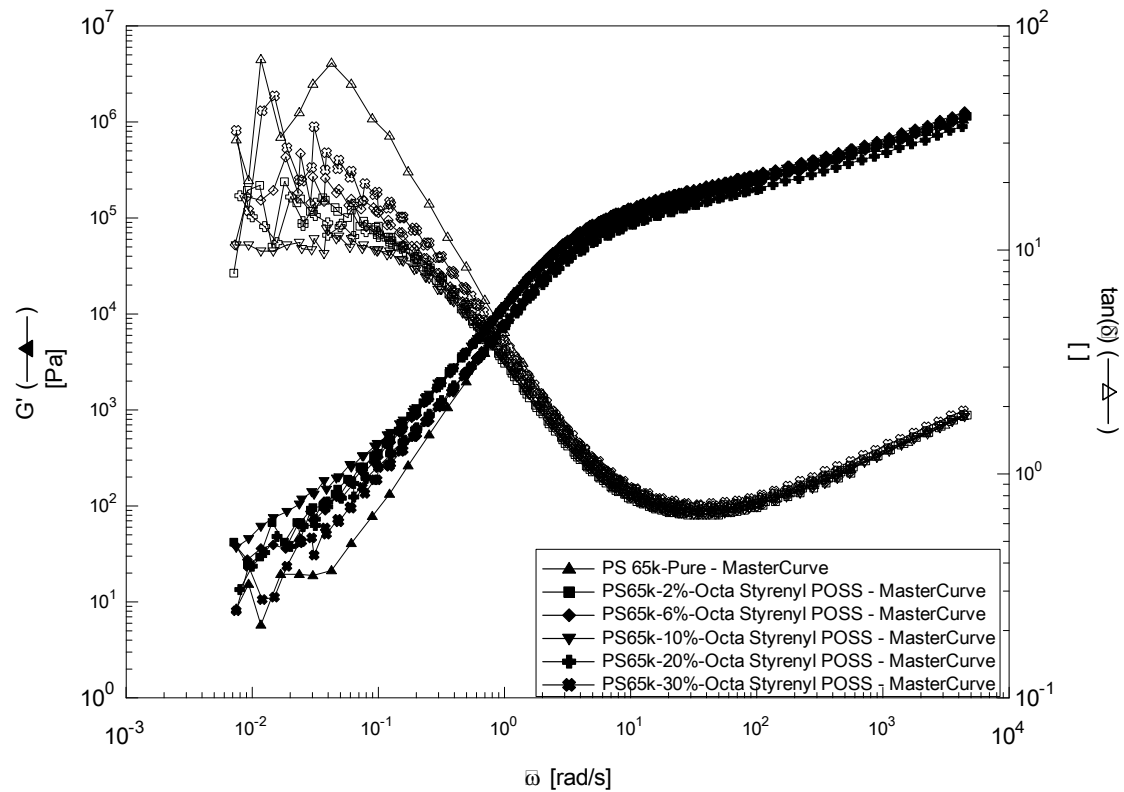


**Figure 4.4 (a)**

**Figure 4.4** Time temperature superposed plots of PS ( $M_w = 65K$  Da) and Styrenyl POSS ( $St_8T_8$ ) blends with varying weight fractions of POSS at  $150^\circ C$  a) Storage Modulus ( $G'$ ) versus Reduced frequency ( $a_T \omega$ ) b) Reduced viscosity ( $\eta^* / a_T$ ) versus Reduced frequency ( $a_T \omega$ ) c) Shift factors ( $a_T$ ) versus Temperature (Temp)

**Figure 4.4 (cont'd)**

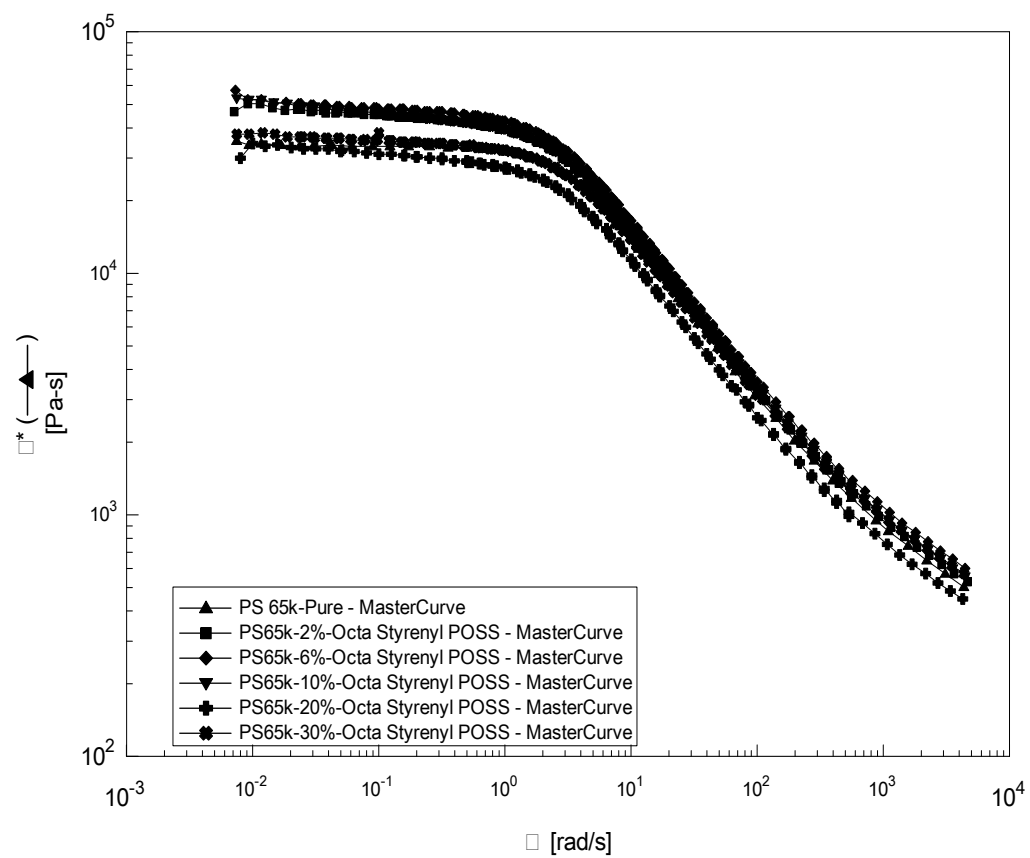


**Figure 4.4 (b)**

**Figure 4.4** (cont'd)

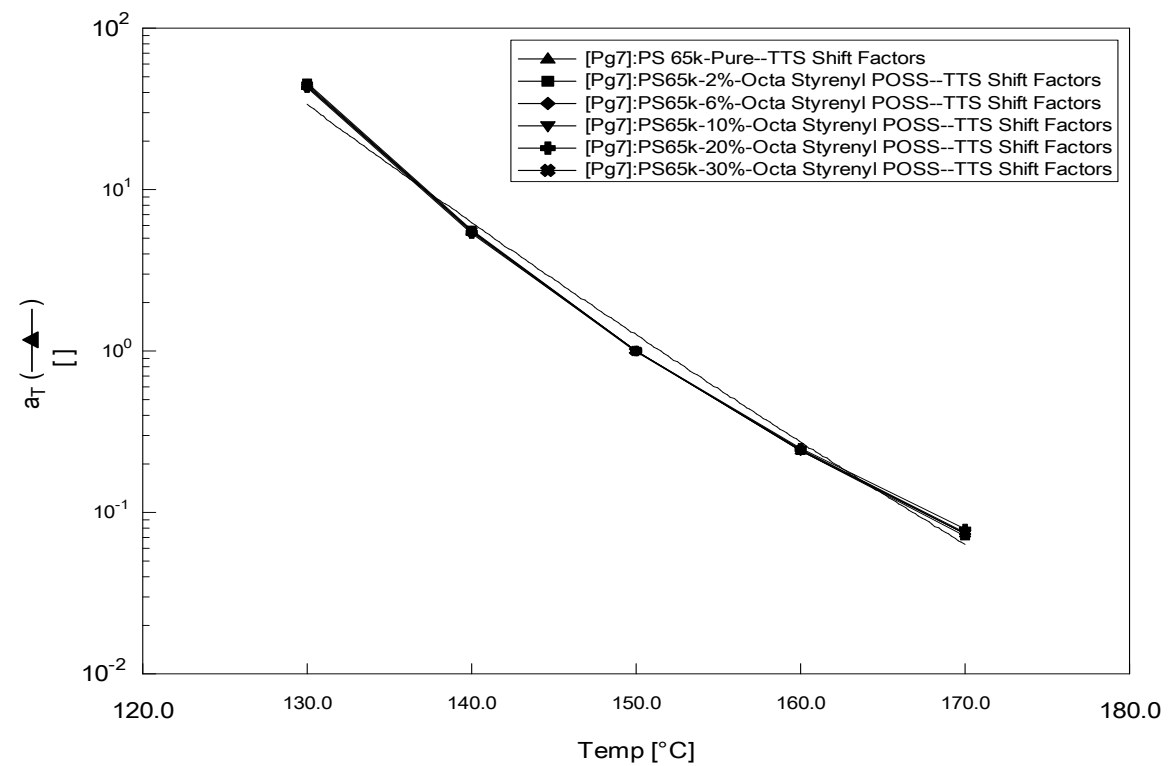


**Figure 4.4** (c)

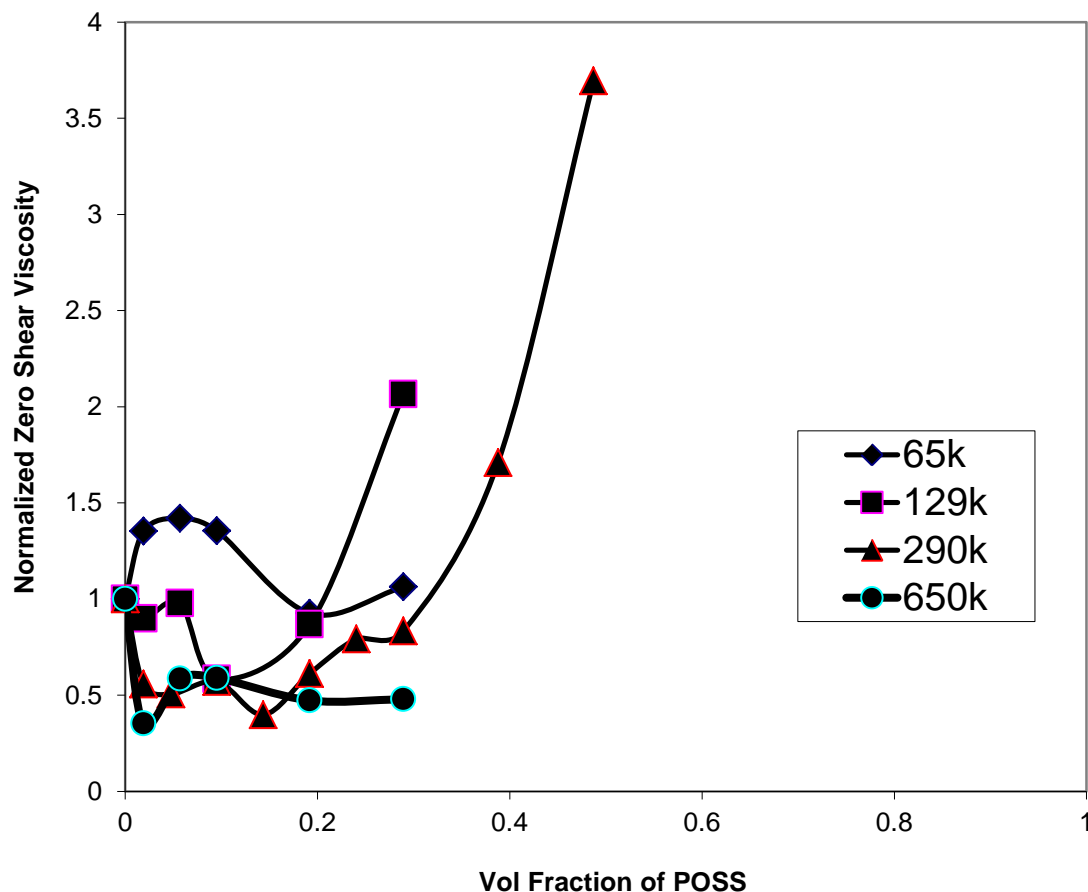


**Figure 4.5** Normalized viscosity ( $\eta^*/a_T$ ) versus volume fraction of Styrenyl POSS

#### 4.4. SUMMARY

Based on our results in the previous chapters which indicate the ability for POSS to very locally interact with the matrix molecules altering their mobility, and thereby able to either stiffen or plasticize the material. The focus of this chapter has been to understand the exact mechanisms which control the dynamics of the polymer chains due to the presence of huge (on a molecular length scale) cage like particles. There are however, many questions left due to the absence of a systematic study.

But with higher molecular weight polymer chains take a longer time to relax due to the interference by POSS macromers, also the dynamics of POSS macromers within the entangled polymer chain play a role in governing the rheological characteristics of these blends. Some of the viscometric and volumetric properties of POSS-PS blends have been studied by varying the molecular weight of the linear nearly monodisperse PS ranging from around 30KDa to around 1.6MDa. Since we already knew from our work in the previous chapter phenethyl POSS acts most likely as a plasticizer focus has been primarily in understanding how styrenyl POSS behaves with varying chain length. Styrenyl POSS blends tend to act as a plasticizer at low weight fractions and also tend to form two phase systems, one polymer rich and the other POSS rich, the molecular weight drives the phase behavior higher or lower depending on the chain length following classic Flory Huggins relationships. As observed in the case of styrenyl blends the presence of the dispersed polymer rich phase gives a unique opportunity in understanding rheological properties of domains filled with soft cores, especially in nonlinear regimes. This led us in a direction of exploring the effects of POSS on the non linear mechanical behavior of POSS polymer blends which is discussed in the next chapter

## **CHAPTER 5**

### **FLOW TRANSITIONS OF POSS – PS BLENDS**

#### **5.1 INTRODUCTION**

Polymer blends are ubiquitous in the polymer industry; the characteristic morphology of these blends plays a crucial role in its applications, since it strongly affects the mechanical response of the blend. Typically either dynamic small amplitude oscillatory shear (SAOS) flow is usually adopted to understand their viscoelastic response. Indeed the dynamic moduli or in general the master curve can be used to correlate the blend morphology for a typical dispersed filler based system. But in the case of nanoparticulate blends shear flows are not strong enough to effectively showcase the differences which originate because of the size of the dispersed phase. Hence the use of large deformations for understanding the characteristic response in nanoparticulate blends has been studied in this chapter, also Dynamic Mechanical Analysis studies have been performed to get an insight into the effects of POSS on the dynamics especially at the transition temperatures where one would see an increased mobility of the backbone polymer network, previous studies by Mulliken and Soong from Boyce and Cohen's group have seen POSS effecting the secondary motions of the polymeric matrix. Their findings suggest that POSS clearly enhanced the mobility of the secondary beta motions, significantly reducing the resistance to high rate elastic and plastic deformation and also POSS was found to plasticize PVC and hence

to dramatically influence its glass transition and corresponding non linear mechanical behavior.

In this chapter the study was based on understanding the effect of the presence of small nanoparticulate domains under large deformations in shear. We discuss the effects of the POSS macromers on PS chain under large deformations.

### **5.1.1 Large Amplitude Oscillatory Shear (LAOS)**

During the oscillation experiment on a rheometer, a sinusoidal deformation is applied to the material. Within the boundaries of the linear viscoelasticity the measured stress at steady state oscillation, preceding the strain remains sinusoidal. The strain rate, the time derivative of the strain has a phase offset of  $90^\circ$  in reference to the strain. This means that the strain is zero, when the strain rate is at a maximum and vice versa.

In order to characterize the time dependent periodic material response, the stress can be decomposed into two waves, one in phase with the strain, one in phase with the strain rate. In analogy to a solid material (strain and stress are in phase) and a simple fluid (strain rate and stress are in phase), the part in phase with the strain is referred to as the elastic (solid) component, the part in phase with the strain rate (out of phase with the strain) is the viscous (fluid) component. Thus the stress can be expressed by the sum of the two components as follows:

$$\sigma(t) = \sigma'(t) + \sigma''(t) \quad (5.1)$$



The amplitude of the measured stress is  $\hat{\sigma}$  and for the two wave components  $\hat{\sigma}'$  and  $\hat{\sigma}''$  in figure 5.1.

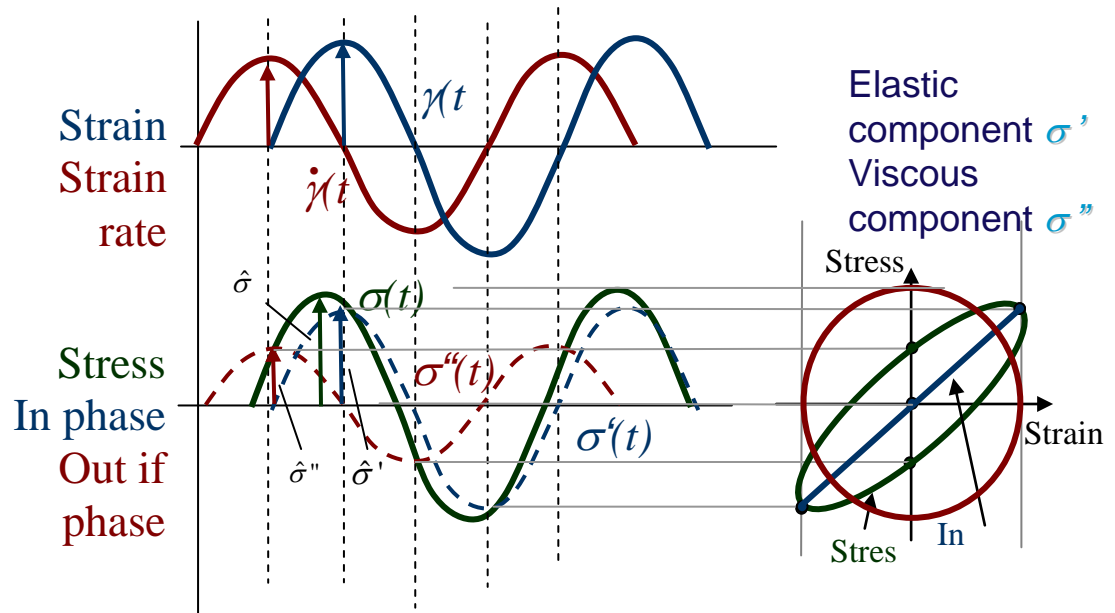


**Figure 5.1:** Stress, Strain and Strain rate waves during an oscillation measurement. The stress can be decomposed in an elastic and a viscous stress wave. The Lissajous figure results from plotting the stress versus the strain.

Instead of representing the stress and strain as sinusoidal waves versus time, they can be plotted as a function of each other. This representation is referred to as Lissajous figure. As long as the measured stress wave is sinusoidal, the Lissajous figure is an ellipsoid. When the stress is in-phase with the strain, the ellipsoid collapses to a straight line

through the origin, in case of the stress being out-of phase with the strain (phase offset  $90^\circ$ ), the ellipsoid changes to a circle.

Although the Lissajous figures represent an excellent visual aid for qualitative analysis, they are more difficult to use when a quantitative evaluation is required. In this case it is more convenient to convert the time dependent periodic signals and evaluate the data in the Fourier space. The Fourier transformation decomposes the stress signal in a series of sinusoidal wave functions with increasing frequency. The results are represented as a magnitude and phase versus frequency. When the stress signal is sinusoidal, the Fourier spectrum shows a single peak at the fundamental frequency. In the linear region (sinusoidal stress response) at a particular strain deformation, only one peak at the excitation frequency (fundamental) is seen. In the non-linear region the peak at the excitation frequency ( $\omega = \omega_0$ ) remains and in addition higher odd harmonics at 3, 5, 7 times the excitation frequency  $\omega_0$  appear. That means, that in order to fully describe the material behavior in the non-linear region, fundamental and harmonics magnitude and phase need to be accounted for.

Until recently, dynamic mechanical data were analyzed only when the conditions of linearity were fulfilled. Manfred Wilhelm was the first to systematically investigate experiments in the non-linear viscoelastic region. He measured the stress response in the time domain during large strain oscillation experiments (LAOS) and evaluated the complete frequency spectrum using discrete Fourier transformation.

At a first glance it might be surprising, that only odd harmonics (3<sup>rd</sup>, 5<sup>th</sup>, 7<sup>th</sup>, etc.) show in the Fourier spectrum. This can be easily shown by developing the expression for the non-linear response of the viscosity to a sinusoidal shear rate input. In order to describe the non-linearity, the viscosity is approximated by a Taylor expansion with even functions in the shear rate.

$$\begin{aligned}\sigma(t) &= \eta \dot{\gamma} \\ \eta &= \eta_o + a\dot{\gamma}^2 + b\dot{\gamma}^4 \dots \\ \dot{\gamma}(t) &\propto e^{i\omega_1 t}\end{aligned}\tag{5.2}$$

With these assumptions the shear stress in the time domain can be expressed as a sum of odd exponentials, their magnitude and phase as follows:

$$\begin{aligned}\sigma(t) &= (\eta_o + a\dot{\gamma}^2 + b\dot{\gamma}^4 \dots)\dot{\gamma} \\ &= \eta_o \dot{\gamma} + a\dot{\gamma}^3 + b\dot{\gamma}^5 \dots \\ &= \sum_{n=odd}^{\infty} a_n e^{-i(n\omega_1 t + \varphi_n)} \\ &= (n=1: a_1 = \eta_o; n=3: a_3 = a; n=5: a_5 = b)\end{aligned}\tag{5.3}$$

At the onset of the non-linear viscoelasticity all higher terms become zero and all reduces to the zero shear viscosity.

The most useful test procedure to analyze non-linear material behavior is the oscillation strain sweep and permits to monitor the

transition from the linear into the non-linear regime. In the linear region the material behavior, typically represented by the storage and loss modulus  $G'$  and  $G''$  are independent of strain. Higher order harmonic contributions are zero. Beyond the onset of non-linear behavior, along with changes of the storage and loss modulus, the third harmonic stress contribution becomes significant.

## **5.2 EXPERIMENTAL**

**5.2.1 Thermo-Mechanical Analysis:** POSS/PS solutions of varying POSS concentrations (0%, 6%, 13.3%, 20% and 30%) were made by dissolving PS ( $M_w = 290K$  Daltons) and POSS macromers in chloroform and stirring the solution for 12 hours using a magnetic stirrer. From this solution films were cast on a glass surface allowing the solvent to evaporate out slowly at room temperature. The films were dried and annealed at 105°C overnight in a vacuum oven to remove trace amounts of solvent and residual stress due to the solvent casting method.

Thermo-mechanical properties of PS/POSS films were analyzed using a Rheometric Scientific Solid Analyzer RSA III operated in a rectangular compression-tension mode. Samples used were in a shape of rectangular film strips with dimensions of  $12 \times 3 \times 0.2 \text{ mm}^3$ . The experiments were performed using an oscillatory frequency of 6.26 radians/second and oscillatory strain amplitude of 0.1%. All

measurements were carried out from room temperature to 120°C for all PS/POSS blends at a heating rate of 2°C per minute.

**5.2.2 Rheological Characterization:** Preparations of POSS/PS blends were performed by dissolving PS and POSS macromers in chloroform and stirring the solution for 12 hours using a magnetic stirrer and crashing the sample out by using a bad solvent methanol. The precipitated sample on crashing out of the solvent is filtered and then dried under vacuum for more than 12 hours at 60°C.

Rheological measurements were carried out using a TA Instruments ARES G2 rheometer equipped with a force convection oven. Parallel plate geometry with diameter of 8 mm and varying gap of 0.3 to 0.5 mm was used for all measurements obtained in this study. Rheological behavior of all samples was investigated using a series of isothermal, large-strain amplitude oscillatory shear with the oscillatory frequency of 6.28radian/second at a temperature of 220C. Strain sweep experiments were performed from 0.1% to 100% strain deformation.

Values of storage modulus,  $G'(\omega)$ , loss modulus,  $G''(\omega)$ , and damping factor,  $\tan\delta(\omega) = G''(\omega)/G'(\omega)$ , were determined using software provided by TA Instruments. Also the harmonic components of the response sinusoidal wave have been obtained using the software which was provided with the rheometer. Samples tested under the same experimental conditions were repeated two to three time to check reproducibility

## 5.3 RESULTS AND DISCUSSION

### 5.3.1 Glass Transition Region

Thermomechanical property of POSS/PS blends in the glassy state was investigated through dynamic thermo-mechanical techniques. Small oscillatory tensile strain at a fixed oscillatory frequency coupled with a simple temperature ramp was applied on films of PS/POSS blends from glassy state through glass transition. The results of the complex elastic modulus,  $E^*$ , and the damping factor,  $\tan \delta$ , for polystyrene blended with varying amount of  $\text{Ph}_8\text{T}_8$  POSS and  $\text{St}_8\text{T}_8$  POSS are depicted in Figures 11 and 12, respectively. In Figure 11, the  $\text{Ph}_8\text{T}_8$  POSS acting with increasing amount of POSS added in PS. In addition, we also observed a systematic decrease of the glassy state complex elastic modulus with increasing weight fractions of POSS as nanoscopic solvent molecule to PS is clearly seen as the  $\tan\delta$  peak shifts to lower temperatures due the plasticization effect.

As depicted in Figure 12, the addition of  $\text{St}_8\text{T}_8$  POSS has a very interesting effect on the glass transition of PS. Although the peak position of the  $\tan\delta$  curve shifts very little with the addition of  $\text{St}_8\text{T}_8$  POSS, the width of glass transition becomes much sharper with increasing amount  $\text{St}_8\text{T}_8$  POSS. Moreover, the onset of glass transition as determined by the complex elastic modulus curve shows a systematic increase as the weight fraction of  $\text{St}_8\text{T}_8$  POSS increase.

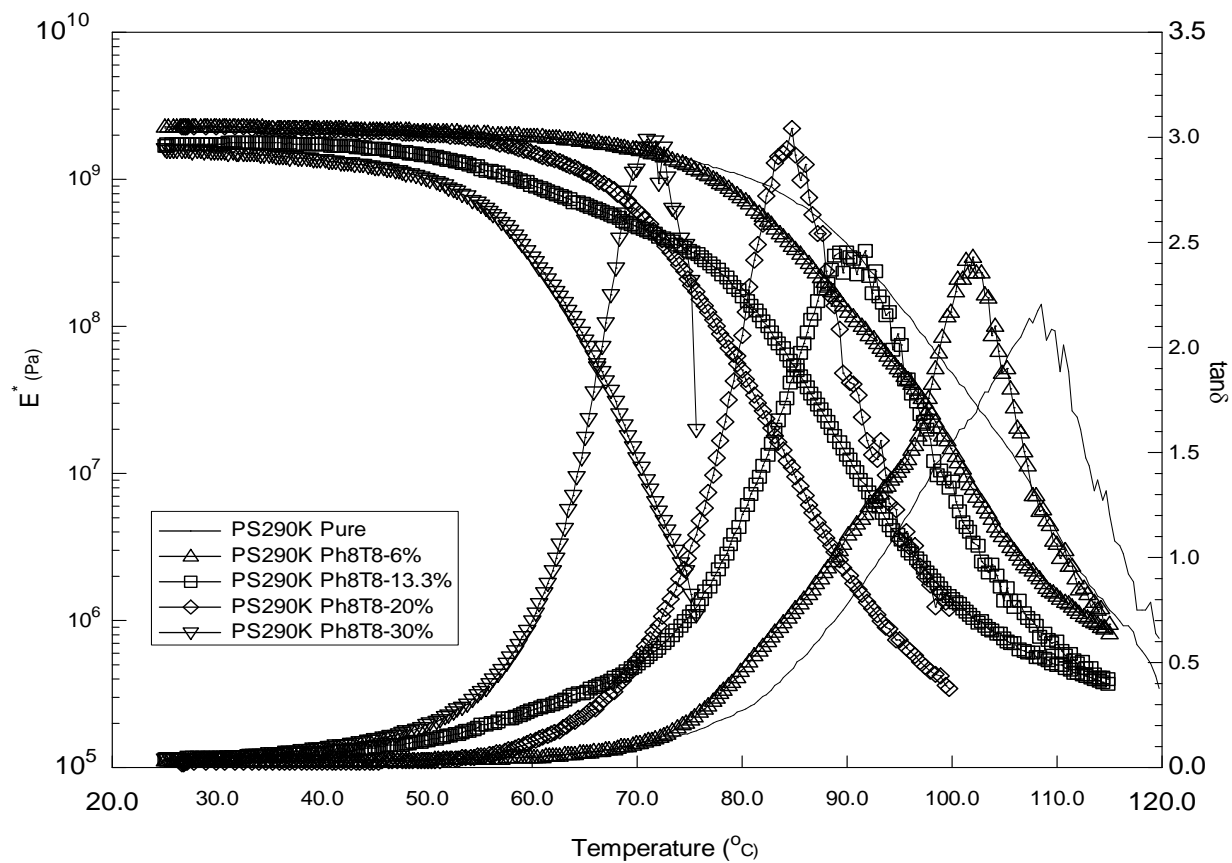


**Figure 5.2** Complex Modulus ( $E^*$ ) and  $\tan\delta$  versus Temperature plot for PS ( $M_w = 290\text{K Da}$ ) and Phenethyl POSS (Ph<sub>8</sub>T<sub>8</sub>) blends with varying weight fractions of POSS

The glass transition in amorphous polymers is very complex; there are many papers published in the past 25 years<sup>68-69</sup>. In general, the dynamics of glass transition is controlled by two molecular properties: order and inter-molecular potentials. The influence of inter-molecular potentials on the value of glass transition temperature,  $T_g$ , is obvious. Higher inter-molecular binding potentials require more energy input to the material as it undergoes transition from the glassy state to the liquid state, thus leading to higher value of  $T_g$ . Similarly the higher the order in the material, the higher the energy input are needed to achieve a complete “disorder” when material undergoes transition from glass-like to liquid-like behavior. We propose that to accommodate molecularly dispersed, nanoscopic rigid fillers such as  $St_8T_8$  POSS, the local polymeric segment may become more “ordered”, which enhances the onset of glass transition temperature. With this increase in the local order, the relaxation spectrum of the polymer chain in the glass transition region becomes narrower, which produces a sharper transition. This local order may persist to the rubbery state, which can facilitate the disentanglement process and leads to the observed reduction in values of  $\lim_{\omega \rightarrow 0} \eta^*(\omega)$  with  $St_8T_8$  POSS addition.



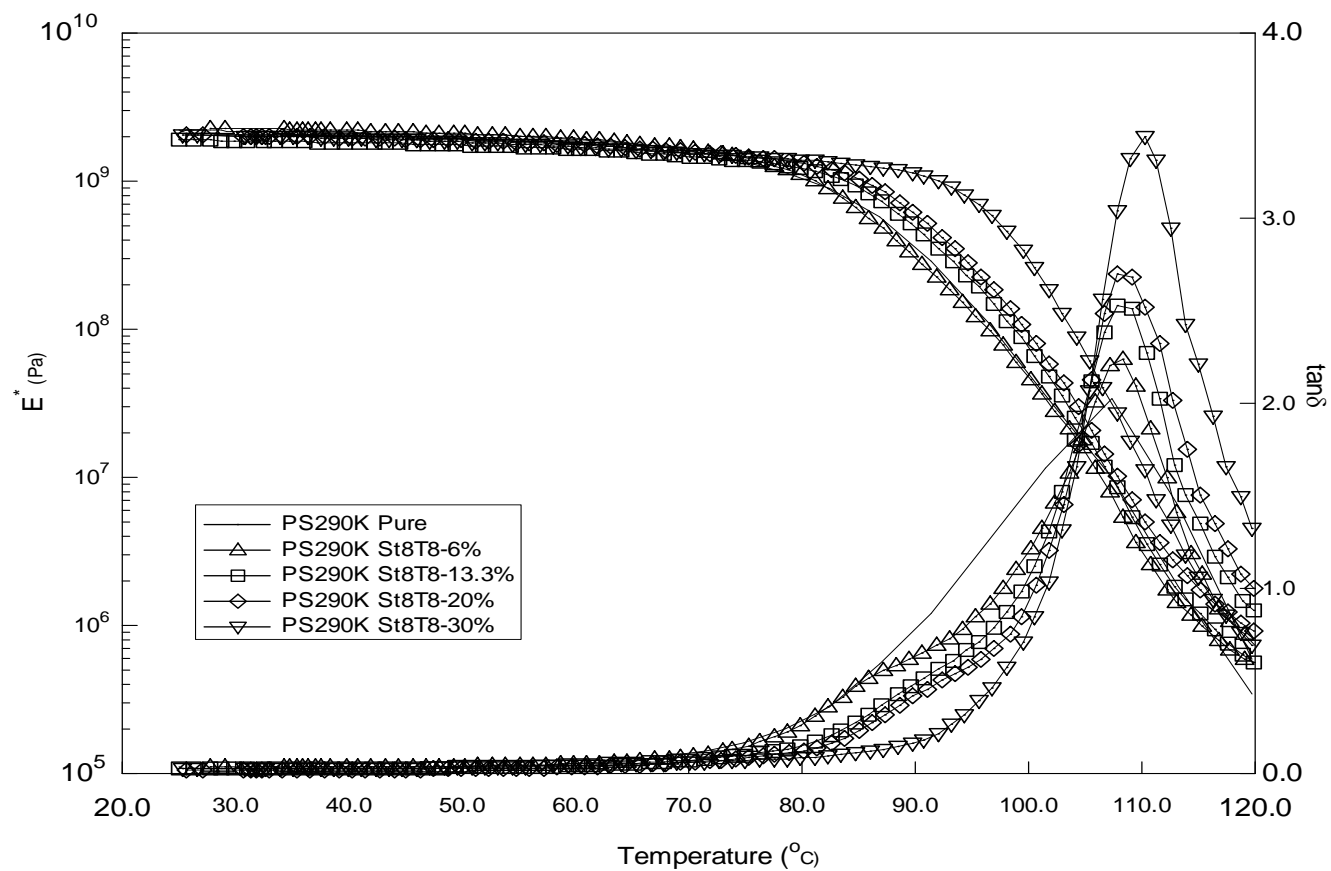


**Figure 5.3** Complex Modulus ( $E^*$ ) and  $\tan\delta$  versus Temperature plot for PS ( $M_w = 290\text{K Da}$ ) and Styrenyl POSS ( $\text{St}_8\text{T}_8$ ) blends with varying weight fractions of POSS

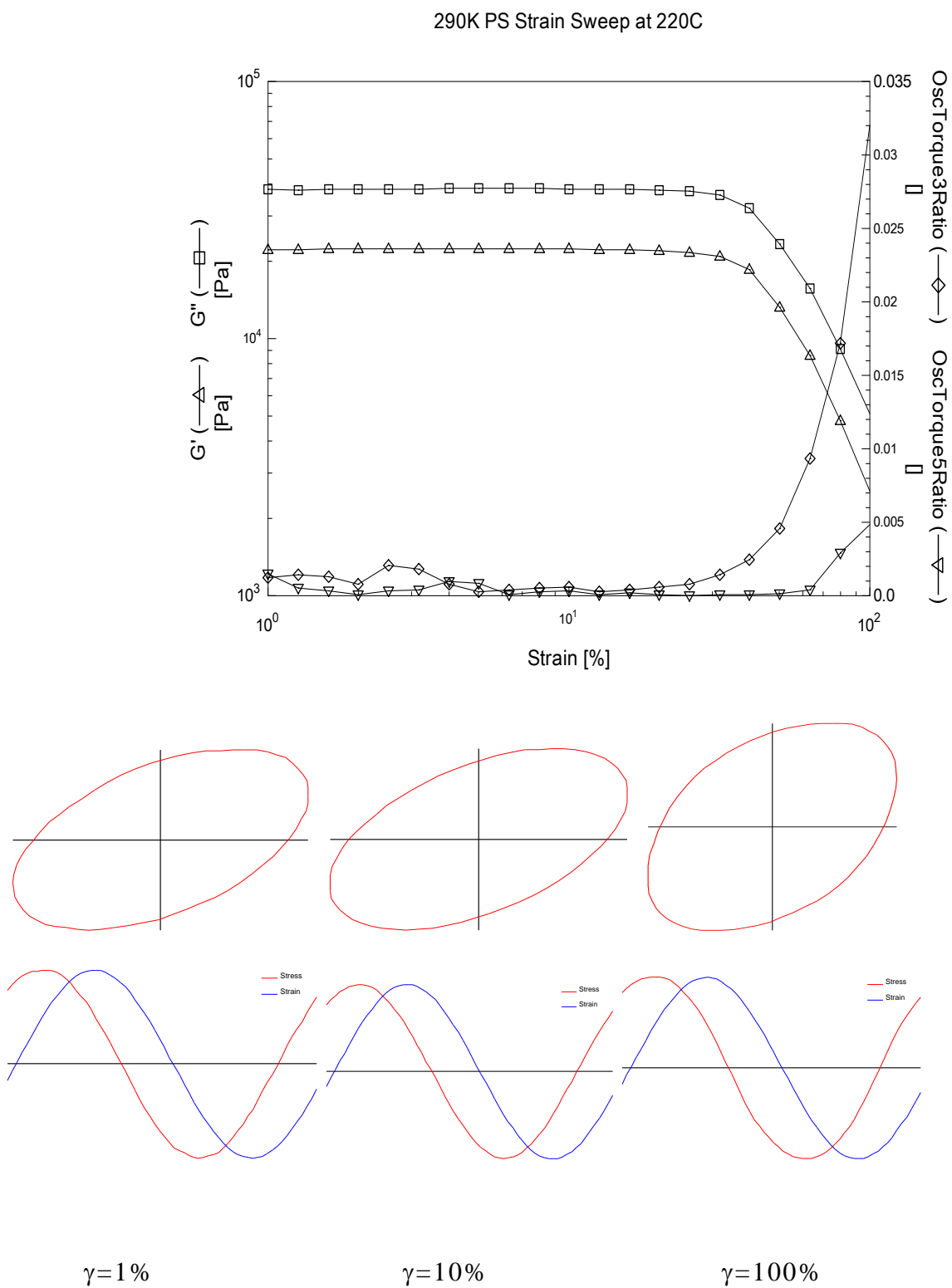


**Figure 5.4:** Strain sweep for the viscoelastic material 290K PS, showing the transition from the linear into the non-linear regime.

### 5.3.2 Non-linear oscillation measurements

For viscoelastic materials such as 290K PS in figure 5.4, both  $G'$  and  $G''$  decrease at the onset of non-linear behavior with increasing strain. The 3<sup>rd</sup> harmonic contribution starts to be significant at the same strain,  $G'$  deviates from linear behavior. The 5<sup>th</sup> harmonic follows the trend of the 3<sup>rd</sup>, only less pronounced and at a higher strain. The higher harmonic contributions are typically presented as the ratio of the magnitude of the  $n^{\text{th}}$  harmonic and the fundamental stress  $I_{n/1} = I(\omega_n)/I(\omega_1)$ , referred to as the “harmonic ratio” in the following. The harmonic ratio increases steadily with increasing strain.

In the non-linear region the symmetry of the stress response can be lost or conserved. For viscoelastic materials such as the reference PS 290K, the symmetry is mostly conserved. The peak of the stress signal in figure 5.4 flattens; the reduction of the peak maximum translates into shear thinning behavior (decrease of  $G'$ ,  $G''$ ) of viscoelastic materials. It is worthwhile to compare the shape of the stress wave at different strain amplitudes in the non-linear region.

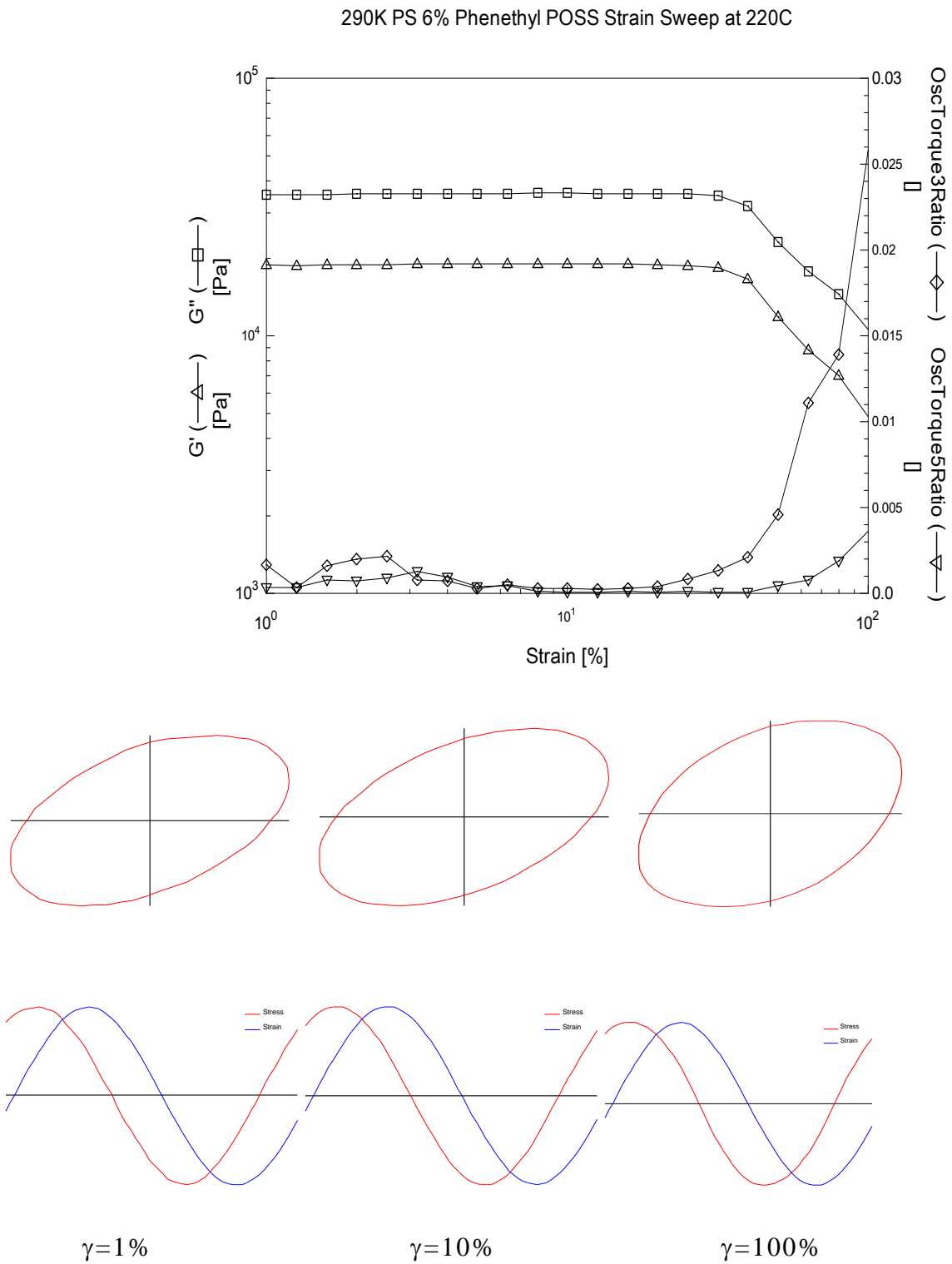


**Figure 5.5:** Strain sweep for the viscoelastic material 6% Phe<sub>8</sub>T<sub>8</sub> PS 290K blend, showing the transition from the linear into the non-linear regime.

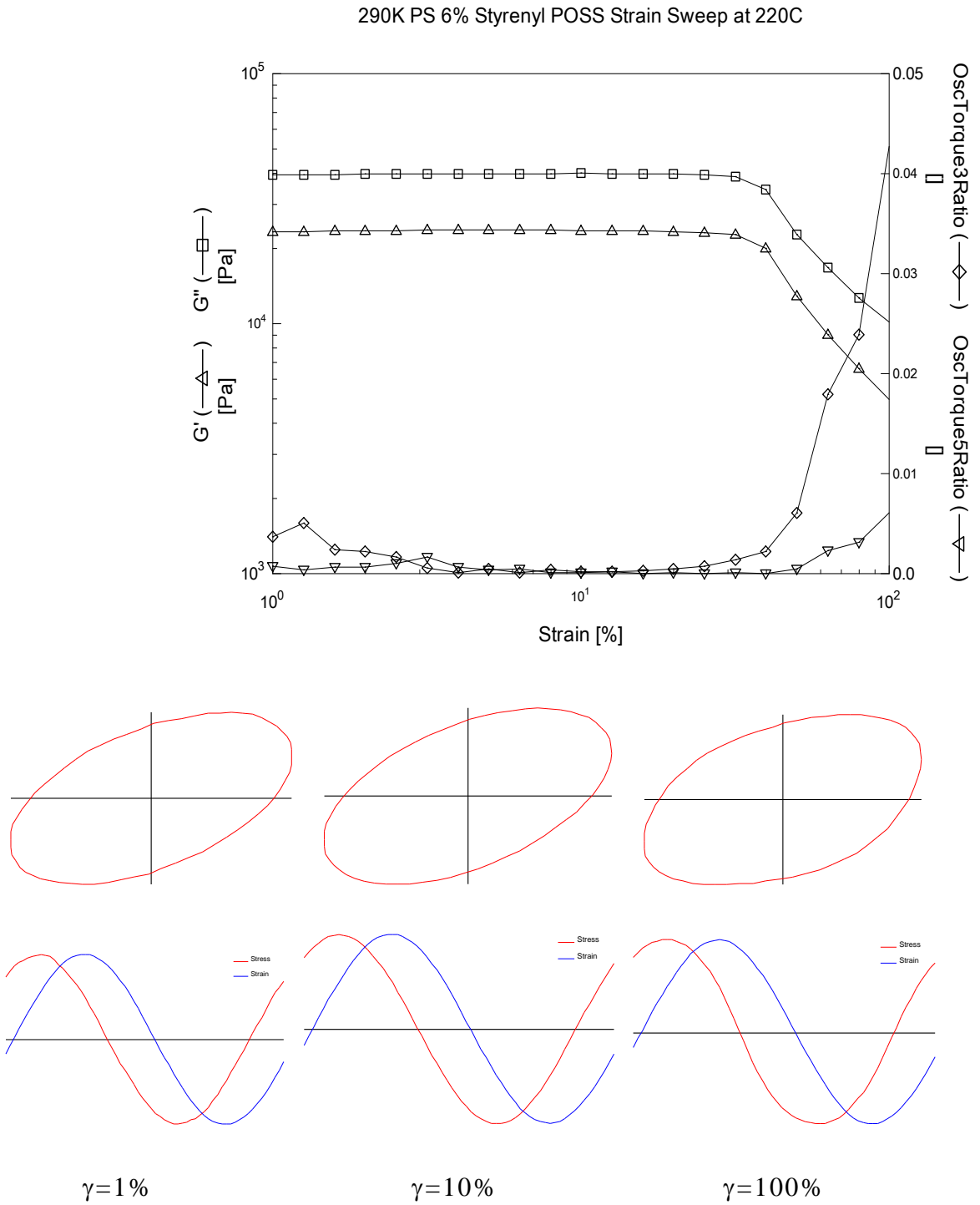


**Figure 5.6:** Strain sweep for the viscoelastic material 6%  $\text{St}_8\text{T}_8$  PS 290K blend, showing the transition from the linear into the non-linear regime.

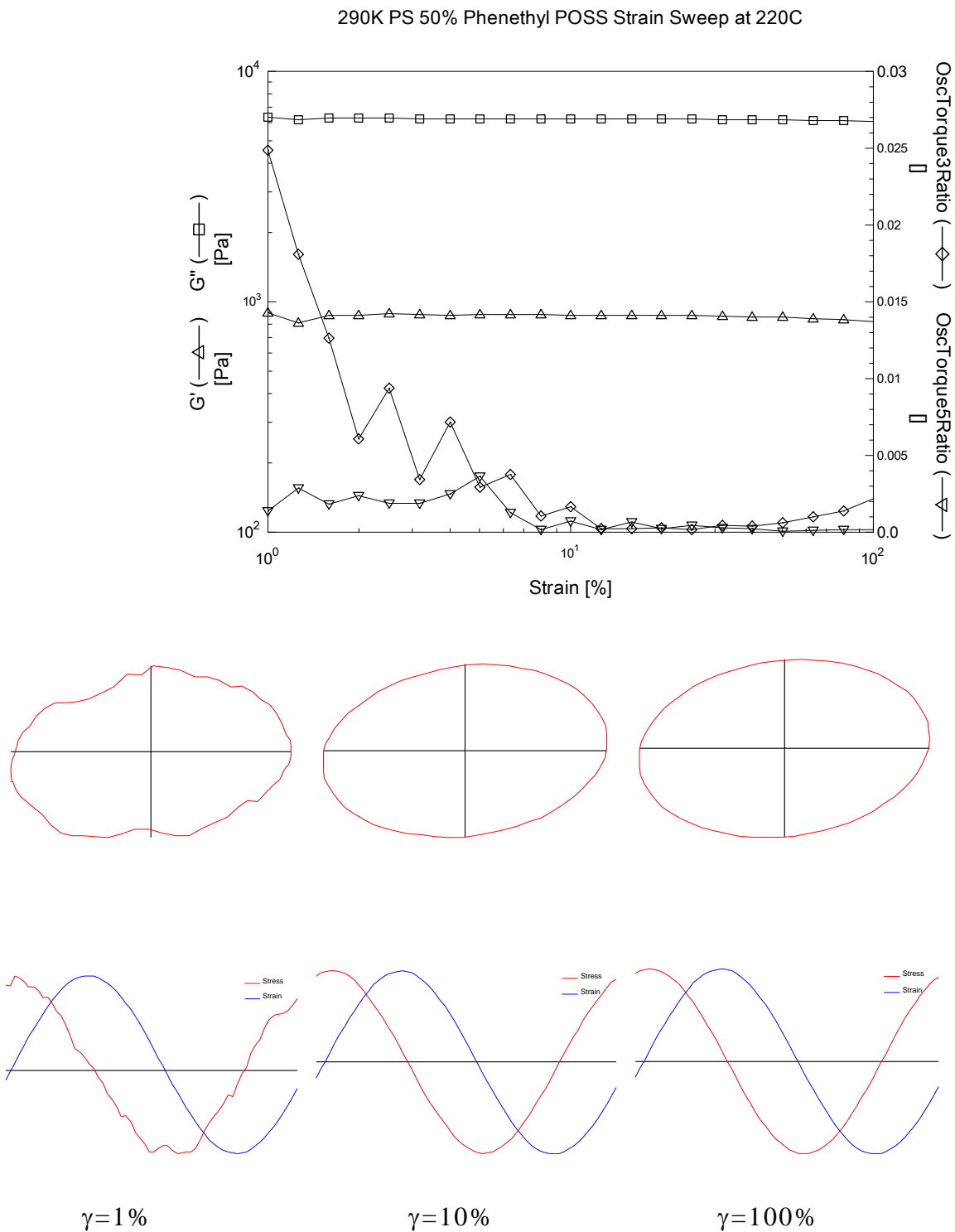


**Figure 5.7:** Strain sweep for the viscoelastic material 50% Phe<sub>8</sub>T<sub>8</sub>/PS blend, showing the transition from the linear into the non-linear regime.

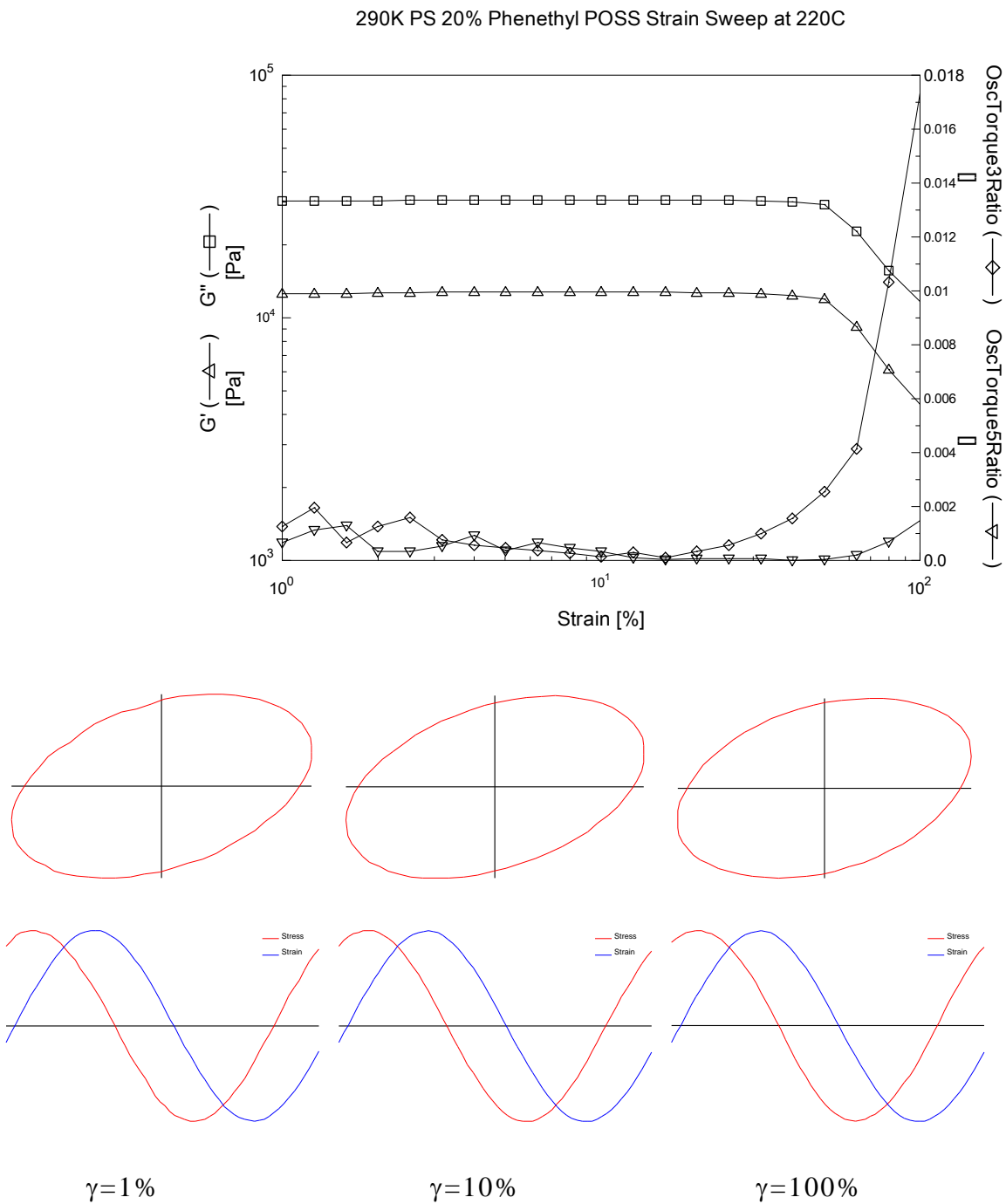


**Figure 5.8:** Strain sweep for the viscoelastic material 20% Phe<sub>8</sub>T<sub>8</sub>/PS blend, showing the transition from the linear into the non-linear regime.

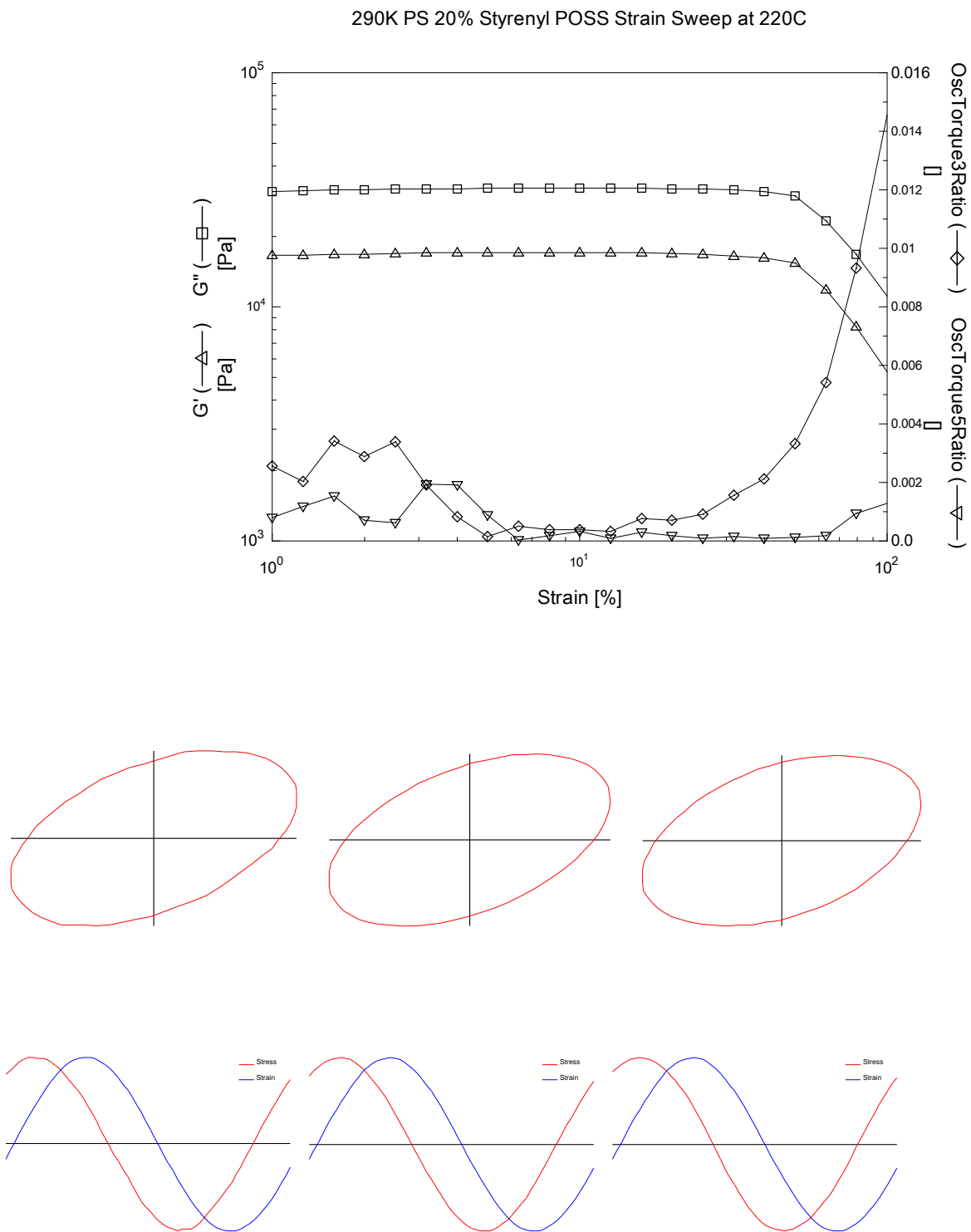


**Figure 5.9:** Strain sweep for the viscoelastic material 20%  $\text{St}_8\text{T}_8/\text{PS}$  blend, showing the transition from the linear into the non-linear regime.



## 5.4 SUMMARY

In this chapter we discuss the effects of the POSS macromers on PS chain under large deformations under flow conditions, also Dynamic Mechanical Analysis studies have been performed to get an insight into the effects of POSS on the dynamics especially at the transition temperatures, previous studies by Mulliken and Soong from Boyce and Cohen's group have seen POSS effecting the secondary motions of the polymeric matrix. Their findings suggest that POSS clearly enhanced the mobility of the secondary beta motions, significantly reducing the resistance to high rate elastic and plastic deformation and also POSS was found to plasticize PVC and hence to dramatically influence its glass transition and corresponding non linear mechanical behavior.

Thermomechanical properties of POSS/PS blends in the glassy state were investigated through dynamic thermo-mechanical techniques. Small oscillatory tensile tests on the Phe<sub>8</sub>T<sub>8</sub>/PS blend films show a gradual decrease in glass transition temperature and elastic modulus with increasing concentration which further confirm the plasticization theory. In the case of St<sub>8</sub>T<sub>8</sub> POSS/PS blends not much variation in glass transition temperature is observed which supports the DSC data, however the width of glass transition becomes much sharper with increasing amount of St<sub>8</sub>T<sub>8</sub> POSS. Moreover, the onset of glass transition as determined by the complex elastic modulus curve shows a systematic increase as the weight fraction of St<sub>8</sub>T<sub>8</sub> POSS increases. Due to the higher order in the St<sub>8</sub>T<sub>8</sub>

POSS as observed from DSC, when material undergoes transition from glass-like to liquid-like behavior we propose to accommodate molecularly dispersed, nanoscopic rigid fillers such as  $\text{Si}_8\text{T}_8$  POSS, the local polymeric segment may become more “ordered”, which enhances the onset of glass transition temperature.

The strain sweep data especially in the non linear regimes on the various POSS PS blends show a delay in the progression from the linear to non linear regimes due to the presence of POSS irrespective of the phase behavior of the blend system, also with increasing weight fractions the effect is magnified suggesting POSS acting as friction points in between the free flowing polymer chains.

POSS nanoparticles which are compatible with the polymer chains could be used to lower the free energy of the polymer mixture and also reduce the viscosity of a polymer mixture as a plasticizer. Though miscibility and aggregation kinetics could be controlled in these types of nanocomposites since the chemistry of POSS particles can be modified depending on the system to be used, it should be noted that restrictions on the organic pendant group on the silicone cage plays an important role in governing the dynamics of systems involving POSS.

## **CHAPTER 6**

### **CONCLUSIONS**

In recent years the blending of 0-, 1-, and 2- dimensional inorganic fillers such as POSS, carbon nanotubes, and nano-clay platelets into polymeric matrices enabled exploration of various filler/matrix combinations on mechanical properties. However, a fundamental understanding of the connections amongst the microstructure and macroscopic properties of polymeric based nanocomposites are yet to be fully explored to optimize the truly multifunctional property potential of polymer nanocomposites.

Several key unifying issues/themes for determining, understanding and optimizing properties for all classes of polymer nanocomposites exist. A key feature of primary importance in understanding the nanocomposite is the actual identification and definition of the structure and the properties of the nanoparticle itself; whether the nanoparticle be OD, ID or 2D, it is critical to provide a well defined description of the particle geometry, structure and properties and its surrounding zone of influence on the matrix morphology and properties and its interface with the matrix in order to assess the impact of the nanoparticle on the nanocomposite property. Similar developments addressed POSS "particles" which are observed to have very different mechanical properties if acting as isolated entities or as crystallized (or near crystallized) rafts - a basic , but somewhat different, observation also seen in nanoclay particles when

comparing intercalated particle structure/properties with that of the exfoliated condition. Furthermore, POSS particles were found to have the ability to act as either stiffening agents or as plasticizing agents depending upon the interactions between the functional groups and the matrix polymer. Another key issue was the development of synthesis and processing routes to (1) properly disperse the particles within the matrix in order to fully make use of their nanoscopic potential and (2) to provide a good interaction with the matrix in order to facilitate load transfer from the matrix to the particle in order to exploit the stiffening and strengthening potential of the nanoparticle. A third key issue is proper identification of the effect of the nanoparticle on the surrounding matrix where use of microscopy and mechanical spectroscopy prove enlightening on identifying the effects on the structure and the local dynamics of the polymer molecules. Details specific to these key issues and others for each material system are presented below where we note that each effect manifests itself differently in each of the nanocomposite material systems.

In Chapter 2, the focus was primarily to investigate the influence of the various organic groups on the interactions between POSS and polymer which would govern the properties of the POSS-polymer blends. The degree of dispersion was investigated using DSC, WAXD and TEM. Even though POSS can be attached onto the backbone of the polymers, in this study we use only fully condensed POSS systems where by altering the organic functional groups appended to Si-O core the different extent of

compatibility can be controlled. The focus of this study is to investigate the influence of the various organic groups on the interactions between POSS and polymer which would govern the properties of the POSS-polymer blends. Samples were prepared using a common solvent and then crashing in a bad solvent and the resulting blend properties characterized by rheology and dynamical thermal analysis.

The architectures of POSS such as size of the inorganic core, pendant organic group and the shape of the POSS can all play some role in governing the microstructure of the blend. Morphological investigations of the POSS blends indicate that there is a significant amount of aggregation (crystallization) of POSS into large particles. In some cases what we found was by controlling the compatibility between the organic group surrounding inorganic silica-like core of POSS and polymer matrix is that the molecular dispersion can be achieved.

In Chapter 3 the effect of concentration on the viscometric properties of the nanocomposite blends have been investigated. Rheological measurements well above  $T_g$  have been used to determine the time-temperature superposition behavior of these thermorheologically simple materials. The size of POSS macromers on similar length scales when compared to the entanglement spacing of the polymer chains makes it interesting to study the role these nano-structured constituents would play in controlling the polymer chain dynamics. However due to the complex morphologies of various POSS/PS blends, similar rheological

behavior may be obtained due to two different mechanisms. To address the above issue we took a POSS macromer having the organic pendant group as the same or nearly similar as the monomer unit as the polymer. DSC, X-ray, TEM were used to understand the morphology of the blends. Rheological characterization was done for understanding the chain dynamics due to the presence of POSS or due to the domains formed due to the presence of POSS.

The shape of the POSS macromers may play an important role in governing the microstructure in the blend. Do these changes in microstructure cause profound changes to the relaxation of the polymer backbones? Our findings clearly suggest that POSS nanoparticles which are compatible with the polymer chains could be used to lower the free energy of the polymer mixture and also reduce the viscosity of a polymer mixture as a plasticizer. Though miscibility and aggregation kinetics could be controlled in these types of nanocomposites since the chemistry of POSS particles can be modified depending on the system to be used, it should be noted that restrictions on the organic pendant group on the silicone cage plays an important role in governing the dynamics of systems involving POSS. Interestingly in the case of Octa styrenyl POSS PS Blends, at small volume fractions, free (untethered) POSS nano-dispersed in the melt appears to act as a plasticizer, reducing the magnitude of selected material properties such as plateau modulus or zero-shear rate viscosity at a given temperature, while simultaneously

causing a decrease in free volume (estimated from WLF coefficient analysis). As the volume of dispersed POSS increases, steric effects of the filler dominate and the rheological properties of the melt (modulus, relaxation time, viscosity) are all enhanced.

In Chapter 4, based on our results in the previous chapters which indicate the ability for POSS to very locally interact with the matrix molecules altering their mobility, and thereby able to either stiffen or plasticize the material. In a confined system like an entangled polymer melt blended with POSS, the motion of either the POSS macromer or the polymer chain or both should in some way be affected. Though this problem is studied previously, several hypotheses have arisen but none conclusive enough to explain what exact mechanisms control the dynamics of the polymer chains due to the presence of huge (on a molecular length scale) cage like particles. There are however, many questions left due to the absence of a systematic study. Will the higher molecular weight polymer chains take a longer time to relax due to the interference by POSS macromers? Or the dynamics of POSS macromers within the entangled polymer chain play a role in governing the rheological characteristics of these blends. We intend to address this problem through the study of POSS-PS blends by varying the molecular weight of the linear nearly monodisperse PS ranging from around 30KDa to around 1.6MDa. As observed in the case of styrenyl blends the presence of the dispersed polymer rich phase gives a unique opportunity in understanding

rheological properties of domains filled with soft cores, especially in nonlinear regimes. This led us in a direction of exploring the effects of POSS on the non linear mechanical behavior of POSS polymer blends.

In Chapter 5 we discuss the effects of the POSS macromers on PS chain previous under large deformations, also Dynamic Mechanical Analysis studies have been performed to get an insight into the effects of POSS on the dynamics especially at the transition temperatures, previous studies by Mulliken and Soong from Boyce and Cohen's group have seen POSS effecting the secondary motions of the polymeric matrix. Their findings suggest that POSS clearly enhanced the mobility of the secondary beta motions, significantly reducing the resistance to high rate elastic and plastic deformation and also POSS was found to plasticize PVC and hence to dramatically influence its glass transition and corresponding non linear mechanical behavior.

In this study we have investigated experimentally the effect of POSS macromers when physically blended in entangled PS matrix. The effect on polymer chain dynamics and the phase characteristics by the presence of POSS macromers in PS blends were discussed.

Using DSC, we were able to determine the melting temperature and the heat of fusion for the two POSS molecules, Styrenyl<sub>8</sub>-POSS (St<sub>8</sub>T<sub>8</sub>) and Phenethyl<sub>8</sub>-POSS (Ph<sub>8</sub>T<sub>8</sub>) used in this study. The hydrogenation of styrenyl to phenethyl reduces the melting temperature from 274°C (St<sub>8</sub>T<sub>8</sub> POSS) to 77°C (Ph<sub>8</sub>T<sub>8</sub> POSS), while the heat of fusion remain unchanged



(37.7 kJ/mole). In addition,  $T_g$  of all POSS/PS blends used in this study was also determined using DSC. No POSS melting peak was observed in all POSS/PS blends used, which suggests the high miscibility between polystyrene and the two POSS molecules used here. The morphologies of the blends were studied by using wide angle X-ray diffraction techniques and TEM. Similar to the DSC observation, X-ray results show the disappearance of the crystalline nature of POSS when blended with PS indicating good compatibility. From the TEM images it was clearly observed that dispersion occurs for all weight fractions of POSS in PS. Different phase behavior was achieved depending on the type of POSS used, for Ph<sub>8</sub>T<sub>8</sub> POSS a homogeneous blend is formed because of the lower POSS-POSS interaction, but phase inversion occurs when solid St<sub>8</sub>T<sub>8</sub> POSS macromers were used which have a high binding energy.

Rheological experiments were performed to investigate the influence of POSS addition on the melt dynamics of the polymer chains. We are particularly interested in the influence of well-dispersed, nanoparticulate additions on the zero-shear viscosity,  $\lim_{\omega \rightarrow 0} \eta^*(\omega)$ , plateau modulus,  $G_N^0$  and the cross-over frequency,  $\omega_C$  of polymer melts.

In the Ph<sub>8</sub>T<sub>8</sub> POSS/PS blends, because of the low POSS-POSS interaction, any POSS interactions are screen-out by the presence of PS. Ph<sub>8</sub>T<sub>8</sub> POSS/PS blend forms a homogeneous solution. The rheological responses of these blends are the same as if as a good solvent was added to PS. We observed a systemic decrease in the zero-shear viscosity,

plateau modulus, cross-over frequency as the concentration of Ph<sub>8</sub>T<sub>8</sub> POSS increases, as shown in Table 1.

For St<sub>8</sub>T<sub>8</sub> POSS/PS blends, due to a stronger POSS-POSS association, the blend forms a two-phase morphology. Regardless to the concentration of St<sub>8</sub>T<sub>8</sub> POSS in PS, the POSS-rich form a continuous phase and PS-rich domain as the discontinuous phase. As we increase the concentration of St<sub>8</sub>T<sub>8</sub> POSS, only the fraction of PS-rich discontinue phase is increased. Since St<sub>8</sub>T<sub>8</sub> POSS is molecularly dispersed in PS, the zero shear viscosity of the blends decreases with the addition of St<sub>8</sub>T<sub>8</sub> POSS which is similar to that observed in the case of Ph<sub>8</sub>T<sub>8</sub>/PS blends (shown in Table 1). However due to persistence of the two-phase morphology, no systematic changes in  $\omega_c$  and  $G_N^0$  was observed with increasing concentration of POSS since phase behavior controls the rheological behavior of these blends.

Thermomechanical properties of POSS/PS blends in the glassy state were investigated through dynamic thermo-mechanical techniques. Small oscillatory tensile tests on the Ph<sub>8</sub>T<sub>8</sub>/PS blend films show a gradual decrease in glass transition temperature and elastic modulus with increasing concentration which further confirm the plasticization theory. In the case of St<sub>8</sub>T<sub>8</sub> POSS/PS blends not much variation in glass transition temperature is observed which supports the DSC data, however the width of glass transition becomes much sharper with increasing amount of St<sub>8</sub>T<sub>8</sub> POSS. Moreover, the onset of glass transition as determined by the

complex elastic modulus curve shows a systematic increase as the weight fraction of  $\text{St}_8\text{T}_8$  POSS increases. Due to the higher order in the  $\text{St}_8\text{T}_8$  POSS as observed from DSC, when material undergoes transition from glass-like to liquid-like behavior we propose to accommodate molecularly dispersed, nanoscopic rigid fillers such as  $\text{St}_8\text{T}_8$  POSS, the local polymeric segment may become more “ordered”, which enhances the onset of glass transition temperature.

## **REFERENCES**

## REFERENCES

1. J. D. Wright, N. Sommerdijk, Sol-Gel Materials: Their Chemistry and Biological Properties, Taylor & Francis Group, London, 2000.
2. U. Schubert, N. Hüsing, A. Lorenz, Hybrid Inorganic-Organic Materials by Sol-Gel Processing of Organofunctional Metal Alkoxides. Chem. Mater. 1995, 7, 2010–2027.
3. C. J. Brinker, G. W. Scherer, Sol-Gel Science: The Physics and Chemistry of Sol-Gel Processing, Academic Press, London, 1990.
4. Hybrid Materials, Special issue of J. Mater. Chem. 2005, 15, 3543–3986.
5. P. Gómez-Romero, C. Sanchez (Eds.) Functional Hybrid Materials, Wiley-VCH, Weinheim, 2004.
6. G. Schottner, Hybrid Sol-Gel-Derived Polymers: Applications of Multifunctional Materials. Chem. Mater. 2001, 13, 3422–3435.
7. G. Kickelbick, U. Schubert, Inorganic Clusters in Organic Polymers and the Use of Polyfunctional Inorganic Compounds as Polymerization Initiators, Monatsh. Chem. 2001, 132, 13.
8. K.-H. Haas, Hybrid inorganic-organic polymers based on organically modified Si-alkoxides. Adv. Eng. Mater. 2000, 2, 571–582.
9. C. Sanchez, F. Ribot, B. Lebeau, Molecular design of hybrid organic-inorganic nanocomposites synthesized via sol-gel chemistry. J. Mater. Chem. 1999, 9, 35–44.
10. K. G. Sharp, Inorganic/organic hybrid materials. Adv. Mater. 1998, 10, 1243–1248.
11. Nanocomposites Special issue of J. Nanosci. and Nanotech. 2006, 6, 265–572.
12. R. M. Laine, Nanobuilding blocks based on the  $[\text{OSiO}_{1.5}]_x$  ( $x = 6, 8, 10$ ) octasilsesquioxanes. J. Mater. Chem. 2005, 15, 3725–3744.
13. A. Usuki, N. Hasegawa, M. Kato, Polymer-clay nanocomposites. Adv. Polym. Sci. 2005, 179, 135–195.
14. B. C. Sih, M. O. Wolf, Metal nanoparticle conjugated polymer nanocomposites. Chem. Commun. 2005, 3375–3384.

- 15.C. Sanchez, B. Julian, P. Belleville, M. Popall, Applications of hybrid organic-inorganic nanocomposites. *J. Mater. Chem.* 2005, 15, 3559–3592.
- 16.P. Gómez-Romero, K. Cuentas-Gallegos, M. Lira-Cantu, N. Casan-Pastor, Hybrid nanocomposite materials for energy storage and conversion applications. *J. Mater. Sci.* 2005, 40, 1423–1428.
- 17.G. Kickelbick, Concepts for Incorporation of Inorganic Building Blocks into Organic Polymers on a Nanoscale. *Progr. Polym. Sci.* 2003, 28, 83–114.
- 18.A. Sayari, S. Hamoudi, Periodic Mesoporous Silica-Based Organic-Inorganic Nanocomposite Materials. *Chem. Mater.* 2001, 13, 3151–3168.
- 19.F. Hoffmann, M. Cornelius, J. Morell, M. Fröba, J. Nanosci. Nanotechnol. 2006, 6, 265–288.
- 20.B. Hatton, K. Landskron, W. Whitnall, D. Perovic, G. A. Ozin, Past, Present, and Future of Periodic Mesoporous Organosilicas – The PMOs. *Acc. Chem. Res.* 2005, 38, 305–312
- 21.J.-L. Shi, Z.-L. Hua, L.-X. Zhang, Nanocomposites from ordered mesoporous materials. *J. Mater. Chem.* 2004, 14, 795–806.
- 22.R. Gangopadhyay, A. De, Conducting Polymer Nanocomposites: A Brief Overview. *Chem. Mater.* 2000, 12, 608–622.
- 23.C. J. Brinker, Y. Lu, A. Sellinger, H. Fan, Evaporation-induced self-assembly. Nanostructures made easy. *Adv. Mater.* 1999, 11, 579–585.
- 24.N. Hüsing, U. Schubert, Aerogels – airy materials: chemistry, structure, and properties. *Angew. Chem. Int. Ed.* 1998, 37, 22–45.
- 25.D. Y. Godovsky, Device applications of polymer nanocomposites. *Adv. Polym. Sci.* 2000, 153, 163–205.
- 26.J. Wen, G. L. Wilkes, Garth L. Organic/Inorganic Hybrid Network Materials by the Sol-Gel Approach. *Chem. Mater.* 1996, 8, 1667–1681.
- 27.G. J. de A. A. Soler-Illia, L. Rozes, M. K. Boggiano, C. Sanchez, C.-O. Turrin, A.-M. Caminade, J.-P. Majoral, New mesotextured hybrid materials made from assemblies of dendrimers and titanium(IV)-oxo-organo clusters. *Angew. Chem. Int. Ed.* 2000, 39, 4249–4254.
- 28.J. L. Hedrick, T. Magbitang, E. F. Connor, T. Glauser, W. Volksen, C. J. Hawker, V. Y. Lee, R. D. Miller, Application of complex

- macromolecular architectures for advanced microelectronic materials. Chem. – Europ. J. 2002, 8, 3308–3319.
- 29.J. W. Kriesel, T. D. Tilley, Carbosilane dendrimers as nanoscopic building blocks for hybrid organic-inorganic materials and catalyst supports. Adv. Mater. 2001, 13, 1645–1648.
  - 30.P. R. Dvornic, C. Hartmann-Thompson, S. E. Keinath, E. J. Hill, Organic-Inorganic Polyamidoamine (PAMAM) Dendrimer- Polyhedral Oligosilsesquioxane (POSS) Nanohybrids. Macromolecules 2004, 37, 7818–7831.
  - 31.R. W. J. Scott, O. M. Wilson, R. M. Crooks, Synthesis, Characterization, and Applications of Dendrimer-Encapsulated Nanoparticles. J. Phys. Chem. B 2005, 109, 692–704.
  - 32.V. Castelvetro, C. De Vita, Cinzia. Nanostructured hybrid materials from aqueous polymer dispersions. Adv. Coll. Interf. Sci. 2004, 108–109, 167–185.
  - 33.E. Bourgeat-Lami, Organic/inorganic nanocomposite colloids in Encyclopedia of Nanoscience and Nanotechnology (Ed. H. S. Nalwa), American Scientific Publishers, Stevenson Ranch 2004.
  - 34.G. Kickelbick, L. M. Liz-Marzán, Core-Shell Nanoparticles in Encyclopedia of Nanoscience and Nanotechnology (Ed. H. S. Nalwa), American Scientific Publishers, Stevenson Ranch, 2004.
  - 35.G. A. Ozin, A. C. Arsenault, Nanochemistry – A Chemical Approach to Nanomaterials, RSC Publishing, London, 2005.
  - 36.Ning, Y.P.; Tang, M.Y.; Jiang, C.Y.; Mark, J.E. and Roth, W.C.; J Appl. Polym. Sci., 1984, 29, 3209
  - 37.Kojima, Y.; Usuki, A.; Kawasumi, M.; Okada, A.; Kurauchi, T. and Kamigaito, J.; J. Polym. Sci: Part A: Polym. Chem.,1993, 31, 983.
  - 38.Wang, M.S. and Pinnavaia, T.J.; Chem. Mat., 1994, 6, 468.
  - 39.Lichtenhan, J.D.; Comments Inorg. Chem., 1995, 17, 115.
  - 40.Geng H. P.; PhD Thesis, Michigan State University, 2001
  - 41.Scott D.W.; J. Am. Chem. Soc., 1946, 68, 356.
  - 42.Brown J.F.; Vogt L.H.; J. Am. Chem. Soc., 1965, 87, 4313.

43. Feher F.J.; Newman D.A.; Walzer J.F.; J. Am. Chem. Soc.,1989, 111, 1741.
44. Feher F.J.; Newman D.A.; J. Am. Chem. Soc.,1989, 112,1931.
45. Lichtenhan J. D.; Schwab J.J.; Feher F.J.; Soulivong D.; U.S. Patent 5942638, 1999.
46. Lichtenhan J. D.; Schwab J.J.; Reinerth W. A. Sr.; Chem. Innovat., 2001, 1, 3.
47. Voronkov M. G.; Lavrent'yev V. I.; Topics Curr. Chem.,1982, 102, 199.
48. Feher F. J.; Terroba R.; Jin R.; Wyndham K. O.; Lucke S.; Brutchey R.; Nguyen F.; Polym. Mater. Sci. Eng, 2001, 82, 301,.
49. Haddad T. S.; Lichtenhan J.D.; Macromolecules, 1996, 29, 7302.
50. Romo-Urbe A.; Mather P. T.; Haddad T. S.; Lichtenhan J.D.; J. of Polym. Sci. Part B: Polym. Phys., 1998, 36, 1857.
51. Lichtenhan JD, Otonari Y, Carr MJ. Macromolecules, 1995, 28, 8435.
52. Mather P. T.; Jeon H. G.; Romo-Urbe A.; Haddad T. S.; Lichtenhan J.D.; Macromolecules, 1999, 32, 1194.
53. Gilman J. W.; Schlitzer D. S.; Lichtenhan J. D.; J. of Appl .Polym. Sci., 1996, 60, 591.
54. Lee A. Y.; Lichtenhan J. D.; Macromolecules, 1998, 31, 4970.
55. Lee A. Y.; Lichtenhan J. D.; J. Appl. Polym. Sci., 1999, 73, 1993
56. Hsiao B. S.; Fu B. X.; Mather P. T.; Chaffee K. P.; Jeon H.; White H.; Rafailovich M.; Lichtenhan J. D.; Schwab J. J.; Polym. Mater. Sci. Eng., 1998, 79, 389.
57. Schwab J. J.; Lichtenhan J.D.; Carr M. J.; Chaffee K. P.; Mather P. T.; Romo-Urbe A.; Polym. Mater. Sci. Eng., 1997, 77, 549.
58. Fu, B. X.; Yang, L.; Somani, R. H.; Zong, S. X.; Hsiao, B. S.; Phillips, S.; Blanski, R.; Ruth, P.; J. Poly. Sci. Part B: Poly. Phy., 2001, 39, 2727.



- 59.Li, G.Z., Wang, L.C., Ni, H.L., and Pittman, C.U.; J. Inorg. Organomet. Polym., 2001, 11, 123.
- 60.Phillips S. H.; Haddad T. S.; Tomczak S. J.; Curr. Opi. Solid State & Mat. Sci. 2004, 8, 21.
- 61.Starr, F.W.; Schroeder, T.B. and Glotzer, S.C.; Phys. Rev. E, 2001, 64, 021802.
- 62.Starr, F.W.; Schroeder, T.B. and Glotzer, S.C.; Macromolecules, 2002, 35, 4481.
- 63.Kopesky E. T.; Haddad, T. S.; Cohen, R. E.; McKinley, G. H.; Macromolecules, 2004, 37, 8992.
- 64.Blanski, R.L.; Lee, A.; Geng, H.P.; Phillips, S.H.; Chaffee, K. and Lichtenhan, J.L.; Polym. Preprint, 2001, 41, 585.
- 65.Baker E. S. Gidden J; Fee D. P.; Kemper P. R.; Anderson S. E.; Bowers M. T.; Intl. J. Mass Spec, 2003, 227, 205.
- 66.Rubinstein M. and Colby R.H; “Polymer Physics”, Oxford University Press, 2003.
- 67.Mackay M. E.; Dao T. T.; Tuteja A.; Ho D. L.; Van Horn B.; Kim H.C.; Hawker C. J.; Nat. Mat.,2003, 2, 762.
- 68.Donth R. J.; “Relaxation and Thermodynamics in Polymers-Glass Transition”, Akademie Verlag, Berlin, 1992.
- 69.Larson R.G.; Chapter 4 of “The Structure and Rheology of Complex Fluids”, Oxford University Press, 1999.